New Method for Directional Modulation using Beamforming: Applications to Simultaneous Wireless Information and Power Transfer and Increased Secrecy Capacity

Randy Matthew Yamada

Dissertation submitted to the faculty of the
Virginia Polytechnic Institute and State University
in partial fulfillment of the requirements for the degree of

Doctor of Philosophy
In
Electrical Engineering

Lamine Mili, Chair
R. Michael Buehrer
T. Charles Clancy
Serkan Gugercin
Allan O. Steinhardt

September 14, 2017
Arlington, Virginia

Keywords: Directional Modulation, Physical Layer Security, Beamforming, Array, Broadcast Channel, Secrecy

New Method for Directional Modulation using Beamforming:
Applications to Simultaneous Wireless Information and Power Transfer and Increased Secrecy Capacity

Randy Matthew Yamada

ABSTRACT

The proliferation of connected embedded devices has driven wireless communications into commercial, military, industrial, and personal systems. It is unreasonable to expect privacy and security to be inherent in these networks given the spatial density of these devices, limited spectral resources, and the broadcast nature of wireless communications systems. Communications for these systems must have sufficient information capacity and secrecy capacity while typically maintaining small size, light weight, and minimized power consumption. With increasing crowding of the electromagnetic spectrum, interference must be leveraged as an available resource.

This work develops a new beamforming method for direction-dependent modulation that provides wireless communications devices with enhanced physical layer security and the ability to simultaneously communicate and harvest energy by exploiting co-channel interference. We propose a method that optimizes a set of time-varying array steering vectors to enable direction-dependent modulation, thus exploiting a new degree of freedom in the space-time-frequency paradigm. We formulate steering vector selection as a convex optimization problem for rapid computation given arbitrarily positioned array antenna elements.

We show that this method allows us to spectrally separate co-channel interference from an information-bearing signal in the analog domain, enabling the energy from the interference to be diverted for harvesting during the digitization and decoding of the information-bearing signal. We also show that this method provides wireless communications devices with not only enhanced information capacity, but also enhanced secrecy capacity in a broadcast channel. By using the proposed method, we can increase the overall channel capacity in a broadcast system beyond the current state-of-the-art for wireless broadcast channels, which is based on static coding techniques. Further, we also increase the overall secrecy capacity of the system by enabling secrecy for each user in the system. In practical terms, this results in higher-rate, confidential messages delivered to multiple devices in a broadcast channel for a given power constraint. Finally, we corroborate these claims with simulation and experimental results for the proposed method.

New Method for Directional Modulation using Beamforming:
Applications to Simultaneous Wireless Information and Power Transfer and Increased Secrecy Capacity

Randy Matthew Yamada

GENERAL AUDIENCE ABSTRACT

The proliferation of connected devices has driven wireless communications into commercial, military, industrial, and personal systems. It is unreasonable to expect privacy and security to be inherent in these networks given the spatial density of these devices, limited available resources, and the broadcast nature of wireless communications systems. Communications for these systems need not only sufficient information capacity, but also the assurance that the available information capacity remains confidential while typically maintaining small size, light weight, and minimized power consumption. With increasing crowding of the electromagnetic spectrum due to the numerous connected devices, interference between them must be leveraged as an available resource.

This work develops a new method for electrically steering an array of antennas to overlay or encode information onto a signal in a way that is direction-dependent and provides wireless communications devices with enhanced security and the ability to simultaneously communicate and harvest energy from interfering devices. We propose a method that optimizes a set of time-varying array steering vectors to enable direction-dependent modulation, thus exploiting a new degree of freedom in the traditional space-time-frequency paradigm. We formulate the selection of steering vectors as a convex optimization problem for rapid computation given arbitrarily positioned array antenna elements in three dimensions.

We show that this method allows us to separate interference from an information-bearing signal in the analog domain, enabling the energy from the interference to be diverted for harvesting during the digitization and decoding of the information-bearing signal. We also show that this method provides broadcast wireless communications devices with not only increased information capacity, but also assured secrecy. By using the proposed time-varying method, we can increase the overall channel capacity in a broadcast system beyond the current state-of-the-art, which is based on static encoding techniques. Further, we also increase the overall secrecy capacity of the system by ensuring that each user in the system receives separate and confidential signals. In practical terms, this results in higher-rate, confidential messages delivered to multiple devices in a broadcast channel for a given power constraint. Finally, we corroborate these claims with simulation and experimental results for the proposed method.

To my family

Acknowledgements

I would first like to thank my advisor, Dr. Lamine Mili, for his enduring support in my education and growth over the years, leading to the completion of this research. I would also like to thank Dr. T. Charles Clancy, Dr. R. Michael Buehrer, and Dr. Serkan Gugercin for participating in my committee. I would like to extend great appreciation to Dr. Allan Steinhardt for nearly a decade of mentorship and to Dr. Joshua Conway for encouragement and support in developing this research. I owe my academic and professional growth to each of you and more.

I must also thank my friends and family for providing me with a strong foundation. I would like to especially thank mom, dad, Roger, and Kevin for the literal lifetime of optimism. I would also like to recognize Phoebe and Petra, for being the reasons that I push myself. Finally, I owe the entirety of this work to my wonderful wife, Esther, whose dedication to our family is the only reason I could complete this work.

Contents

List of Figures

List of Tables

Chapter 1

Introduction

Beamforming is often implemented in capable communications systems to increase the efficiency and security of a communications link by spatial filtering [1], [2]. This technique enables a transmitter (the source) to focus energy in the direction of an intended receiver (the destination), and minimize the energy transmitted in the direction of an unintended receiver or Eavesdropper. Reciprocally, spatial filtering enables a receiver to focus in the direction of the transmitter, and de-focus or null interference from other directions occupying the same frequency bandwidth as the communications link, called co-channel interference. Generally speaking, increasing (respectively decreasing) the signal-to-interference-plus-noise ratio (SINR) decreases (respectively increases) the rate of bit errors in the information signal recovered at the receiver. As such, a common approach to providing security for a communications link at the physical layer (PHY-layer) is to minimize the power spectral density of the information-bearing signal

transmitted towards potentially vulnerable directions, or to specifically steer a null in the direction of an Eavesdropper if it is known [2]. Similarly, a null is placed in the direction of received co-channel interference to minimize the impact of co-channel interference on the desired signal [1]. Other, more complex beamforming techniques have been explored for multiple input, single output (MISO) systems intended to reduce the SINR to provide secrecy [3], [4]. For example, the Artificial Noise or Null Space method for MISO systems allocates some transmit power from the information-bearing signal to a pseudo-random noise signal projected into the null space between the transmitter and receiver, which is partially directed at the Eavesdropper [5]. In practical use, this method requires allocation of 50% or more of the transmit power to transmitting only noise as shown in [5]; however, as demonstrated in [6], the Artificial Noise or Null Space method for MISO systems can be overcome by an Eavesdropper using a steerable antenna array.

Let us first consider a Wireless Communications Device with an antenna array serviced by two additional devices: a Base Station transmitting an information-bearing signal and a Wireless Power Transfer System transmitting a signal intended for power harvesting. The Base Station and the Wireless Power Transfer System are spatially separated, in the far-field, and within line-of-sight with respect to the Wireless Communications Device. We seek to enable the Wireless Communications Device to receive the information-bearing signal uninterrupted from the Base Station while simultaneously harvesting power from the Wireless Power Transfer System, given that both signals occupy the same time-frequency sub-space. Such modulation is more effective than nulling either the information-bearing signal or the power transfer signal to access the other, because they can be accessed simultaneously.

Let us next consider a Wireless Communications Device with an antenna array communicating with a counterpart Receiver while in range of an Eavesdropper. The Receiver and Eavesdropper are spatially separated, in the far-field, and within line-of-sight with respect to the Wireless Communications Device. We seek to prevent the Eavesdropper from successfully demodulating and decoding the information-bearing signal transmitted by the Wireless Communications Device. Furthermore, we seek to simultaneously transmit an independently controlled information-bearing signal to the Eavesdropper. Such a technique is more effective than steering a null in the direction of the Eavesdropper because it allows us to achieve security that cannot be overcome by increased sensitivity, reduced range, and larger aperture, to name a few. It ensures that the Eavesdropper receives and decodes an arbitrary bit stream that is completely independent of the original transmitted signal, but may still contain valid data and pass valid redundancy and error correction checks, which is referred to as a spoofed signal hereafter. The original signal is then unrecoverable from the wireless medium.

Finally, let us consider a Wireless Communications Device with an antenna array communicating with two legitimate counterpart Receivers. The Receivers are spatially separated, in the far-field, and within line-of-sight with respect to the Wireless Communications Device. We seek to transmit independent and confidential messages to each Receiver with the maximum possible capacity per bandwidth over a broadcast channel. That is, we expect that each Receiver is within range of the Wireless Communications Device and capable of receiving the signal intended for the other Receiver. From the perspective of the transmitter, we seek to maximize the secrecy capacity of the entire system.

1.1 Research Objectives

In this dissertation, we seek to develop a new array beamforming method for communications devices based on the concepts of direction-dependent modulation. The proposed beamforming method should enable simultaneous wireless information and power transfer that outperforms other switching and multiplexing methods [7]–[13]. The proposed beamforming method should also natively provide secrecy at the PHY-layer in a broadcast channel at a reduced implementation cost compared to existing methods [5], [14]. The implementation cost should consider the computational burden of steering vector formation compared to other methods [14], [15], as well as the analog hardware required to implement the beamformer compared to other methods [16]. Finally, the proposed beamforming method should enable enhanced secrecy capacity in a wireless broadcast channel beyond the current state-of-the-art [17].

1.2 Literature Review of Directional Modulation

Direction-dependent modulation, also called directional modulation, is a new approach to spatial filtering. It was initially proposed as time-varying array parameters such as current distribution, phase center, or physical dimensions to observe a time-varying, spatially-varying array response for radar [18], [19], and later implemented by rapidly commutating a receiver among array elements [20], [21] in an effort to overlay a known modulation to energy incident away from broadside to the array. Directional modulation implemented by on-off keying the antenna elements has been proposed for multipath mitigation in communications systems [22] and the method has been refined through optimization of key performance parameters, such as bit error

rate [23]–[25]. Directional modulation was later proposed and demonstrated by perturbing the near-field of the antenna for PHY-layer security, negating the need for an array [26]–[28]. Recent work has proposed implementing directional modulation by beamforming for PHY-layer security [14], [29], [16], [30], [15], [31].

1.2.1 Pioneering Work on Time Modulated Arrays

The concept of time-varying the characteristics of an antenna element or array of elements to increase information handling capacity or enhance the array gain pattern response was gaining traction in the late 1950s, first proposed by Shanks and Bickmore [18]. Shanks and Bickmore suggest a variety of parameters be modulated, including physical dimensions, current distribution, frequency, or phase center location [18]. This technique was demonstrated to reduce array sidelobe levels by sequentially activating pairs of elements about the array phase center [19]. These approaches exploit spatial and temporal degrees-of-freedom to manipulate array response characteristics.

1.2.2 Directional Modulation by Commutating Among Antenna Array Elements

Directional modulation is later published in 1964 [20], and identifies the potential of distinguishing targets in the sidelobe of a radar system from targets in the main lobe by inducing a Doppler shift in the signals off of the main axis of the array. This is proposed in by continuously time-varying the phase center of the array along a path normal to the direction of maximum radiation of the antenna array, instantiated by a pair of horn antennas rapidly scanning across a

reflector or as a switched array of antenna elements [20]. This differs from [19] in that symmetry about the array phase center is not preserved. The Naval Research Laboratory (NRL) published study and simulation of this concept nearly 20 years later, claiming the added value of limiting the spectral sidelobes of a transmitted signal [21]. They also identified implementation issues in synchronizing the directional modulation with the radar pulses and the grating lobes that exist when the array is switched to a spatially under-sampled configuration [21]. In the late 1980s, a technique designed to separate multipath signals from the direct-path signals called induced directional frequency modulation (IDFM) was introduced from Massachusetts Institute of Technology (MIT) [22]. Though this technique was initially modeled using a physically moving antenna, it is later instantiated as a switched array of antenna elements, or on-off keyed elements [22] for the sake of practicality. Further, the IFDM technique is recognized as able to be used to induce direction-dependent frequency spreading for interference reduction and transmitter camouflage.

After many years without significant work on time-modulated linear arrays (TMLAs), a number of publications have emerged focused on beam pattern control through the optimization of array element switch-on time sequences [23]–[25], [32]–[35]. These publications describe the numerical optimization of element switch-on time to suppress sideband radiation and simultaneously optimize the beampattern through commutation of the antenna elements. Researchers from the University of Electronic Science and Technology in China formalized directional modulation for communications, in what they termed a “4D array”, using the previously described array commutation technique for suppression of side-lobes [36]. This was later demonstrated in hardware [37], and analyzed using signal to noise ratio (SNR) as a performance

benchmark [38]. Researchers at the University of Texas at Austin extend the original array time-modulation concept to millimeter-wave arrays, which are expected to be significantly more dense in practical applications based on the wavelength [39]. They describe design methods for the selection of antenna array elements and commutation sequences for optimized sidelobe response [39].

1.2.3 Directional Modulation by Near-field Direct Antenna Modulation

Approximately 20 years after directional modulation was initially applied to communications systems [22], a team from the California Institute of Technology (CalTech) introduces direction-dependent modulation in a communications transmitter for security purposes [26]. It should be noted that this is the first appearance in the literature of using directional modulation for wireless communications security. Rather than mitigating interference or introducing Doppler shifts, the researchers at CalTech purposefully perturb the array in the near-field to alter the transmitted communications symbol constellation directions away from the intended receiver by introducing and modulating nearby structures such as reflecting dipoles [26]. The near-field direct antenna modulation technique is further developed and explored in the literature in [40]–[43].

Several researchers have proposed procedures and designs to implement directional modulation by near-field direct antenna modulation. Researchers from the University of Illinois at Urbana-Champagne (UIUC) implemented this technique in a phased array of reconfigurable elements, using square spiral printed microstrip antennas with switches that reconfigure the element pattern at will to enable directional modulation [27]. Similarly, researchers from Nanjing

University used separately synthesized antenna beams for the in-phase and quadrature signals to implement directional modulation by alternating between beams [28].

1.2.4 Directional Modulation by Phased Array

Researchers from University of Illinois Urbana-Champaign (UIUC) have led increased activity in directional modulation since 2009. They introduce a technique for directional modulation using a phased array by properly selecting array steering vectors to enhance wireless communications security in a binary phase shift keying (BPSK) system [14]. A key contribution of [14] is the concept of intentionally sending an incorrect symbol in the undesired direction, rather than a reduced signal-to-noise ratio (SNR) or a random degraded symbol, which narrows the spatial region where the signal can be properly demodulated. Researchers at UIUC also experimentally demonstrated the directional modulation array for quadrature phase shift keying (QPSK) [29] and simulated the array for 16-QAM [16]. The implementation only uses element phase shifting and arithmetic computation of results, but a later publication describes an optimization algorithm for steering vector determination that minimizes the sum of the squares of the distances between constellation points for wireless communications security [16].

Researchers from Aalborg University later formalized directional modulation into a space-time array processing framework, showing that a series of steering vectors could be derived that superimpose a varying interfering component orthogonal to the transmit direction at the modulation rate to provide additional security over conventional noise-injection techniques [6]. This concept was experimentally demonstrated using a Fourier Rotman lens beamforming network in [44]. Optimization methods for selecting array steering vectors to synthesize a transmitter

capable of directional modulation are described in [15] for a four-element uniform linear array using QPSK modulation. A Fourier transform method that ensures recoverable data in the desired direction while maximizing bit error rate in other directions for transmitter synthesis is described in [45]. Another technique is communications security-focused and recommends optimization of the Symbol Equivocation Metric (SEM), which describes the symbol constellation zones and their intersections causing bit errors [31].

Beginning in 2013, researchers from Queens University of Belfast proposed and demonstrated a synthesis strategy based on bit error rate-driven optimization for directional modulation for the security of wireless communications [30], [46]. They also proposed a transmitted far-field power pattern-based optimization criteria to establish communications security [47], [48], and extended the directional modulation to a retrodirective array [49], further providing wireless communications security.

Researchers from Nanjing University in China showed that directional modulation could be used not only to focus the information being sent in a particular direction, but could be used to enable direction finding by a receiver, even with only a single antenna [50]. They used the original antenna commutating techniques to create the direction-dependent modulation, and extended use to phased array radars through work showing that matched filters could be developed with strong angle-dependent response [51].

1.2.5 Direct Sequence Spread Spectrum Modulation Induced by Directional Modulation

Researchers have suggested that array elements could be time-modulated to implement direct-sequence spread spectrum for communications security [28]. In 2011, researchers from Nanjing University in China showed that directional modulation layered onto direct-sequence spread spectrum provided security by narrowing the physical region over which the correlation sequence is recoverable [50], [52].

1.3 Contributions

Following this line of research, we develop a new array beamforming method for communications devices based on the concepts of direction-dependent modulation in this dissertation. The proposed beamforming method is formulated as a convex optimization problem, which reduces the computational burden of steering vector formation compared to other methods [14], [15]. It is also constrained to be implemented as a passive beamformer, in contrast to other techniques [16]. The proposed beamforming method provides PHY-layer secrecy with better efficiency than existing methods [5], [14], [15] and enables simultaneous wireless information and power transfer using a common time-frequency subspace, outperforming switching methods [7]–[13]. Furthermore, the proposed beamforming method enables enhanced secrecy capacity in a wireless broadcast channel beyond the current state-of-the-art [17].

In contrast to the literature review summarized in this dissertation, the proposed beamforming method exhibits improvements in the formulation, implementation, application, and performance of directional modulation for systems. First, and unique compared to the published literature, the proposed method for directional modulation is formulated using an array processing construct that allows for computation of steering vectors for arbitrary volumetric arrays, rather than uniformly spaced linear or planar arrays. Second, the proposed method for directional modulation is implemented as an overlay modulation by inducing direction-specific phase shift keying (PSK) modulation rather than by optimizing the transmitted constellation for individual symbol spoiling. This allows such a system to be retro-fitted onto a conventional array by enabling time-varying beamforming, allows for multicasting, and is suitable for use during reception. The proposed method is also distilled into a convex optimization function for rapid computation of optimal steering vectors that can be implemented in a completely passive beamformer. This is in contrast to other techniques that propose non-convex algorithms for steering vector determination, such as genetic algorithms, that risk convergence on local minima [14], [30], [48].

We also propose a novel application for the proposed beamforming method implemented during reception. By overlaying received signals with the appropriate direction-dependent modulation sequences, we enable the separation of energy within the same time and frequency sub-space from the desired information-bearing signal in the analog domain, such that the separated energy can be harvested. It enables selective spectral manipulation of co-channel interference without corrupting the desired information-bearing signal. Using a simple diplexer, we can then isolate the information-bearing signal from a large fraction of the energy from the interfering signal, such as a wireless power transfer signal, which now occupies a different

frequency band. This technique can enhance the performance of far field directive power beaming compared to techniques proposed in the literature such as time domain switching [7], power splitting [7]–[10], antenna switching [11], [12], and spatial switching [13], which seek an optimal allocation of energy from a single transmitter to information and power harvesting circuits using the available degrees of freedom. In contrast, our method enables the analog isolation of interfering energy from the same time and frequency sub-space as the information signal. Thus, multiple, spatially separated transmitters can reuse the same time and frequency sub-space to convey both information and power to a single receiver. Consequently, our technique enables a denser frequency re-use pattern and enables the re-use of the same spectrum for both communications and wireless power transfer. The proposed method is the first implementation of directional modulation for harvesting of co-channel interference.

In addition to simultaneous wireless information and power transfer when implemented during reception, the proposed method can be applied during transmission to provide PHY-layer secrecy for wireless communications devices. We can consider the proposed beamforming method as overlaying direction-dependent modulation on a transmitted signal. Rather than minimizing the signal energy transmitted away from the intended receiver, we selectively transform the energy to natively provide PHY-layer secrecy in a broadcast channel. A novel contribution of this dissertation is that the proposed method can be used to provide PHY-layer secrecy at a reduced implementation cost compared to existing methods [5], [14]–[16], including in the computational burden of steering vector formation and the analog hardware required to implement the beamformer. Finally, the increased efficiency of the proposed beamforming method in terms of the transmitter power sacrificed to implement the proposed beamforming method can enable an

overall increase in the sum-rate secrecy capacity in a wireless broadcast channel compared to the currently accepted state-of-the-art [17], which is a major contribution of this work.

1.4 Dissertation Organization

The remainder of this dissertation is organized into three parts. In Chapter 2, we present a novel phased array beamforming method to implement direction-dependent modulation. In Chapters 3 and 4, we develop applications of the method developed in Chapter 2, intended for use in wireless communications systems. In Chapters 5 and 6, we summarize simulation and experimental results that demonstrate the feasibility and performance of the technique developed in Chapter 2.

In Chapter 2, we design a time-varying array steering vector following a typical array processing construct by defining a series of constraints that implement directional modulation. We achieve this by designing a BPSK overlay modulation able to independently address two different users, or two directions of interest. We introduce design methods to extend this technique to additional users, additional directions of interest, and higher order PSK or QAM schema. To design a passive beamformer, we impose a practical constraint that none of the elements in the steering vectors can have net gain. Further, we define a design objective that maximizes the array response in the directions of interest for overall implementation efficiency with the goal of outperforming the implementation cost of Time-division multiplexing (TDM). Lastly, we formulate the beamforming technique as a convex optimization problem, allowing for rapid computation of a globally optimal solution with commercially-available solvers.

In Chapter 3, we study the application of the proposed beamforming technique for simultaneous wireless information and power transfer. We implement the proposed beamforming technique on receive to selectively modulate co-channel interference corrupting an information signal. We explore methods to isolate the co-channel interference in the analog domain, such that the energy contained in the interference can be harvested by the receiver. We compare this method to publications, noting that it provides access to energy in the co-channel subspace, which has not been previously proposed. Specifically, we note that this method can be used to re-use spectrum for wireless information and power transfer without simply dividing resources, as is done in TDM, frequency division multiplexing (FDM), or by power splitting.

In Chapter 4, we study the application of the proposed beamforming technique for physical layer security in wireless communications systems. First, we implement the proposed beamforming technique on transmit to selectively modulate the transmitted signal into a spoofed signal in directions away from the intended receiver. We compare the achievable secrecy capacity of this method to other wireless physical layer secrecy techniques, including the Artificial Noise or Null-Space method. Given that the spoofed signal generated can be arbitrarily independent of the intended signal, we explore the capability to transmit two completely independent signals to two different users over a broadcast channel. We show that the proposed method can increase the secrecy capacity for two users in a wireless broadcast channel beyond the currently accepted state-of-the-art [17].

In Chapter 5, we summarize simulation results from various studies. First, we explore the implementation cost of the proposed beamforming method, benchmarked by the average array gain in the directions of interest subject to each of the steering vectors. We analyze various array

element spacing and geometries of receivers. Next, we present a summary of simulation results for the achievable sum-rate secrecy capacity for two users in a wireless broadcast channel. Again, we analyze various array element spacing and geometries of interest, and compare the results to the currently accepted state-of-the-art, known as Dirty Paper Coding. We follow this with a summary of simulation results for simultaneous wireless information and power transfer using the proposed technique.

In Chapter 6, we summarize the procedures for and results of laboratory experimentation carried out to validate the proposed technique. First, we describe at length the experimental setup, plan, and rigorous calibration. Next, we provide a series of results with the express purpose of 1) verifying the quality of the direction-dependent modulation overlay using the proposed beamforming technique and 2) measuring the implementation cost of the proposed beamforming technique.

We conclude this dissertation in Chapter 7 by proposing future work, including further analyses of the proposed method, additional applications of the proposed method, and practical limitations of the proposed method. We suggest further analysis, linearization, and performance characterization of the proposed beamforming method using non-uniform array layouts. We recommend further exploration of additional applications, such as multi-rate, multiple access communications. We also propose further analysis and experimentation investigating the practical implementation of the proposed method, such as imperfect synchronization, imperfect hardware implementation, and imperfect knowledge of the channel state information and channel model.

Chapter 2

A Proposed Method for Directional Modulation Using Beamforming

In this Chapter, we develop a novel method for directional modulation using phased arrays. We design a set of time-varying array steering vectors following a typical array processing construct by defining a series of constraints that control the direction-dependent modulation overlay. First, we design a BPSK overlay modulation able to independently address two different users located in two different directions relative to the array. Next, we design a passive beamformer to implement the overlay modulation by imposing a practical constraint that none of the steering vector elements can require net gain. Then, we introduce a design objective that maximizes the array response in the directions of interest for overall implementation efficiency with the goal of outperforming the implementation cost of other multiple access methods. We then formulate the

beamforming technique as a convex optimization problem, allowing for rapid computation of globally optimal steering vectors given the defined constraints. Lastly, we introduce design methods to extend this technique to support additional users and higher order PSK or QAM modulation schema.

2.1 Array Processing Construct and Signal Model

Invoking the array processing construct described in [1], we define the array manifold, $\boldsymbol{V}$, expressed as

$$\boldsymbol{V} = \begin{bmatrix} e^{-j\hat{\boldsymbol{k}}_0^T \boldsymbol{p}_0} & e^{-j\hat{\boldsymbol{k}}_1^T \boldsymbol{p}_0} & \cdots & e^{-j\hat{\boldsymbol{k}}_{R-1}^T \boldsymbol{p}_0} \\ e^{-j\hat{\boldsymbol{k}}_0^T \boldsymbol{p}_1} & e^{-j\hat{\boldsymbol{k}}_1^T \boldsymbol{p}_1} & \cdots & e^{-j\hat{\boldsymbol{k}}_{R-1}^T \boldsymbol{p}_1} \\ \vdots & \vdots & \ddots & \vdots \\ e^{-j\hat{\boldsymbol{k}}_0^T \boldsymbol{p}_{N-1}} & e^{-j\hat{\boldsymbol{k}}_1^T \boldsymbol{p}_{N-1}} & \cdots & e^{-j\hat{\boldsymbol{k}}_{R-1}^T \boldsymbol{p}_{N-1}} \end{bmatrix}. \quad (1)$$

The array manifold geometrically describes the array, including the locations of N array elements in a Cartesian coordinate system,

$$\boldsymbol{p_n} = \begin{bmatrix} x_n \\ \mathrm{y_n} \\ z_n \end{bmatrix}, \quad (2)$$

and the array response toward R different directions from the geometric center of the array. Directions relative to the geometric center of the array are expressed as a unit vector based on angles from the positive $\hat{x}$ and $\hat{z}$ axes (θ and ϕ, respectively), as follows:

$$\widehat{\boldsymbol{a}}_{\boldsymbol{r}} = \begin{bmatrix} \sin(\theta_r)\cos(\phi_r) \\ \sin(\theta_r)\sin(\phi_r) \\ \cos(\theta_r) \end{bmatrix}. \tag{3}$$

One assumption underlying the proposed method is that all waves considered are plane waves propagating in a homogeneous medium, such that the wavenumber corresponding to a direction from the geometric center of the array is given by $\widehat{\boldsymbol{k}}_{\boldsymbol{r}} = \frac{2\pi}{\lambda}\,\widehat{\boldsymbol{a}}_{\boldsymbol{r}}$, where λ is the operating wavelength.

Continuing to follow a classical array processing construct [1], we exercise individual phase and amplitude control by applying a complex weight at each element in the array. The vector of complex weights at a given time t is denoted by $\boldsymbol{w}(t)$, called the weight vector or the steering vector. We compute the time-varying complex channel transfer function between the array and a point in the far field of the array in the direction $\widehat{\boldsymbol{k}}$ under the array steering vector $\boldsymbol{w}$ using the appropriate column of $\boldsymbol{V}$, $\boldsymbol{v}_{\boldsymbol{k}}(\widehat{\boldsymbol{k}})$, as

$$H(\boldsymbol{w}, \widehat{\boldsymbol{k}}, t) = \boldsymbol{v}_k^H(\widehat{\boldsymbol{k}})\mathbf{w}(t). \tag{4}$$

We assume that the channel under a given steering vector, in each direction, for a given time interval is static and ignore any other time-varying effects, such as those introduced by motion or the environment. The channel transfer function $H(\boldsymbol{w}, \widehat{\boldsymbol{k}}, t)$ is then manipulated as a function of time by using multiple steering vectors to overlay a modulation on existing signals. The minimum number of complex steering vectors, S, required to achieve the desired, independent modulation depends on the number of directions of interest, R, the modulation format, the desired array performance (i.e., array gain), and the modulation quality (e.g., modulation error ratio).

Throughout this chapter, we address the case where there are two directions of interest. We form a matrix of S steering vectors, $\boldsymbol{W} \in \mathbb{C}^{N\times S}$, as

$$\boldsymbol{W} = [\boldsymbol{w}_0 \quad \cdots \quad \boldsymbol{w}_{S-1}] = \begin{bmatrix} w_{0,0} & \dots & w_{S-1,0} \\ w_{0,1} & \dots & w_{S-1,1} \\ \vdots & \ddots & \vdots \\ w_{0,N-1} & \cdots & w_{S-1,N-1} \end{bmatrix}. \tag{5}$$

We also explicitly assume a narrowband, line-of-sight channel model and ignore other effects, such as propagation, since they could be compensated for separately.

2.2 Applying Directional Modulation

We seek to determine a matrix of array steering vectors, $\boldsymbol{W}$, that can independently modulate the channel $H(\boldsymbol{w}, \widehat{\boldsymbol{k}}, t)$ in different directions, $\widehat{\boldsymbol{k}}$, without modifying the array manifold, $\boldsymbol{V}$. The minimum size of the array steering vector matrix, $\boldsymbol{W}$, depends on the number of independently controlled elements in the array, N, and the number of desired independently modulated directions, R. In this chapter, we specifically consider Binary Phase-Shift Keying (BPSK) modulation for simplicity; however, this method is applicable to a variety of modulation schemes, including higher-order M-ary phase-shift keying (PSK) modulation or quadrature amplitude modulation (QAM).

For BPSK modulation and two directions of interest, denoted $\widehat{\boldsymbol{k}}_{\boldsymbol{0}}$ and $\widehat{\boldsymbol{k}}_{\boldsymbol{1}}$ (though $\widehat{\boldsymbol{k}}_{\boldsymbol{r}}$ is a wavenumber, we shall refer to it as a direction throughout this dissertation), we require a pair of array steering vectors, denoted $\boldsymbol{w}_{\boldsymbol{0}}$ and $\boldsymbol{w}_{\boldsymbol{1}}$. In an abuse of notation, we denote the complex channel

in the direction $\widehat{\boldsymbol{k}}_r$ under steering vector $\boldsymbol{w}_s$ as $\boldsymbol{H}_{r,s}$. We can express the $R \times S$ matrix of channels by

$$\boldsymbol{H} = \begin{bmatrix} H_{0,0} & H_{0,1} \\ H_{1,0} & H_{1,1} \end{bmatrix} = \boldsymbol{V}^H \boldsymbol{W}. \tag{6}$$

For this example, we seek $\{\boldsymbol{w_0}, \boldsymbol{w_1}\}$ such that by alternating between steering vectors we can selectively induce a symbol transition in the direction $\widehat{\boldsymbol{k}}_{\boldsymbol{0}}$ independently from the direction $\widehat{\boldsymbol{k}}_{\boldsymbol{1}}$. Concisely, we seek $\{\boldsymbol{w_0}, \boldsymbol{w_1}\}$ such that

$$\begin{gathered} \arg\left(\boldsymbol{v}_k^H\left(\widehat{\boldsymbol{k}}_1\right)\boldsymbol{w_1} * \left(\boldsymbol{v}_k^H\left(\widehat{\boldsymbol{k}}_1\right)\boldsymbol{w_0}\right)^*\right) = \pi, \text{ and} \\ \arg\left(\boldsymbol{v}_k^H\left(\widehat{\boldsymbol{k}}_0\right)\boldsymbol{w_1} * \left(\boldsymbol{v}_k^H\left(\widehat{\boldsymbol{k}}_0\right)\boldsymbol{w_0}\right)^*\right) = 0. \end{gathered} \tag{7}$$

We can formalize two requirements to induce time-varying, overlay modulation in the arbitrary direction $\widehat{\boldsymbol{k}}_{\boldsymbol{1}}$ independently from the direction $\widehat{\boldsymbol{k}}_{\boldsymbol{0}}$. First, we require the ability to achieve a phase shift of approximately π radians in the wireless channel in the direction $\widehat{\boldsymbol{k}}_{\boldsymbol{1}}$ when switching from array steering vector $\boldsymbol{w_0}$ to array steering vector $\boldsymbol{w_1}$, which can be written as a constraint expressed as

$$|H_{1,0} * exp(-j\pi) - H_{1,1}| \leq \varepsilon, \tag{8}$$

where ε denotes a parameter that controls the resulting modulation error ratio (MER), signal-to-interference-plus-noise ratio (SINR), and degradation of the overall bit error rate. For the sake of example, by choosing $\varepsilon = 0.05$ we can achieve a worst-case modulation error ratio of $26dB$ for the overlaid symbol and worst case modulation error ratio of $-6dB$ for the original symbol.

Simultaneously, we require a phase shift of approximately zero radian in the arbitrary direction $\widehat{\boldsymbol{k}}_{\boldsymbol{0}}$ when switching from array steering vector $\boldsymbol{w}_{\boldsymbol{0}}$ to array steering vector $\boldsymbol{w}_{\boldsymbol{1}}$, which can be written as

$$\left|H_{0,0} - H_{0,1}\right| \leq \varepsilon. \tag{9}$$

As above, a modest $\varepsilon = 0.05$ introduces a worst-case modulation error ratio of $26dB$ to the channel. With this pair of array steering vectors, $\boldsymbol{w}_{\boldsymbol{0}}$ and $\boldsymbol{w}_{\boldsymbol{1}}$, that can satisfy the stated requirements, we are able to independently control BPSK modulation in the directions $\widehat{\boldsymbol{k}}_{\boldsymbol{1}}$ and $\widehat{\boldsymbol{k}}_{\boldsymbol{0}}$.

2.3 Efficiency of Directional Modulation

To practically implement directional modulation, we impose three constraints. First, we allow for some maximum allowable implementation loss, as shown in (8) and (9). Second, we require this proposed method to be implemented in a passive beamformer with fixed transmit power using only phase delays and amplitude attenuation for each element, or $\left|\boldsymbol{W}_{n,s}\right| \leq 1$. This model is physically accurate for communication systems which tend to operate in or near saturation conditions, where phase embeds information, but no amplitude modulation is desired for SNR considerations. This differs from other work that requires the array steering vectors to be of unit magnitude [14] and work that requires the real and imaginary parts of the complex array steering vectors to each be less than unit magnitude [53], which limits the available solution space and results in steering vectors that enable directional modulation but at a significant cost to array gain. Lastly, given that this is a broadcast system, we attempt to maximize the sum-rate capacity

without minimizing or zeroing capacity to a disadvantaged user. That is, we wish to maximize the square of the norm of every wireless channel transfer function, $\left|\boldsymbol{H}_{r,s}\right|^2$.

The array steering vector matrix has a direct impact on the array beam patterns and resulting link efficiency of the wireless communication system. We seek to constrain the array beam pattern loss in each of the R directions subject to each of the S array weight vectors, such that the beam pattern gain is greater than some factor ξ of the maximum achievable beam pattern gain. The square of the norm of the wireless channel transfer function, $\left|\boldsymbol{H}_{r,s}\right|^2$, is equivalent to the array beam pattern in each direction, $\widehat{\boldsymbol{k}}_{\boldsymbol{r}}$, subject to the array weight vector, $\boldsymbol{w}_{\boldsymbol{s}}$. Formally, we have

$$\left|\boldsymbol{H}_{r,s}\right|^2 \geq \xi * \max_{s,r}\left|\boldsymbol{H}_{r,s}\right|^2. \tag{10}$$

Many adaptive array processing techniques select an array steering vector to maximize the output signal-to-noise ratio in a desired direction, typically for an intended receiver, and by minimizing the array gain in undesired directions, typically towards interferers or unintended receivers [1]. We consider the product of the array beam patterns in each direction under each steering vector to ensure that there are no nulls placed under any array steering vector or in any direction; however, we recognize that there are scenarios where the maximum achievable array gain is not necessarily desired.

2.4 Array Steering Vector Formulation

2.4.1 Passive Beamformer

One contribution of this research to the current state-of-the-art consists of conforming the objectives for directional modulation into a convex optimization problem to enable rapid selection of the solution matrix of passive steering vectors $\boldsymbol{W}$ using readily available solvers. First, for practicality, $\boldsymbol{W}$ is constrained such that each individual complex element weight, $\boldsymbol{W}_{n,s}$, has a norm of less than or equal to unity. Thus, the array can be implemented with phase shifters and attenuators and do not require additional gain. Formally, we define the convex subset Ω as

$$\Omega = \left\{\boldsymbol{W}: \left|\boldsymbol{W}_{n,s}\right| \leq 1, \forall n \in [0, \dots \mathrm{N}-1],\ \forall s \in [0, \dots, S-1]\right\}. \tag{11}$$

2.4.2 Time-Varying Beamformer

A summary of the operation for executing directional modulation is shown in the state diagram in Figure 2.1. We seek an appropriate set of steering vectors, $\boldsymbol{W}$, capable of independently modulating the wireless channel transfer function in two different directions, $\widehat{\boldsymbol{a}}_{\boldsymbol{m}}$ and $\widehat{\boldsymbol{a}}_{\boldsymbol{n}}$. In the case of two users, BPSK modulation, and the steering vector solution $\boldsymbol{W} = [\boldsymbol{w_0}, \boldsymbol{w_1}]$, we can specify two different states for the array – one where the steering vector $\boldsymbol{w_0}$ is applied, and one where the steering vector $\boldsymbol{w_1}$ is applied. As indicated in Figure 2.1 for the case of BPSK, we can choose to or choose not to induce a symbol transition from either state in the direction $\widehat{\boldsymbol{a}}_{\boldsymbol{n}}$, which represents half of the required control. Since we have control of the transmitted data, $d_m(t)$, we

inherit the other half of the required control, i.e., by inverting $d_m(t)$ we can selectively modulate the channel in the direction $\hat{\boldsymbol{a}}_{\boldsymbol{m}}$ instead of $\hat{\boldsymbol{a}}_{\boldsymbol{n}}$.

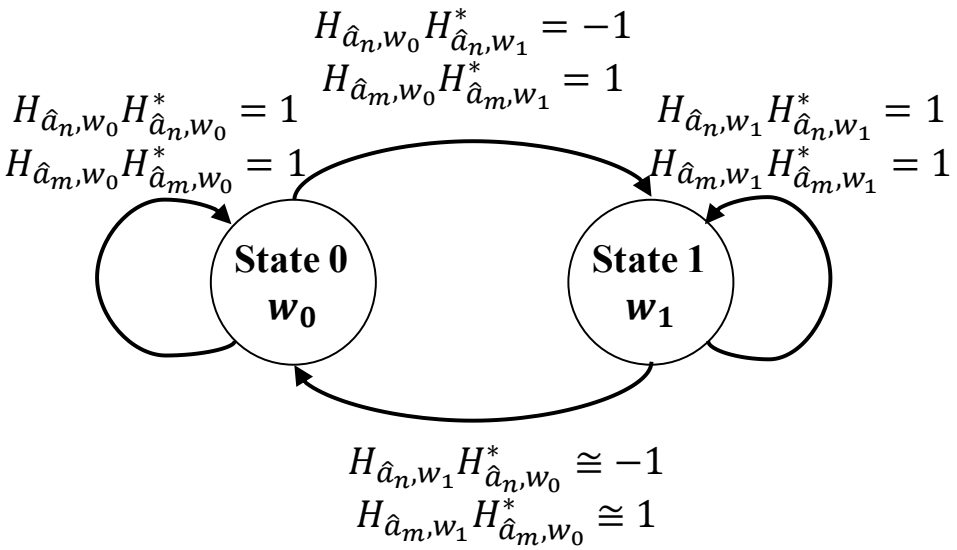

Figure 2.1: A state diagram of the array control system for directional modulation is shown. Here, we specify two different states for the array – one where the steering vector $\boldsymbol{w_0}$ is applied, and one where the steering vector $\boldsymbol{w_1}$ is applied. The desired modulation overlay induced in the directions of interest, $\hat{\boldsymbol{a}}_{\boldsymbol{m}}$ and $\hat{\boldsymbol{a}}_{\boldsymbol{n}}$ are indicated for each transition for the two User case with BPSK overlay modulation. The transitions shown in this state diagram represent half of the required control for directional modulation; the other half of the required control is inherited by inverting the input signal to the array.

2.4.3 Achieving Direction-Dependent Modulation

To achieve direction-dependent modulation, we define a set of constraints, given in (8) and (9), as the convex subset Ψ, expressed as

$$\Psi = \left\{ \boldsymbol{W}: \begin{bmatrix} \boldsymbol{v}_k^H(\hat{\boldsymbol{k}}_{\mathbf{m}}) & -\boldsymbol{v}_k^H(\hat{\boldsymbol{k}}_{\mathbf{m}}) \\ -\boldsymbol{v}_k^H(\hat{\boldsymbol{k}}_{\boldsymbol{m}}) & \boldsymbol{v}_k^H(\hat{\boldsymbol{k}}_{\mathbf{m}}) \\ \boldsymbol{v}_k^H(\hat{\boldsymbol{k}}_{\boldsymbol{n}}) & \boldsymbol{v}_k^H(\hat{\boldsymbol{k}}_{\boldsymbol{n}}) \\ -\boldsymbol{v}_k^H(\hat{\boldsymbol{k}}_{\boldsymbol{n}}) & -\boldsymbol{v}_k^H(\hat{\boldsymbol{k}}_{\boldsymbol{n}}) \end{bmatrix} \begin{bmatrix} \boldsymbol{w_0} \\ \boldsymbol{w_1} \end{bmatrix} \leq \begin{bmatrix} \varepsilon \\ \varepsilon \\ \varepsilon \\ \varepsilon \end{bmatrix} \right\}. \tag{12}$$

These modulation requirements can be easily extended to higher-order modulation and multiple directions of interest by considering all the desired channel states and transitions. Examples for higher-order modulation and additional directions are provided later in this Chapter.

Given the convex subset $\Omega \cap \Psi$, we form the objective function from the efficiency criteria given in (10). We transform the requirement in (10) into a convex objective function to be minimized as the negative sum of the of log of all the beam pattern responses in question. Formally, we have

$$\begin{gathered} \min(f(\boldsymbol{V},\boldsymbol{W})) \\ s.t.\ \boldsymbol{W} \in \Omega \cap \Psi, \\ \text{where } f(\boldsymbol{V},\boldsymbol{W}) = -\sum_{\substack{s=0,\dots,S-1 \\ r=0,\dots,R-1}} \ln\left(\left|\boldsymbol{H}_{r,s}\right|^2\right). \end{gathered} \tag{13}$$

Lemma 1: Let $\mathbf{W} \in \mathbb{C}^{\mathrm{N}\times\mathrm{S}}$ and $\boldsymbol{V} \in \mathbb{C}^{\mathrm{N}\times\mathrm{R}}$. If $\left|\boldsymbol{V}_{n,r}\right| = 1, \forall \mathrm{n} \in [0, \dots, \mathrm{N}-1], \forall \mathrm{r} \in [0, \dots \mathrm{R}-1]$, then the function $f(\boldsymbol{V},\boldsymbol{W})$ is convex. A proof of Lemma 1 can be found at the end of this Chapter.

2.4.4 Extension to 3 Directions of Interest

A summary of the operation for implementing BPSK directional modulation given three arbitrary directions of interest is shown in the state diagram in Figure 2.2. We seek an appropriate set of steering vectors, $\boldsymbol{W}$, capable of independently modulating the wireless channel transfer function in three different directions, $\widehat{\boldsymbol{k}}_{\boldsymbol{0}}$, $\widehat{\boldsymbol{k}}_{\boldsymbol{1}}$, and $\boldsymbol{k}_{\boldsymbol{2}}$. In the case of three users, BPSK modulation, and the steering vector solution $\boldsymbol{W} = [\boldsymbol{w}_{\boldsymbol{0}}, \boldsymbol{w}_{\boldsymbol{1}}, \boldsymbol{w}_{\boldsymbol{2}}, \boldsymbol{w}_{\boldsymbol{3}}]$, we can specify four necessary states for the array, where each state represents a different steering vector applied to the array. Each transition between states is marked by a modulation overlay pair for the forward direction, $[x, y, z]$,

which is conjugated in the reverse direction. The modulation overlay pair is a simplified representation of the modulation observed in the directions $\hat{k}_0$ and $\hat{k}_1$ when transitioning from State a to State b, expressed as

$$[x, y, z] = \begin{Bmatrix} H_{\hat{k}_0,a} H^*_{\hat{k}_0,b} \cong x_{a\to b} \\ H_{\hat{k}_1,a} H^*_{\hat{k}_1,b} \cong y_{a\to b} \\ H_{\hat{k}_2,a} H^*_{\hat{k}_2,b} \cong z_{a\to b} \end{Bmatrix}. \tag{14}$$

For the simplicity of Figure 2.2, we do not show the identity transition at each state. Further, the state diagram represents half of the required control for independent messaging between the transmitter and each of the receivers. Since we have control of the source data, we inherit the other half of the required control without the need for additional states.

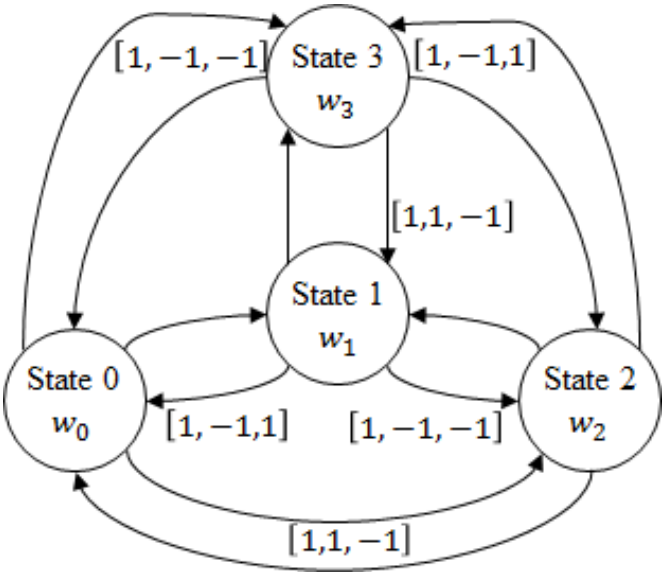

Figure 2.2: A state diagram of the array control system for directional modulation for the three User case and BPSK overlay modulation is shown. Here, we specify four necessary states and steering vectors for the array to overlay modulation in the directions of interest, $\hat{\boldsymbol{a}}_0$, $\hat{\boldsymbol{a}}_1$, and $\hat{\boldsymbol{a}}_2$. The transitions shown in this state diagram represent half of the required control for directional modulation; the other half of the required control is inherited by inverting the input signal to the array. The desired effect on the wireless channel transfer functions in each of the directions of interest is given in (14).

From the state diagram in Figure 2.2, we seek to define a set of constraints similar to (12) that can be used in (13) to determine a set of complex steering vectors that enable directional modulation. We formalize these constraints to enable directional modulation in the three-User case for BPSK modulation as the convex subset $\Psi_{\mathrm{R=3}}$, expressed as

$$\Psi_{\mathrm{R=3}} = \left\{ \boldsymbol{W}: \left\{ \left\{ \begin{bmatrix} \boldsymbol{A}\otimes\boldsymbol{v}_k^H(\widehat{\boldsymbol{k}}_0) \\ \boldsymbol{B}\otimes\boldsymbol{v}_k^H(\widehat{\boldsymbol{k}}_1) \\ \boldsymbol{A}\otimes\boldsymbol{v}_k^H(\widehat{\boldsymbol{k}}_2) \end{bmatrix} \begin{bmatrix} w_0 \\ w_1 \end{bmatrix} \leq \begin{bmatrix} \varepsilon \\ \varepsilon \\ \varepsilon \\ \varepsilon \\ \varepsilon \\ \varepsilon \end{bmatrix} \right\}, \quad \left\{ \begin{bmatrix} \boldsymbol{A}\otimes\boldsymbol{v}_k^H(\widehat{\boldsymbol{k}}_0) \\ \boldsymbol{A}\otimes\boldsymbol{v}_k^H(\widehat{\boldsymbol{k}}_1) \\ \boldsymbol{B}\otimes\boldsymbol{v}_k^H(\widehat{\boldsymbol{k}}_2) \end{bmatrix} \begin{bmatrix} w_0 \\ w_2 \end{bmatrix} \leq \begin{bmatrix} \varepsilon \\ \varepsilon \\ \varepsilon \\ \varepsilon \\ \varepsilon \\ \varepsilon \end{bmatrix} \right\}, \right. \right.$$
$$\left. \left\{ \begin{bmatrix} \boldsymbol{A}\otimes\boldsymbol{v}_k^H(\widehat{\boldsymbol{k}}_0) \\ \boldsymbol{B}\otimes\boldsymbol{v}_k^H(\widehat{\boldsymbol{k}}_1) \\ \boldsymbol{B}\otimes\boldsymbol{v}_k^H(\widehat{\boldsymbol{k}}_2) \end{bmatrix} \begin{bmatrix} w_0 \\ w_3 \end{bmatrix} \leq \begin{bmatrix} \varepsilon \\ \varepsilon \\ \varepsilon \\ \varepsilon \\ \varepsilon \\ \varepsilon \end{bmatrix} \right\}, \quad \left\{ \begin{bmatrix} \boldsymbol{A}\otimes\boldsymbol{v}_k^H(\widehat{\boldsymbol{k}}_0) \\ \boldsymbol{B}\otimes\boldsymbol{v}_k^H(\widehat{\boldsymbol{k}}_1) \\ \boldsymbol{B}\otimes\boldsymbol{v}_k^H(\widehat{\boldsymbol{k}}_2) \end{bmatrix} \begin{bmatrix} w_1 \\ w_2 \end{bmatrix} \leq \begin{bmatrix} \varepsilon \\ \varepsilon \\ \varepsilon \\ \varepsilon \\ \varepsilon \\ \varepsilon \end{bmatrix} \right\}, \right\}, \quad (15)$$
$$\left. \left\{ \begin{bmatrix} \boldsymbol{A}\otimes\boldsymbol{v}_k^H(\widehat{\boldsymbol{k}}_0) \\ \boldsymbol{A}\otimes\boldsymbol{v}_k^H(\widehat{\boldsymbol{k}}_1) \\ \boldsymbol{B}\otimes\boldsymbol{v}_k^H(\widehat{\boldsymbol{k}}_2) \end{bmatrix} \begin{bmatrix} w_1 \\ w_3 \end{bmatrix} \leq \begin{bmatrix} \varepsilon \\ \varepsilon \\ \varepsilon \\ \varepsilon \\ \varepsilon \\ \varepsilon \end{bmatrix} \right\}, \quad \left\{ \begin{bmatrix} \boldsymbol{A}\otimes\boldsymbol{v}_k^H(\widehat{\boldsymbol{k}}_0) \\ \boldsymbol{B}\otimes\boldsymbol{v}_k^H(\widehat{\boldsymbol{k}}_1) \\ \boldsymbol{A}\otimes\boldsymbol{v}_k^H(\widehat{\boldsymbol{k}}_2) \end{bmatrix} \begin{bmatrix} w_2 \\ w_3 \end{bmatrix} \leq \begin{bmatrix} \varepsilon \\ \varepsilon \\ \varepsilon \\ \varepsilon \\ \varepsilon \\ \varepsilon \end{bmatrix} \right\} \right\} \right\}$$

where $\boldsymbol{A} = \begin{bmatrix} 1 & -1 \\ -1 & 1 \end{bmatrix}$, $\boldsymbol{B} = \begin{bmatrix} -1 & -1 \\ 1 & 1 \end{bmatrix}$, and $\boldsymbol{X}\otimes\boldsymbol{Y}$ denotes the Kronecker product of the matrix $\boldsymbol{X}$ and the matrix $\boldsymbol{Y}$. Though (15) is a compact representation, it is extremely similar in structure to (12). The steering vectors for directional modulation varied according to the state diagram in Figure 2.2 can be implemented in a beamformer for transmission or reception. A schematic diagram showing one possible implementation of such a beamformer configured to transmit three independent information signals in three different directions, $\widehat{\boldsymbol{k}}_0$, $\widehat{\boldsymbol{k}}_1$, and $\widehat{\boldsymbol{k}}_2$ using the state machine described in Figure 2.2 is shown in Figure 2.3.

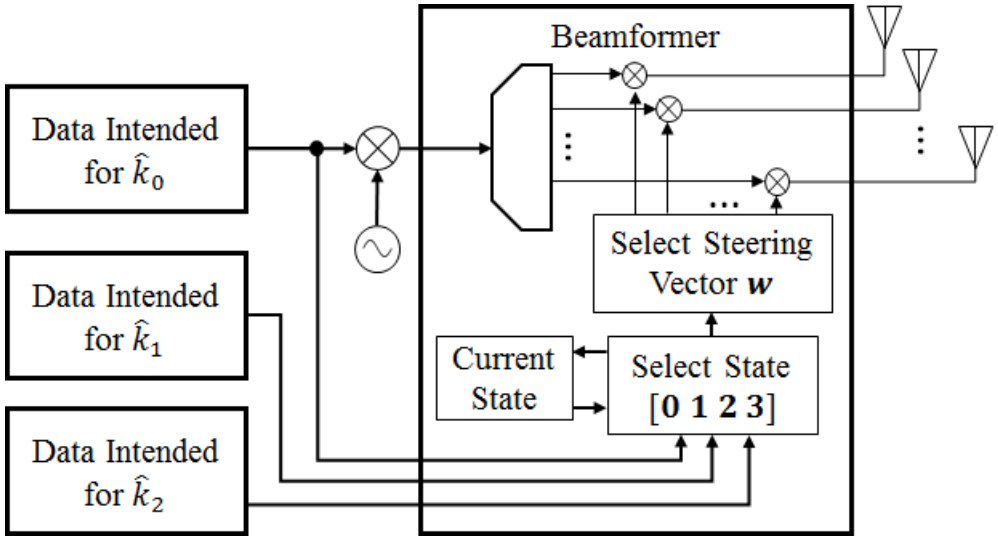

Figure 2.3: Schematic diagram showing a beamformer implementing directional modulation by time-varying the array steering vector. The beamformer behavior is controlled by a state machine that is driven by the desired overlay modulation pattern, as described in Figure 2.2.

2.4.5 Extension to QPSK

For any given symbol constellation point in a Quadrature Phase Shift Keying (QPSK) modulation constellation, we seek steering vectors capable of remapping that constellation point to each of the other constellation points. The modulation constraints for QPSK require 4 steering vectors or states to individually address each of these specific modulations, as shown in Figure 2.4. Each transition between states is marked by a modulation overlay pair for the forward direction, $[x, y]$, which is conjugated in the reverse direction. The modulation overlay pair is a simplified representation of the modulation observed in the directions $\hat{k}_0$ and $\hat{k}_1$ when transitioning from State a to State b, expressed as

$$[x, y] = \begin{Bmatrix} H_{\hat{k}_0,a} H^*_{\hat{k}_0,b} \cong x_{a\to b} \\ H_{\hat{k}_1,a} H^*_{\hat{k}_1,b} \cong y_{a\to b} \end{Bmatrix} . \tag{16}$$

We observe that from each state in Figure 2.4, the QPSK symbol transmitted in the direction $\hat{k}_0$ can be remapped to any QPSK symbol in the direction $\hat{k}_1$ by varying the steering vector. Similar state diagrams can be constructed for modulation schemes requiring manipulation of amplitude and phase, such as 16-QAM. Introducing relative rotation and scale to the set of linear inequality constraints in (12) will remain affine and preserve the convexity of the subset.

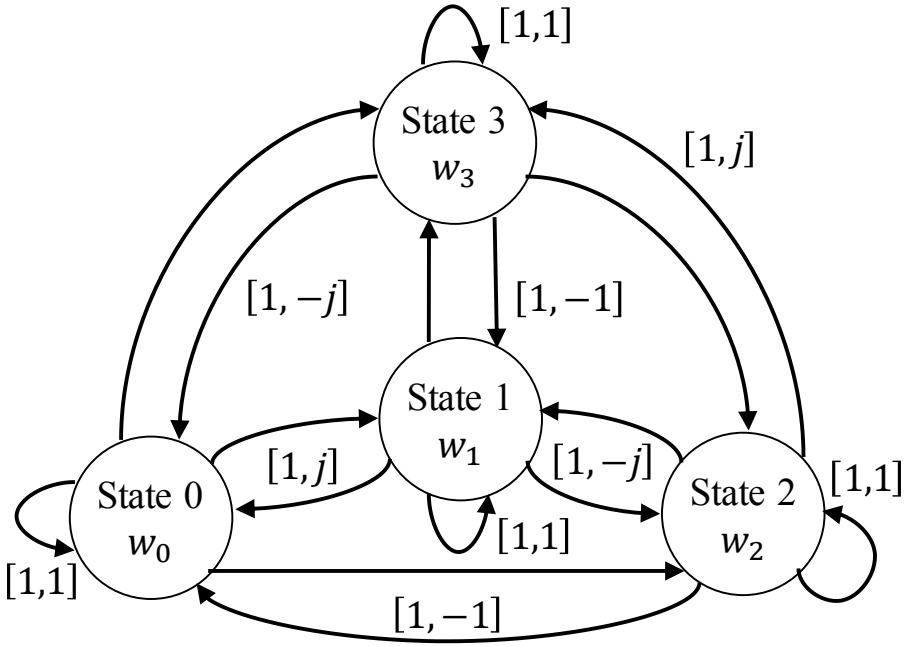

Figure 2.4: A state diagram of the array control system for directional modulation for the two User case and QPSK overlay modulation is shown. Here, we specify four necessary states and steering vectors for the array to overlay modulation in the directions of interest, $\widehat{\boldsymbol{k}}_{\boldsymbol{0}}$ and $\widehat{\boldsymbol{k}}_{\boldsymbol{1}}$. The transitions shown in this state diagram represent half of the required control for directional modulation; the other half of the required control is inherited by inverting the input signal to the array. The desired effect on the wireless channel transfer functions in each of the directions of interest is given in (16).

From the state diagram in Figure 2.4 we seek to define a set of constraints similar to (12) that can be used in (13) to determine a set of complex steering vectors that enable directional modulation. We formalize these constraints to enable directional modulation in the two-User case for QPSK modulation as the convex subset Ψ_{QPSK}, expressed as

$$\Psi_{\text{QPSK}} = \left\{ \begin{bmatrix} \boldsymbol{v}_k^H(\widehat{\boldsymbol{k}}_0) & -\boldsymbol{v}_k^H(\widehat{\boldsymbol{k}}_0) & 0 & 0 \\ -\boldsymbol{v}_k^H(\widehat{\boldsymbol{k}}_0) & \boldsymbol{v}_k^H(\widehat{\boldsymbol{k}}_0) & 0 & 0 \\ \boldsymbol{v}_k^H(\widehat{\boldsymbol{k}}_0) & 0 & -\boldsymbol{v}_k^H(\widehat{\boldsymbol{k}}_0) & 0 \\ -\boldsymbol{v}_k^H(\widehat{\boldsymbol{k}}_0) & 0 & \boldsymbol{v}_k^H(\widehat{\boldsymbol{k}}_0) & 0 \\ 0 & \boldsymbol{v}_k^H(\widehat{\boldsymbol{k}}_0) & -\boldsymbol{v}_k^H(\widehat{\boldsymbol{k}}_0) & 0 \\ 0 & -\boldsymbol{v}_k^H(\widehat{\boldsymbol{k}}_0) & \boldsymbol{v}_k^H(\widehat{\boldsymbol{k}}_0) & 0 \\ \boldsymbol{v}_k^H(\widehat{\boldsymbol{k}}_0) & 0 & 0 & -\boldsymbol{v}_k^H(\widehat{\boldsymbol{k}}_0) \\ -\boldsymbol{v}_k^H(\widehat{\boldsymbol{k}}_0) & 0 & 0 & \boldsymbol{v}_k^H(\widehat{\boldsymbol{k}}_0) \\ 0 & \boldsymbol{v}_k^H(\widehat{\boldsymbol{k}}_0) & 0 & -\boldsymbol{v}_k^H(\widehat{\boldsymbol{k}}_0) \\ 0 & -\boldsymbol{v}_k^H(\widehat{\boldsymbol{k}}_0) & 0 & \boldsymbol{v}_k^H(\widehat{\boldsymbol{k}}_0) \\ 0 & 0 & \boldsymbol{v}_k^H(\widehat{\boldsymbol{k}}_0) & -\boldsymbol{v}_k^H(\widehat{\boldsymbol{k}}_0) \\ 0 & 0 & -\boldsymbol{v}_k^H(\widehat{\boldsymbol{k}}_0) & \boldsymbol{v}_k^H(\widehat{\boldsymbol{k}}_0) \\ \boldsymbol{v}_k^H(\widehat{\boldsymbol{k}}_1) & j\boldsymbol{v}_k^H(\widehat{\boldsymbol{k}}_1) & 0 & 0 \\ -\boldsymbol{v}_k^H(\widehat{\boldsymbol{k}}_1) & -j\boldsymbol{v}_k^H(\widehat{\boldsymbol{k}}_1) & 0 & 0 \\ \boldsymbol{v}_k^H(\widehat{\boldsymbol{k}}_1) & 0 & \boldsymbol{v}_k^H(\widehat{\boldsymbol{k}}_1) & 0 \\ -\boldsymbol{v}_k^H(\widehat{\boldsymbol{k}}_1) & 0 & -\boldsymbol{v}_k^H(\widehat{\boldsymbol{k}}_1) & 0 \\ \boldsymbol{v}_k^H(\widehat{\boldsymbol{k}}_1) & 0 & 0 & -j\boldsymbol{v}_k^H(\widehat{\boldsymbol{k}}_1) \\ -\boldsymbol{v}_k^H(\widehat{\boldsymbol{k}}_1) & 0 & 0 & -j\boldsymbol{v}_k^H(\widehat{\boldsymbol{k}}_1) \\ 0 & \boldsymbol{v}_k^H(\widehat{\boldsymbol{k}}_1) & 0 & \boldsymbol{v}_k^H(\widehat{\boldsymbol{k}}_1) \\ 0 & -\boldsymbol{v}_k^H(\widehat{\boldsymbol{k}}_1) & 0 & -\boldsymbol{v}_k^H(\widehat{\boldsymbol{k}}_1) \\ 0 & \boldsymbol{v}_k^H(\widehat{\boldsymbol{k}}_1) & j\boldsymbol{v}_k^H(\widehat{\boldsymbol{k}}_1) & 0 \\ 0 & -\boldsymbol{v}_k^H(\widehat{\boldsymbol{k}}_1) & -j\boldsymbol{v}_k^H(\widehat{\boldsymbol{k}}_1) & 0 \\ 0 & 0 & \boldsymbol{v}_k^H(\widehat{\boldsymbol{k}}_1) & j\boldsymbol{v}_k^H(\widehat{\boldsymbol{k}}_1) \\ 0 & 0 & -\boldsymbol{v}_k^H(\widehat{\boldsymbol{k}}_1) & -j\boldsymbol{v}_k^H(\widehat{\boldsymbol{k}}_1) \end{bmatrix} \begin{bmatrix} \boldsymbol{w}_0 \\ \boldsymbol{w}_1 \\ \boldsymbol{w}_2 \\ \boldsymbol{w}_3 \end{bmatrix} \leq \begin{bmatrix} \varepsilon \\ \varepsilon \end{bmatrix} \right\}. \tag{17}$$

2.4.6 Extension to M-QAM

We seek to form a convex subset, Ψ_{M-QAM}, that constrains a set of steering vectors $\boldsymbol{W}$. Each of the $M(M-1)$ rows of the matrix in Ψ_{M-QAM} is specification for mapping one constellation point in the direction $\widehat{\boldsymbol{k}}_m$ to a constellation point in the direction $\widehat{\boldsymbol{k}}_n$. We can consider a state diagram similar to Figure 2.4 as a graphical representation of the overlay modulations possible.

Rather than specifying the absolute location of the desired constellation point in the direction $\widehat{\boldsymbol{k}}_n$, we specify the relative mapping between the two constellation points as a rotation and scale in the matrix in Ψ_{M-QAM}, rather than just the rotation, as in Ψ. The subset Ψ_{M-QAM} would still be affine and convex. For QAM, we would also modify the objective function to only consider the array response of the corner constellation points.

We recognize that the convex subset Ψ_{M-QAM} would become particularly large. At most, we would need a library of M^2 steering vectors to enable us to remap any of M transmitted constellation points to any other constellation point. By recognizing that constellation mapping pairs separated by identical translations can employ the same steering vector, we can reduce the number of steering vectors needed to $\frac{M(M-1)}{2}$. Due to the need for the modulus operator, the number of rows in the matrix of Ψ_{M-QAM} is $M(M-1)$.

2.4.7 Selection of the Inequality Constraint Parameter ε

The selection of the parameter ε in the linear inequality constraints for directional modulation as in (12), (15), and (17), is not only critical to the performance in terms of achieved modulation error ratio, but also affects the achievable array gain. We recognize that it is not necessary for the inequality constraint parameter to be applied uniformly across each inequality constraint; however, we do so for the ease of analysis, and the gains achieved by individually tuning this parameter per user is left as a topic for future research.

The set of inequality constraints, Ψ, describes the overlay modulation we seek to achieve. These constraints are critical to directional modulation to achieve independent, confidential links to multiple users as opposed to simply increasing the bit error rate everywhere but the intended

direction as in [6], [31], [54]. Further, we note that if we impose equality constraints rather than inequality constraints for the overlay modulation as in [14], [29], [53], a solution may not exist that satisfies all the constraints . This would also necessitate an iterative algorithmic approach to determining the steering vectors, which is unattractive due to the time required to converge to a solution and the non-convex nature of the optimization.

In the set of inequality constraints, Ψ, we can consider the parameter ε as a surrogate for the modulation error ratio, as shown in Figure 2.5. The arbitrary received signal subject to the channel transfer function H_a is shown. The channel transfer function is manipulated by updating the array steering vector, and represented as H_b. We are concerned principally with the new measured symbol relative to the original symbol, shown as $H_a * H_b^*$, and note that H_a can also represent the desired symbol rather than the actual symbol without loss of generality. We specify ε as the maximum allowable norm of the distance between H_a and $H_a * H_b^*$. Clearly, ε should be small relative to the SNR of the measured symbol to avoid unwanted symbol errors or an observable modulation structure even without symbol transition.

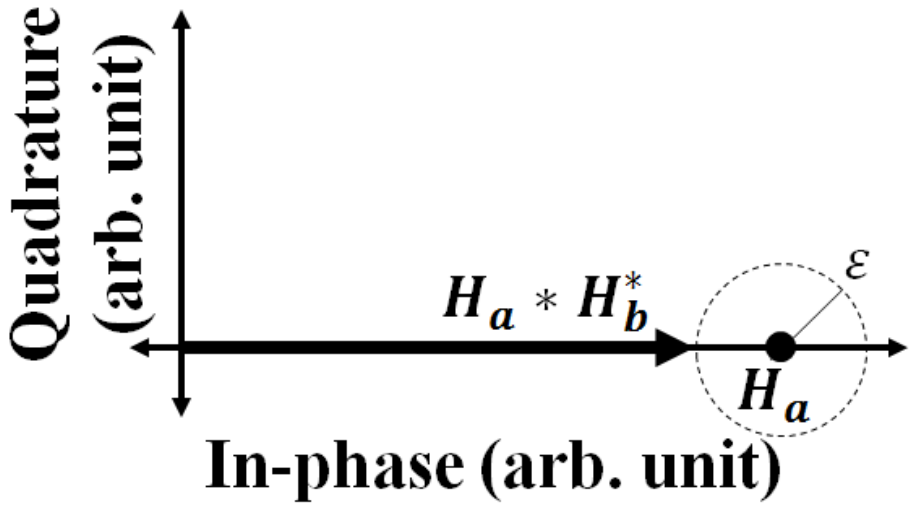

Figure 2.5: Graphical representation of the control parameter ε, a surrogate for the modulation error ratio possible in the set of inequality constraints, Ψ, for directional modulation. The channel transfer functions resulting from a set of steering vectors are given by H_a and H_b. We are concerned principally with the resulting overlay modulation, $H_a * H_b^*$, and note that H_a can also represent the desired symbol rather than the actual symbol without loss of generality. We specify ε as the maximum allowable norm of the distance between H_a and $H_a * H_b^*$, which allows us to quantify and specify a worst-case increase in bit error rate resulting from directional modulation.

We can quantitatively relate the control parameter ε to a worst-case reduction in SNR and worst-case bit error rate, as follows. The well-known probability of bit error for a BPSK-modulated signal with energy per bit, E_b, in additive white Gaussian noise with power spectral density N_0 is given by [55] $P_b\left(\frac{E_b}{N_0}\right) = Q\left(\sqrt{2\frac{E_b}{N_0}}\right)$, where $Q(x)$ is the statistical Q-function. Phase errors, ϕ, possibly resulting from imperfect synchronization or multipath affect the energy per bit to noise power spectral density ratio (E_b/N_0) and thus the probability of bit error by

$$P_b\left(\frac{E_b}{N_0}|\phi\right) = Q\left(\sqrt{2\frac{E_b}{N_0}} * \cos(\phi)\right). \tag{18}$$

Selection of the parameter ε will similarly affect the probability of bit error by reducing the effective overall E_b/N_0, resulting from a decreased received bit energy, but unchanged noise

power spectral density. The expected overall probability of bit error given two channel transfer functions H_a and H_b, assuming $|H_a| > |H_b|$ and knowing the fraction of time the channel transfer function can be characterized as H_a as opposed to H_b, P_{H_a}, can be computed as

$$P_b = P_{H_a} Q\left(\sqrt{\frac{2E_{b,H_a}}{N_0}}\right) + \left(1 - P_{H_a}\right) Q\left(\sqrt{\frac{2E_{b,H_a}}{N_0}}\left(\frac{|H_a|^2 + |H_b|^2}{2|H_a|^2} - \frac{\varepsilon^2}{2|H_a|^2}\right)\right). \quad (19)$$

Here, we note that if only one channel, H_a is used, this reduces to the traditional bit error rate calculation. If we assume an equal use of the BPSK symbols $\{-1, +1\}$, such that $P_{H_a} = P_{H_b} = 0.5$, we observe that the overall E_b/N_0 is penalized by any magnitude imbalance between the channels (i.e., $|H_b|^2 < |H_a|^2$) and the magnitude of the vector difference between channels (i.e., $\varepsilon^2 = |H_a - H_b|^2$). For a given ε, the worst-case reduction in E_b/N_0 is realized when H_a and H_b are collinear. The penalty term above reduces to a simple scaling, given by

$$\frac{|H_b|}{|H_a|} = 1 - \frac{\varepsilon}{|H_a|} \quad (20)$$

By specifying the fixed parameter ε rather than a relative quantity, we are able to maintain the convexity of (13). The worst case reduction in E_b/N_0 is less than $0.5dB$ for $\varepsilon = 0.05 * |H_a|$ for typical operating ranges of BPSK with a bit error rate of less then 10^{-3} ($6dB < E_b/N_0 < 12dB$), as shown in Figure 2.6. If we are able to normalize the measured channel state information, prior to executing the optimization in (13), we can specify the fixed parameter ε without loss of generailty. Here, we are particularly concerned with efficiency, and are interested in cases where $|H_b|$ and $|H_a|$ are within $3dB$ of the peak achievable channel transfer function. As such, we choose $\varepsilon = 0.05$ as the design parameter such that the loss due to modulation error.

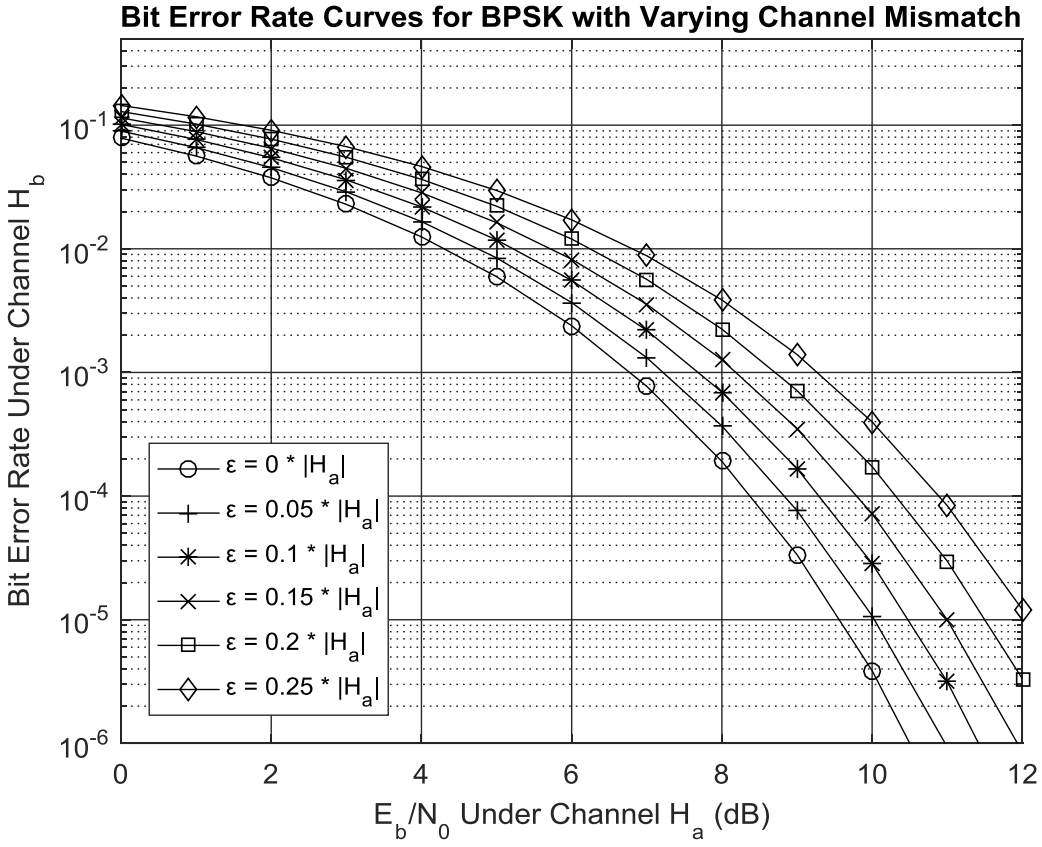

Figure 2.6: Plot of curves showing the worst-case increase in bit error rate under the channel transfer function H_b based on the bit energy to noise power spectral density ratio, E_b/N_0, of H_a and the directional modulation constraint control parameter ε. We observe that the worst-case reduction in $E_b/N_0$is less than $0.5dB$ for $\varepsilon = 0.05 * |H_a|$ for typical operating ranges of BPSK with a bit error rate of less then 10^{-3} ($6dB < E_b/N_0 < 12dB$).

2.4.8 Proof of Lemma 1

Proof of Lemma 1: Let $\mathbf{w_s} \in \mathbb{C}^{\mathrm{N}}$ and $\mathbf{v_k}(\hat{\mathbf{k}}_\mathbf{r}) \in \mathbb{C}^{\mathrm{N}}$. The magnitude of the channel is given by $g(\boldsymbol{w_s^*}, \boldsymbol{w_s})$: $\mathbb{C}^N \rightarrow \mathbb{R}$, where

$$g(\boldsymbol{w_s^*}, \boldsymbol{w_s}) = \left|\boldsymbol{H}_{r,s}\right|^2 = \mathbf{w_s^H}\mathbf{v_k}(\hat{\mathbf{k}}_\mathbf{r})\mathbf{v_k^H}(\hat{\mathbf{k}}_\mathbf{r})\mathbf{w_s}. \tag{21}$$

Making use of Wirtinger derivatives, we can easily show that the gradient of $g(\boldsymbol{w}_s^*, \boldsymbol{w}_s)$ is given by

$$\nabla_{\boldsymbol{w}_s^*} g(\boldsymbol{w}_s^*, \boldsymbol{w}_s) = \mathbf{v_k}(\hat{\mathbf{k}}_\mathbf{r})\mathbf{v_k^H}(\hat{\mathbf{k}}_\mathbf{r})\mathbf{w_s}, \tag{22}$$

and the Hessian of $g(\boldsymbol{w}_s^*, \boldsymbol{w}_s)$ is given by

$$\nabla^2_{\boldsymbol{w}_s^*, \boldsymbol{w}_s} g(\boldsymbol{w}_s^*, \boldsymbol{w}_s) = \mathbf{v_k}(\hat{\mathbf{k}}_\mathbf{r})\mathbf{v_k^H}(\hat{\mathbf{k}}_\mathbf{r}) = \boldsymbol{R}_r. \tag{23}$$

To prove that $f(\boldsymbol{V}, \boldsymbol{W})$ is convex, we can show that $d(\boldsymbol{w}_s^*, \boldsymbol{w}_s) = \ln\left(\left|\mathbf{w_s^H}\mathbf{v_k}(\hat{\mathbf{k}}_\mathbf{r})\mathbf{v_k^H}(\hat{\mathbf{k}}_\mathbf{r})\mathbf{w_s}\right|^2\right)$ is concave by examining the derivatives, since convexity is preserved under nonnegative weighted sums [56]. Since $d(\boldsymbol{w}_s^*, \boldsymbol{w}_s) = h(x) \circ g(\boldsymbol{w}_s^*, \boldsymbol{w}_s)$ is a composite function, the second derivative is given by

$$\begin{aligned} d''(\boldsymbol{w}_s^*, \boldsymbol{w}_s) = h''\big(g(\boldsymbol{w}_s^*, \boldsymbol{w}_s)\big)\left(\nabla_{\boldsymbol{w}_s^*} g(\boldsymbol{w}_s^*, \boldsymbol{w}_s)\right)^2 + \\ h'\big(g(\boldsymbol{w}_s^*, \boldsymbol{w}_s)\big)\nabla^2_{\boldsymbol{w}_s^*, \boldsymbol{w}_s} g(\boldsymbol{w}_s^*, \boldsymbol{w}_s) \ . \end{aligned} \tag{24}$$

It follows from (24) that $d(\boldsymbol{w}_s^*, \boldsymbol{w}_s)$ is concave if $h\big(g(\boldsymbol{w}_s^*, \boldsymbol{w}_s)\big)$ is concave and nondecreasing, and $g(\boldsymbol{w}_s^*, \boldsymbol{w}_s)$ is concave, which is the case here. The non-negative eigenvalues of $\nabla^2_{\boldsymbol{w}_s^*, \boldsymbol{w}_s} g(\boldsymbol{w}_s^*, \boldsymbol{w}_s)$ indicate that it is positive semidefinite. Upon closer inspection, we observe that

$$d''(\boldsymbol{w}_s^*, \boldsymbol{w}_s) = -\frac{(\boldsymbol{R}_r \mathbf{w_s})^H \boldsymbol{R}_r \mathbf{w_s}}{\left(\mathbf{w_s^H} \boldsymbol{R}_r \mathbf{w_s}\right)^2} + \frac{\boldsymbol{R}_r}{\mathbf{w_s^H} \boldsymbol{R}_r \mathbf{w_s}}, \tag{25}$$

which is always negative since the norm of the elements of the matrix $\boldsymbol{R}_r = \mathbf{v_k}(\hat{\mathbf{k}}_\mathbf{r})\mathbf{v_k^H}(\hat{\mathbf{k}}_\mathbf{r})$ are always equal to 1. Therefore, since $d(\boldsymbol{w}_s^*, \boldsymbol{w}_s)$ is concave, $f(\boldsymbol{V}, \boldsymbol{W})$ is convex.

Chapter 3

Simultaneous Wireless Information and Power Transfer Using Directional Modulation

The current state of spectrum regulation in the Americas, Europe, and Asia has herded many wireless communications devices into crowded bandwidths [57]. As such, it is quite possible that a significant amount of energy available for harvesting exists in the same time and frequency sub-spaces as the desired signal. We apply the proposed beamforming method for directional modulation described in Chapter 2 to enable a device to harvest interfering energy that is spatially separated from an information signal, but within the same time and frequency subspaces. The proposed thus enables simultaneous wireless information and power transfer with high system spectral efficiency.

3.1 Overview

First, we apply the proposed beamforming method to a receiver harvesting energy from co-channel interferers. Early research of methods for harvesting microwave electromagnetic energy using antennas with rectifiers [58] was focused on delivering energy to aerospace vehicles. The so-called “rectennas” placed rectifiers with a matching circuit directly onto the antennas [59] and were dedicated to maximizing the efficiency of wireless power transfer from the transmitter to the receiver. A simple way for wireless communications devices to harvest microwave electromagnetic energy while communicating is to separate the desired signal energy from any noise and interference energy. Signals can be designed to occupy predictable time and bandwidth; therefore, simple switches and multiplexers can divert energy from unnecessary time and frequency sub-spaces to an energy-harvesting subsystem. Unfortunately, any energy within the desired time and frequency sub-space that is not related to the desired signal can degrade performance and is difficult to divert and harvest, requiring strict synchronization across the communications system. Any interfering energy that is spatially separated from the desired signal can be nulled to minimize the effect on the desired signal, but then cannot be harvested.

Given the reciprocal nature of array beamforming, we implement the proposed directional modulation method during reception. In this application, we enable the separation of signal energy from interfering energy within the same time and frequency sub-space in the analog domain, such that the interfering energy can be separated and harvested for power while simultaneously decoding the information-bearing signal. The proposed method enables selective spectral manipulation of co-channel interference without corrupting the desired signal. Specifically, we

frequency modulate interfering signals far enough out of band such that they can be easily harvested using a passive diplexer as shown in Figure 3.1. Using a diplexer, we can then isolate the information-bearing signal from a large fraction of the energy from an interferer, such as a wireless power transfer system, which now occupies a different frequency band.

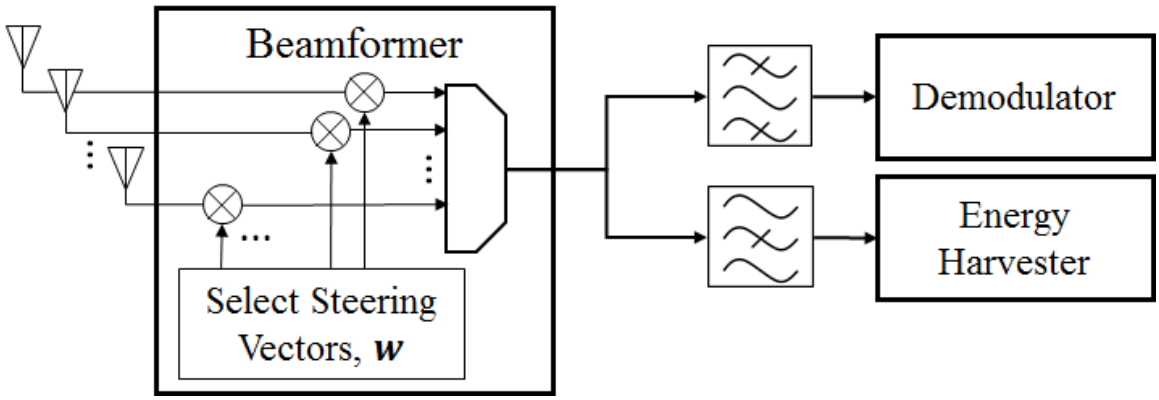

Figure 3.1: Schematic diagram showing a beamformer implementing directional modulation by time-varying the array steering vector. The output of the beamformer is connected to a diplexer that diverts in-band frequencies containing the information signal to a demodulator and now out-of-band frequencies carrying the power transfer signal to an energy harvesting circuit.

The proposed directional modulation method would enable communications systems with designed layouts (such as mobile wireless communications systems served by fixed base stations) to reuse the same frequencies for information and for power transfer, so long as they are spatially separated. This can be easily implemented, for example, in a cellular sector as shown in Figure 3.2. The sector is served by three base stations, each with two antennas providing service with a simple frequency re-use scheme to provide wireless power transfer in addition to information transfer. A user inside the sector can use the proposed beamforming method to separate the information and wireless power transfer signals on any frequency since they will be spatially separated. Depending on the specific frequency allocation, it is possible to access more than one frequency simultaneously.

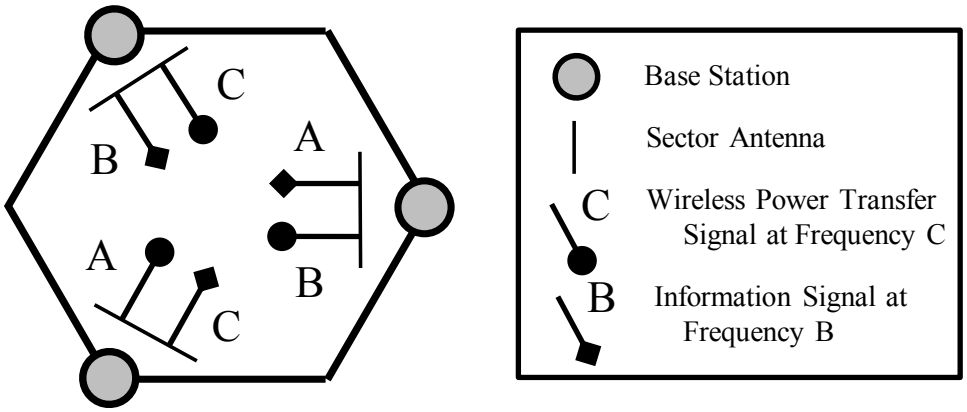

Figure 3.2: Example of a cellular sector served by three base stations, each with an antenna providing service to the sector. The frequency allocations are planned such that the base stations serving a sector do not interfere with each other. This notional layout also shows a simple scheme to re-use these frequencies to provide wireless power transfer. A user inside the sector can use the proposed beamforming method to use any of the frequencies available for information and wireless power transfer since they are spatially separated. Depending on the specific frequency allocation, it is possible to access more than one frequency simultaneously.

3.2 Prior Art

The proposed directional modulation method can be applied to enhance far field directive power beaming, which is able to transfer several orders of magnitude more power than far field ambient scavenging techniques [60]–[62], at ranges several times further than near field power transfer [62]. Other far field directive power beaming techniques proposed in the literature such as time domain switching [7], power splitting [7]–[10], antenna switching [11], [12], and spatial switching [13] seek an optimal allocation of energy from a single transmitter to information and power harvesting circuits using available degrees of freedom. Allocations for far field directive power beaming techniques have been proposed that consider the security needs of wireless information and power transfer systems [63].

In contrast, the proposed method enables the isolation and harvesting of interfering energy from the same time and frequency sub-space as the information signal. Thus, multiple, spatially separated transmitters can occupy the same time and frequency sub-space, and convey both information and power to a single receiver. Consequently, our method enables a denser frequency re-use pattern in communications systems while providing energy to mobile devices. Additionally, it enables a system to operate within a narrower frequency allocation by re-using the same spectrum for both communications and wireless power transfer.

3.3 Harvesting Energy from Co-channel Interferers Using Beamforming

We apply the proposed method to develop a new array beamforming technique for simultaneous wireless information and power transfer for communications devices based on concepts of direction-dependent modulation. The proposed method is formulated as a convex optimization problem, which reduces the computational burden of steering vector formation compared to other methods [14], [15]. It is also constrained to be implemented as a passive beamformer, in contrast to other techniques [16], [53]. Simulation and experimentation showing both the proof of concept and potential performance of the proposed method is shown in Chapters 5 and 6.

3.3.1 Signal Model

Our received signal model, $\boldsymbol{x}(t)$, consists of the sum of a plane wave information signal of interest in the direction $\widehat{\boldsymbol{k}}_{\boldsymbol{s}}$, a plane wave wireless power transfer signal in the direction $\widehat{\boldsymbol{k}}_{\boldsymbol{p}}$, and isotropic noise η. Each of these signals occupies the same time and frequency sub-space, and is given by $\boldsymbol{x}(t) = b_s\boldsymbol{v}_{\boldsymbol{k}}(\widehat{\boldsymbol{k}}_{\boldsymbol{s}}) + b_p\boldsymbol{v}_{\boldsymbol{k}}(\widehat{\boldsymbol{k}}_{\boldsymbol{p}}) + \eta$ where b_s and b_p are arbitrary scalars. We seek to apply an overlay modulation to the power transfer signal independent of the desired information signal using a time-varying array steering vector. This signal model assumes an otherwise static channel during the time scales of interest. The array output is given by $y(t) = \boldsymbol{x}^H(t)\boldsymbol{w}(t)$. In the case of overlaying a BPSK modulation, we identify two steering vectors, $\boldsymbol{w}_0$ and $\boldsymbol{w}_1$, such that the transition between $\boldsymbol{v}_k^H(\widehat{\boldsymbol{k}}_p)\boldsymbol{w}_0$ and $\boldsymbol{v}_k^H(\widehat{\boldsymbol{k}}_p)\boldsymbol{w}_1$ induces a sufficient phase shift while the transition between $\boldsymbol{v}_k^H(\widehat{\boldsymbol{k}}_s)\boldsymbol{w}_0$ and $\boldsymbol{v}_k^H(\widehat{\boldsymbol{k}}_s)\boldsymbol{w}_1$ does not. Furthermore, we must sufficiently modulate the power transfer signal in frequency such that it can be harvested while preserving the desired information signal.

Once modulated in frequency, the power transfer signal can be isolated using a diplexer and diverted to the energy harvesting circuit. To maintain a usable efficiency, we only consider beamforming using phase delays and attenuation, such that the power transfer signal harvesting system is comprised of the antenna array, a matching network, a passive phase delay device, an attenuator, a combiner, and the energy harvesting circuit. We select an optimal set of steering vectors per (13) and predictably time-vary them to achieve the desired modulation in separate directions. Given that this is an array processing technique that can be added to existing energy

harvesting circuitry, practical constraints such as transmission efficiency, path loss, and receive circuit efficiency have not been taken into consideration.

3.3.2 Spectral Manipulation of Co-channel Interference

From (13) we have identified an optimal pair of steering vectors to modulate the wireless power transfer signal without distorting the desired information signal, while maintaining adequate array gain in both directions. We then vary the steering vector between $\boldsymbol{w_0}$ and $\boldsymbol{w_1}$ to overlay a phase-shift keying (PSK) modulation only to the wireless power transfer signal. Throughout this paper, we assume that both transmitted signals—the information-bearing signal and the wireless power transfer signal—are BPSK-modulated signals occupying the same bandwidth. In the case where there is bandwidth mismatch, system parameters should be designed based on the wider bandwidth. The power spectral density of BPSK-modulated signals is given by [64]

$$P_{BPSK}(f) = 2E_b \left(\frac{\sin\left(\frac{\pi f}{f_c}\right)}{\frac{\pi f}{f_c}} \right)^2, \tag{26}$$

where E_b is the bit energy, f is the signal center frequency, and f_c is the modulation chip rate. For an un-spread BPSK-modulated signal, the modulation chip rate is equal to the symbol rate.

There are well known PSK modulation sequences and rates that can be applied to manipulate the signal power spectrum. For example, we can apply a direct sequence spread spectrum (DSSS) modulation by applying a BPSK-modulated waveform of a pseudo-random sequence at a modulation chip rate significantly higher than the symbol rate, which spreads the typical sinc-shaped power spectrum and reduces the peak power spectral density as shown in Figure 3.3.

Knowing that we seek to minimize the power spectral density about the carrier frequency within the information bandwidth and maximize the power transferred outside the information bandwidth, we employ Binary Offset Carrier (BOC) modulation, which has been designed specifically for broadcast scenarios of multiple signals sharing the same time-frequency subspace [65].

3.3.3 Binary Offset Carrier (BOC) Modulation

Binary Offset Carrier (BOC) modulation was designed for spectrum re-use among conventional PSK-modulated signals [65] and is currently employed on satellite navigation systems to enable signals to effectively share spectrum [66]. The power spectral density of a BOC-modulated signal using the chip rate f_c and subcarrier frequency f_s, denoted $BOC(f_s, f_c)$, is given by [65]

$$P_{BOC(f_s,f_c)}(f) = f_c \left(\frac{\sin\left(\frac{\pi f}{2f_s}\right)\sin\left(\frac{\pi f}{f_c}\right)}{\pi f cos\left(\frac{\pi f}{2f_s}\right)} \right)^2 . \tag{27}$$

The power spectral density of a BPSK-modulated signal is compared to that of a spread spectrum-modulated signal and that of a BOC(10,2)-modulated signal in Figure 3.3. It is clear by inspection that we can increase the instantaneous bandwidth of the BPSK-modulated signal by modulating the signal at a rate faster than the symbol rate. The ratio of the maximum chipping or subcarrier rate to the symbol rate is known as the spreading factor; the latter is a measure of intercept probability as well as a robustness measure against multipath fading. We can uniformly spread the signal energy across a wide bandwidth by using direct sequence spread spectrum

(DSSS) modulation or deliberately shift the vast majority of the signal located within the information bandwidth outside that bandwidth using BOC modulation.

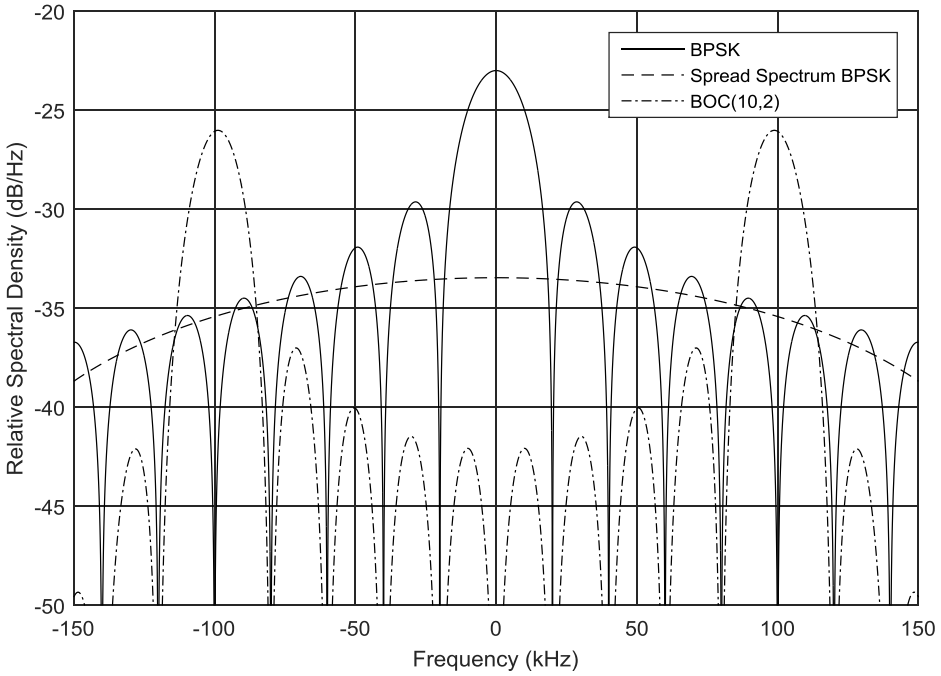

Figure 3.3: Comparison of theoretical spectra of BPSK modulation, spread spectrum BPSK modulation, and BOC(10,2) modulation, at the same center frequency. The spread spectrum BPSK chipping rate and the BOC(10,2) subcarrier frequency in this example are a factor of 5 higher than the BPSK symbol rate.

3.3.4 Preservation of the Desired Signal and Synchronization

The proposed beamforming method is designed to allow simultaneous wireless information and power transfer from signals that share the same time and frequency sub-space. The proposed method selectively modulates the wireless power transfer signal out-of-band, but must not irreversibly distort the information-bearing signal. As such, the array steering vector optimization

criteria given in (13) reflect a requirement of a distortionless response in the direction of the information signal.

The distortionless response criteria in (13) removes the requirement for the system to synchronize to the information signal; however, to effectively overlay the BOC modulation, the receiver must be synchronized to the wireless power transfer signal. Assessing the sensitivity of BOC modulation to the subcarrier misalignment is beyond the scope of this work. Here, we assume that the receiver is able to synchronize to the wireless power transfer signal through a search algorithm assisted by global timing, such as the one provided by the Global Positioning System (GPS).

Further, the proposed beamforming method relies on knowledge of the incoming direction of both the information signal and the wireless power transfer signal. The directions of arrival should be estimated as part of the receiver synchronization (signal acquisition and tracking). Multiple signal classification is outside the scope of this paper; however, integrating direction-of-arrival estimation into the beamformer weight selection process is a topic recommended for future research.

Chapter 4

Increased Secrecy Capacity Using Directional Modulation

The proposed beamforming method can improve the performance of Internet of Things (IoT) systems by increasing the overall secrecy capacity of a wireless broadcast system without increasing the size, weight, or power consumption of IoT devices. Unlike traditional beamforming techniques [1], [2] which focus energy in the direction of an intended receiver and minimize the total energy transmitted in the direction of an eavesdropper, the proposed method uses time-varying beamforming to induce physical layer symbol transitions in the energy transmitted in the direction of an eavesdropper, resulting in an entirely new "cover" signal to mask the original message. This is accomplished by overlaying a direction-dependent modulation onto the transmitted signal. This technique, called directional modulation, has been proposed previously for physical layer security when considering a single user and one or more eavesdroppers by

sufficiently increasing the signal-error-vector magnitude in the direction of the eavesdroppers [6], [14], [26], [30], [52], [67], [68]. Other techniques, such as the artificial noise method or null-space method for multiple-input single-output (MISO) systems are formulated to do the same [5]. With the exception of [67], these publications aim to increase the overall secrecy capacity of the system by preventing the eavesdropper from receiving a message rather than increasing the overall capacity of the system. This work is the first to consider directional modulation in a broadcast scenario and increases the achievable secrecy capacity in a wireless broadcast channel by increasing the sum-rate wireless broadcast channel capacity and increasing the PHY-layer secrecy of the transmitted signals.

PHY-layer secrecy in wireless communications systems tends to leverage a simple rule of thumb: increasing the signal-to-interference-plus-noise ratio (SINR) of a transmission decreases the rate of bit errors at the receiver, and vice versa [69]. As such, Eavesdroppers desire the maximum possible SINR for signals intended for other receivers. Cognizant communications systems might reduce the power transmitted in the directions of suspected eavesdroppers in an attempt to increase the eavesdroppers received bit error rate and mask as much of the transmission as possible [2]. Unfortunately, many techniques exist to increase the SINR of a received signal, possibly to an intelligible level, including increasing the antenna size or decreasing the distance between the transmitter and the eavesdropper [70].

If we assume that an Eavesdropper is not sufficiently within the line-of-sight between a transmitter and a receiver pair such that the array manifold and wireless channel between the transmitter and the eavesdropper is different than the array manifold and wireless channel between the transmitter and receiver, then directional modulation may be applied to provide additional

PHY-layer secrecy. Recent research has described approaches to time-varying beamforming techniques to enable directional modulation for the purposes of PHY-layer secrecy [6], [14], [26], [30], [36], [52]. These techniques attempt to intentionally modulate the amplitude and phase of transmitted symbols in directions away from the intended receiver, thus randomly inducing additional bit errors in the transmitted signal at the PHY-layer. A sufficient rate of these bit errors would reduce the signal received by an eavesdropper to a random string of bits lacking any meaningful information.

Given knowledge of the direction from the array toward the eavesdropper, the proposed beamforming method can be used to overlay a second information signal in the direction of the eavesdropper that is completely independent of the genuine information signal. The proposed method independently modulates the array manifold and consequently, the wireless channel between the transmitter and the eavesdropper and the wireless channel between the transmitter and the receiver. Rather than simply reducing the signal power in the direction of the eavesdropper and relying on either the eavesdropper's internal noise or external noise to induce sufficient bit errors, the eavesdropper can be spoofed by completely replacing the genuine signal with an incorrect but valid information signal, because the proposed method is capable of arbitrary modulation at the PHY-layer. Further, as a PHY-layer technique, directional modulation can be applied independent of other security protocols at other layers of the Open Systems Interconnection (OSI) model, including encryption.

4.1 Disguising Transmissions for Physical Layer Secrecy

Consider a Base Station transmitter with N antennas communicating with a legitimate user in the direction $\hat{a}_m$, known as User 0. There is an Eavesdropper in the direction $\hat{a}_n$, known as User 1, as shown in Figure 4.1. We let $N = 2$ and restrict the transmit power of the Base Station to P_T. We assume that both User 0 and User 1 are externally noise limited with noise level σ_m^2 and σ_n^2, respectively.

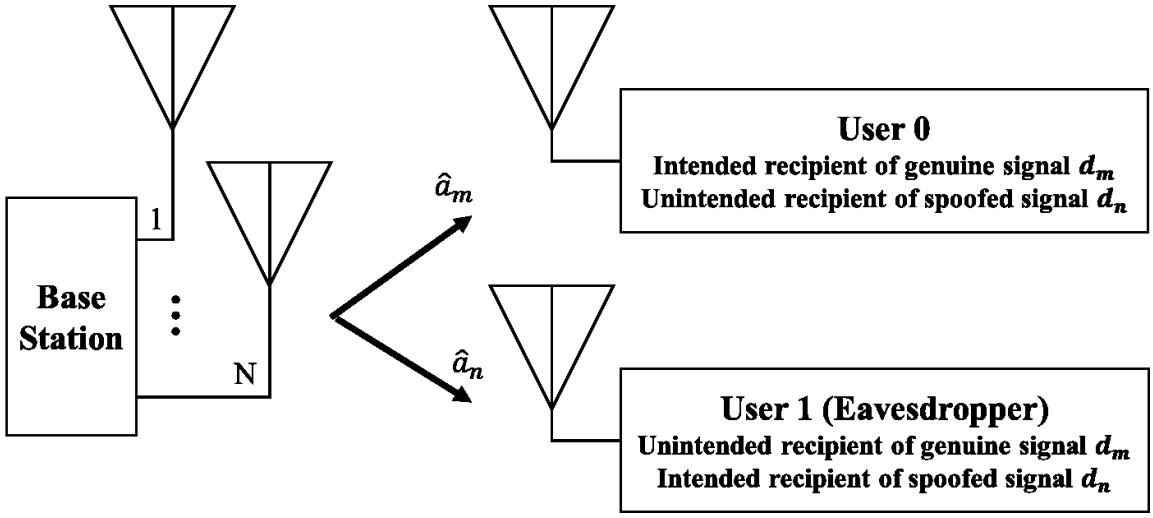

Figure 4.1: Diagram of Base Station transmitter array servicing a User (User 0) spatially separated from an Eavesdropper (User 1). The Base Station possesses two messages: a genuine signal, d_m, intended for User 0 and a spoofed signal, d_n, intended for User 1. Due to the broadcast nature of the Base Station and expected wireless channels, we expect that both messages are perceptible by their respective unintended receivers.

The data intended for User 0 in the direction $\hat{\boldsymbol{a}}_{\boldsymbol{m}}$ is denoted by $d_m(t)$. Arbitrarily independent data intended for the Eavesdropper (User 1) in the direction $\hat{\boldsymbol{a}}_{\boldsymbol{n}}$ is denoted by $d_n(t)$. A typical

array modulates $d_m(t)$ onto a carrier frequency and selects a steering vector that attempts to simultaneously maximize the array gain towards $\hat{\boldsymbol{a}}_{\boldsymbol{m}}$ and minimize the array gain towards $\hat{\boldsymbol{a}}_{\boldsymbol{n}}$ [71]. Unfortunately, reduced signal power spectral density towards $\hat{\boldsymbol{a}}_{\boldsymbol{n}}$ can be overcome by the Eavesdropper (User 1) in a variety of ways, e.g., by increasing the receiver sensitivity, by increasing the antenna aperture area, or by reducing the distance to the signal source. To provide additional security at the PHY- layer, we overlay a signal modulation towards $\hat{\boldsymbol{a}}_{\boldsymbol{n}}$ by time-varying the array steering vector, $\boldsymbol{w}(t)$, in the pattern given by $d_m(t) \oplus d_n(t)$, as shown in Figure 4.2, where $\oplus$ denotes the exclusive disjunction. The steering vector update rate will be matched to the symbol rate, and will only need to be recomputed if the Eavesdropper (User 1) or User 0 directions change relative to the Base Station. This results in $d_m(t)$ being transmitted in the direction $\hat{\boldsymbol{a}}_{\boldsymbol{m}}$, and the spoofed signal $d_n(t)$ being transmitted in the direction $\hat{\boldsymbol{a}}_{\boldsymbol{n}}$.

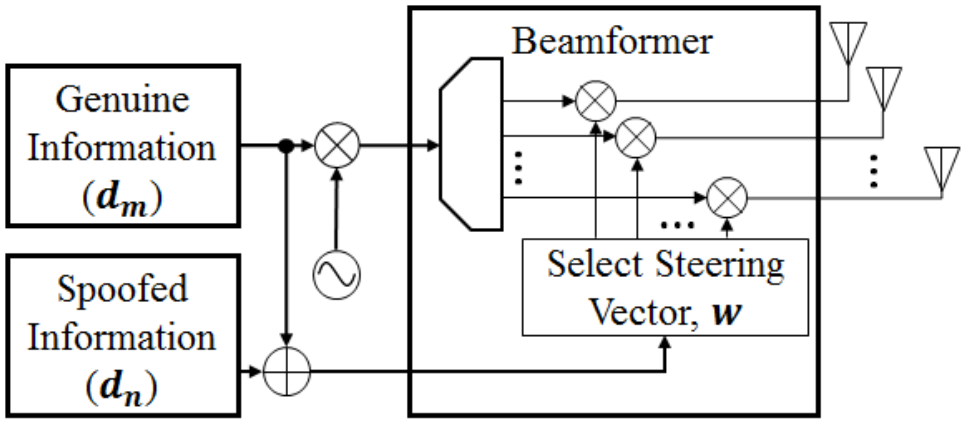

Figure 4.2: Schematic diagram showing a genuine binary information sequence, d_m being sent to the beamformer which is modulated according the exclusive disjunction of d_m and the spoofed information sequence, d_n. This results in the genuine information sequence, d_m, being transmitted in the direction $\hat{k}_m$, and the spoofed information sequence, d_n, being transmitted in the direction $\hat{k}_n$. This directional modulation technique provides physical layer security since the genuine information sequence, d_m, becomes unrecoverable in the direction $\hat{k}_n$.

Critical to the benefits of the proposed method is that directional modulation transforms the signal in different directions rather than simply reducing the signal power into noise. In contrast to the well-studied Dirty Paper Coding technique for broadcast channels [72] where the transmitted power is shared between two signals and only User 0 receives an interference-free signal, the proposed method transmits only one signal and sacrifices overall transmitted power to transform it towards User 1. This results in both User 0 and User 1 receiving a nearly interference-free signal, which is controlled by the implementation loss parameter ε. This will lead to a modest increase in the sum-rate broadcast channel capacity beyond published upper bounds for systems that do not account for controlled variation of the array steering over time as an available degree of freedom and a line-of-sight channel, which is the currently accepted state-of-the-art for wireless broadcast channels [73]. Furthermore, this will lead to substantial gains in the overall secrecy capacity of the wireless communications system since the confidential signals are selectively transformed in directions away from the intended user.

4.1.1 Signal Model

We consider a multiple-input multiple-output (MIMO) broadcast channel with a transmitter or Base Station with an N-element phased array antenna and R receivers that are spatially separated. In this paper, we consider $R = 2$ receivers – one user in the direction $\widehat{\boldsymbol{a}}_{\boldsymbol{m}}$ and another user in the direction $\widehat{\boldsymbol{a}}_{\boldsymbol{n}}$, each with a single antenna as shown in Figure 4.1. In this scenario, we consider two independent and confidential messages to be broadcasted: $d_m(t)$ intended for User 0 in the direction $\widehat{\boldsymbol{a}}_{\boldsymbol{m}}$ and $d_n(t)$ intended for User 1 in the direction $\widehat{\boldsymbol{a}}_{\boldsymbol{n}}$. In this scenario, both users are considered to be legitimate receivers of their own message and eavesdroppers of the other users' messages. Directions are expressed in the spherical coordinate system relative to the

geometric center of the transmit array as a unit vector based on angles θ and ϕ from the positive $\hat{x}$ and $\hat{z}$ axes, as $\widehat{\boldsymbol{a}}_{\boldsymbol{r}} = [\sin(\theta)\cos(\phi), \sin(\theta)\sin(\phi), \cos(\theta)]^T$. The positions of the N elements of the antenna array are described in a Cartesian coordinate system, $\boldsymbol{p_n} = [x_n, y_n, z_n]^T$. We restrict the transmit power of the Base Station to P_T and assume that both users are externally noise limited with unit noise levels, $\sigma_{\widehat{\boldsymbol{a}}_{\boldsymbol{m}}} = \sigma_{\widehat{\boldsymbol{a}}_{\boldsymbol{n}}} = 1$.

The proposed beamforming method is applied by the Base Station during transmission. Our signal consists of the phase-modulated information signal, $d_m(t) \in \{0,1\}$, given by $x(t) = b_s cos(2\pi f_c t + \pi d_m(t))$ where b_s is an arbitrary scalar and f_c is the signal carrier frequency. We seek to overlay a direction-dependent modulation, as summarized in Figure 4.3. Specifically, we seek to transmit the data contained in $d_m(t)$ towards $\widehat{\boldsymbol{a}}_m$ and the arbitrarily different data $d_n(t)$ towards $\widehat{\boldsymbol{a}}_n$ by only manipulating the array steering vector $\boldsymbol{w}$. The array output towards $\widehat{\boldsymbol{a}}_m$ is given by $\boldsymbol{z}(\widehat{\boldsymbol{a}}_m, t) = \boldsymbol{v}_k^H(\widehat{\boldsymbol{k}}_m)\boldsymbol{w}(t)x(t)$. The array output towards $\widehat{\boldsymbol{a}}_n$ is given by $\boldsymbol{z}(\widehat{\boldsymbol{a}}_n, t) = \boldsymbol{v}_k^H(\widehat{\boldsymbol{k}}_n)\boldsymbol{w}(t)x(t)$. In the case of overlaying a BPSK modulation, we again seek to identify two steering vectors, $\boldsymbol{w}$, such that

$$\begin{aligned} \boldsymbol{v}_k^H(\widehat{\boldsymbol{k}}_n)\boldsymbol{w}(t+1) * \left(\boldsymbol{v}_k^H(\widehat{\boldsymbol{k}}_n)\boldsymbol{w}(t)\right)^* &= -1, \text{ and} \\ \boldsymbol{v}_k^H(\widehat{\boldsymbol{k}}_m)\boldsymbol{w}(t+1) * \left(\boldsymbol{v}_k^H(\widehat{\boldsymbol{k}}_m)\boldsymbol{w}(t)\right)^* &= 1 \ . \end{aligned} \tag{28}$$

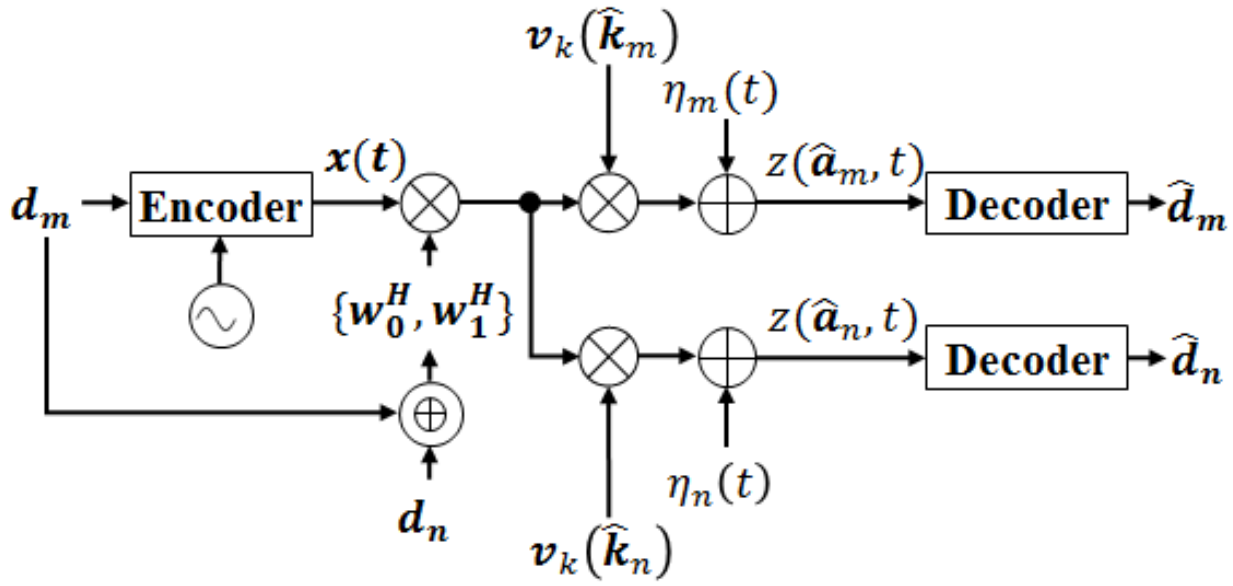

Figure 4.3: Graphical representation of the signal model for implementation of directional modulation in the two-user scenario. The information, d_m, is phase-modulated and encoded onto a carrier signal and transmitted by the array. The array steering vector is time-varied per the exclusive disjunction between the information d_m and the information d_n. Given the known array manifold in the directions $\widehat{\boldsymbol{k}}_{\boldsymbol{m}}$ and $\widehat{\boldsymbol{k}}_{\boldsymbol{n}}$, and the appropriately designed steering vectors $\boldsymbol{w}_{\boldsymbol{0}}^{\boldsymbol{H}}$ and $\boldsymbol{w}_{\boldsymbol{1}}^{\boldsymbol{H}}$, the information signal decoded in the direction $\widehat{\boldsymbol{k}}_{\boldsymbol{m}}$ yields d_m, and the information signal decoded in the direction $\widehat{\boldsymbol{k}}_{\boldsymbol{n}}$ yields d_n.

If we allow for some implementation loss denoted ε, the modulation requirements in (28) can be written as the convex subset Ψ, given (12). Further applying the practical constraint of not requiring any active gain in the array, we can solve this problem using the constrained optimization given by (13). We assume a simple, static line of sight channel model with no diffraction, dispersion, or multipath between the transmitter and the receivers during the time scales of interest. As such, we assume that the transmitter does not have access to any channel state information (CSI), which would manifest here as a bulk rotation and scale of the constellation for each receiver. Here, we assume that the receiver and eavesdropper are independently and correctly synchronized by estimating their respective channel transfer functions by measuring the orientation of their respective received constellations.

4.1.2 Secrecy Capacity

Using the antenna array, we seek to transmit different, confidential messages to multiple receivers that occupy the same time-frequency subspace. Further, we seek to maximize the sum-rate channel capacity between the broadcast transmitter and all the receivers with enhanced physical layer security of confidential messages. In order to assess the effectiveness of this technique in providing PHY-layer security, we consider the secrecy capacity defined as [74]

$$C_s = \begin{cases} C_{\hat{\boldsymbol{k}}_m} - C_{\hat{\boldsymbol{k}}_n}, & \gamma_{\hat{\boldsymbol{k}}_m} > \gamma_{\hat{\boldsymbol{k}}_n} \\ 0, & \gamma_{\hat{\boldsymbol{k}}_m} \leq \gamma_{\hat{\boldsymbol{k}}_n} \end{cases}, \tag{29}$$

where $\gamma_{\hat{\boldsymbol{k}}_m}$ and $C_{\hat{\boldsymbol{k}}_m}$ are the SNR and the channel capacity of User 0 in the direction $\hat{\boldsymbol{k}}_m$, respectively, and $\gamma_{\hat{\boldsymbol{k}}_n}$ and $C_{\hat{\boldsymbol{k}}_n}$ are the SNR and the channel capacity of User 1 in the direction $\hat{\boldsymbol{k}}_n$, respectively. We define the overall transmitted SNR in the direction $\hat{\boldsymbol{k}}$ as $\bar{\gamma}_{\hat{\boldsymbol{k}}} = P_T/\sigma^2$. We define the overall received SNR as $\dot{\gamma}_{\hat{\boldsymbol{k}}} = P_T \left|\left|\boldsymbol{H}_{\hat{\boldsymbol{k}}}\right|\right|^2 /\sigma^2$, where $\boldsymbol{H}_{\hat{\boldsymbol{k}}}$ is the complex channel in the direction $\hat{\boldsymbol{k}}$. Finally, we define $\gamma_{\hat{\boldsymbol{k}}}$ as the final received SNR considered for use in computation of the channel capacity.

The SNRs for typical intended and unintended users for the signal $d_m(t)$ are given by

$$\begin{aligned} \gamma_{typical,\hat{\boldsymbol{k}}_m} &= \frac{P_T}{\sigma_m^2}\left|\left|\boldsymbol{H}_{\hat{\boldsymbol{k}}_m}\right|\right|^2 = \dot{\gamma}_{\hat{\boldsymbol{k}}_m}, \text{and} \\ \gamma_{typical,\hat{\boldsymbol{k}}_n} &= \frac{P_T}{\sigma_n^2}\left|\left|\boldsymbol{H}_{\hat{\boldsymbol{k}}_n}\right|\right|^2 \end{aligned} \tag{30}$$

Assuming that User 0 and User 1 have equivalent system noise and their wireless channel transfer functions have equal norms, there is no secrecy capacity in this system. Any secrecy capacity would be due to additional gain in the direction $\widehat{\boldsymbol{k}}_{\boldsymbol{m}}$ as compared to the direction $\widehat{\boldsymbol{k}}_{\boldsymbol{n}}$.

First, we compare this to a MIMO technique for establishing physical layer secrecy for a single transmitter-receiver pair called the Artificial Noise method or the Null-Space method proposed by Yang et al [5]. The Artificial Noise method or the Null-Space method diverts some fraction $\alpha \in [0,1]$ of the signal transmit power P_T to generating a second signal, typically only carrying noise, exclusively in the direction $\widehat{\boldsymbol{k}}_{\boldsymbol{n}}$, away from the intended user. This has the desired effect of reducing the SINR in the direction of the unintended user (User 1); however, the natural extension of this technique to transmit multiple signals requires halving the transmit time, thus halving the overall capacity of the system. The Artificial Noise method or Null-Space method has been shown to marginally outperform Time-division multiplexing (TDM) [5]. The SNRs for intended and unintended users for the signal $d_m(t)$ using this method are given by

$$\begin{aligned} \gamma_{Artificial\ Noise,\widehat{\boldsymbol{k}}_{\boldsymbol{m}}} &= \alpha \frac{P_T}{\sigma_m^2} \left|\left| \boldsymbol{H}_{\widehat{\boldsymbol{k}}_{\boldsymbol{m}}} \right|\right|^2 = \alpha \dot{\gamma}_{\widehat{\boldsymbol{k}}_{\boldsymbol{m}}}, \text{and} \\ \gamma_{Artificial\ Noise,\widehat{\boldsymbol{k}}_{\boldsymbol{n}}} &= \frac{\alpha P_T \left|\left| \boldsymbol{H}_{\widehat{\boldsymbol{k}}_{\boldsymbol{n}}} \boldsymbol{W}_{\boldsymbol{IS}} \right|\right|^2}{\frac{1-\alpha}{N-1} P_T \left|\left| \boldsymbol{H}_{\widehat{\boldsymbol{k}}_{\boldsymbol{n}}} \boldsymbol{W}_{\boldsymbol{AN}} \right|\right|^2 + \sigma_n^2}. \end{aligned} \tag{31}$$

By contrast, the proposed beamforming method for directional modulation coherently overlays a modulation and interfering signal over the original information-bearing signal, causing the SNR in the direction of the unintended user (User 1) to be dramatically reduced. For the proposed beamforming method, the SNRs for User 0 in the direction $\widehat{\boldsymbol{k}}_{\boldsymbol{m}}$ and User 1 in the direction $\widehat{\boldsymbol{k}}_{\boldsymbol{n}}$ are given by

$$\gamma_{\hat{\boldsymbol{k}}_{\boldsymbol{m}}} = \frac{P_T}{\sigma_m^2}\left|\left|\boldsymbol{H}_{\hat{\boldsymbol{k}}_{\boldsymbol{m}}}\right|\right|^{\mathbf{2}} = \dot{\gamma}_{\hat{\boldsymbol{k}}_{\boldsymbol{m}}}, \text{and}$$
$$\gamma_{\hat{\boldsymbol{k}}_{\boldsymbol{n}}} = \frac{1}{2}\left(\frac{P_T}{\sigma_n^2}\left|\left|\overline{\boldsymbol{H}}_{\hat{\boldsymbol{k}}_{\boldsymbol{n}}}\right|\right|^{\mathbf{2}} + \frac{P_T\left|\left|\overline{\boldsymbol{H}}_{\hat{\boldsymbol{k}}_{\boldsymbol{n}}}\right|\right|^{\mathbf{2}}}{2P_T\left|\left|\overline{\boldsymbol{H}}_{\hat{\boldsymbol{k}}_{\boldsymbol{n}}}\right|\right|^{\mathbf{2}} + \sigma_n^2}\right). \quad (32)$$

The secrecy capacities for typical broadcast, Artificial Noise, and the proposed methods as a function of the SNR of the signal intended for User 0 received by User 0, $\dot{\gamma}_{\hat{k}_m}$, are compared in Figure 4.4. The secrecy capacities for a typical system and a system using the proposed beamforming method for directional modulation assume a two-element array spaced by 0.75λ where the users are spaced by 40° about the boresight of the Base Station transmit array. Performance calculations for the Artificial Noise (Null-Space) method assumes a three-element array, as in [5]. The proposed beamforming method for directional modulation easily outperforms calculated performance for both the typical system and the system using the Artificial Noise method due to the fact that the original signal is modulated into an interferer at the PHY-layer in the direction $\widehat{\boldsymbol{k}}_{\boldsymbol{n}}$.

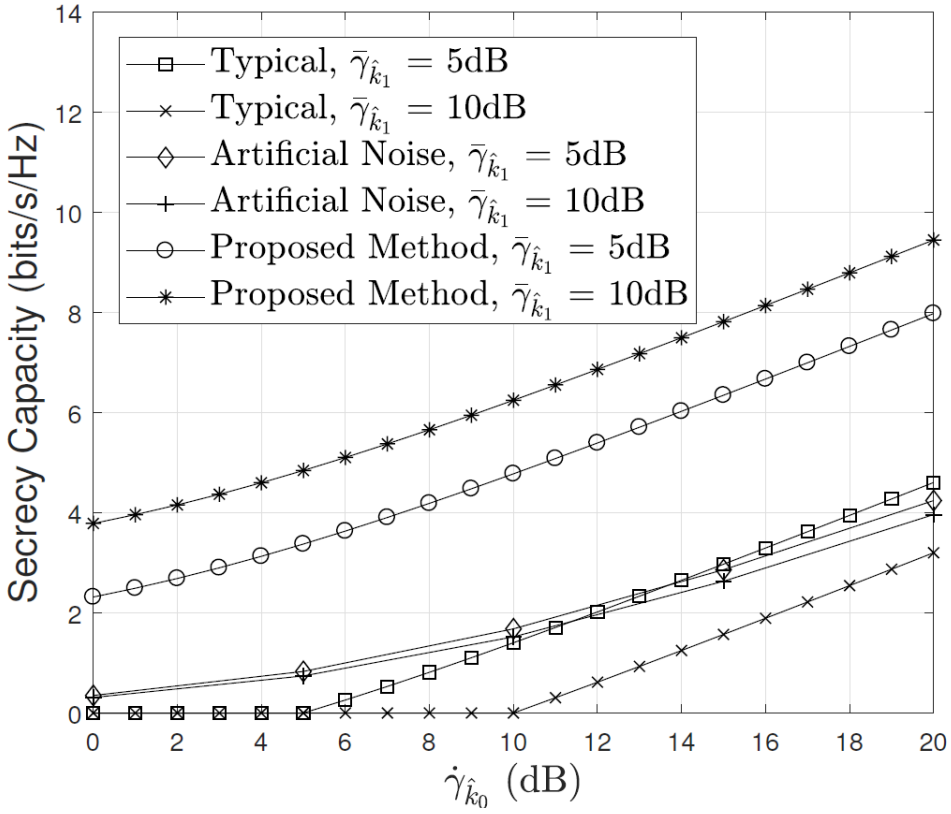

Figure 4.4: Comparison of the secrecy capacities for typical broadcast, Artificial Noise, and the proposed methods as a function of the SNR of the signal intended for User 0 received by User 0, $\dot{\gamma}_{\hat{k}_m}$. Performance calculations for the secrecy capacities for a typical system and a system using the proposed beamforming method for directional modulation assume a two-element array spaced by 0.75λ where the users are spaced by 40° about the boresight of the Base Station transmit array, whereas the performance calculations for the Artificial Noise (Null-Space) method assumes a three-element array, as in [5]. The proposed beamforming method for directional modulation easily outperforms calculated performance for both the typical system and the system using the Artificial Noise method.

4.2 Increasing the Capacity of Confidential Messages over Wireless Broadcast Channels

The proliferation of embedded devices attached to networks, commonly referred to as the Internet-of-Things (IoT), has driven wireless communications into commercial, military,

industrial, and personal devices, estimated to number in excess of 6 billion devices in 2016 and projected to exceed 20 billion devices by 2020 [75]. Given these staggering numbers, limited spatial and spectral resources, and the broadcast nature of wireless communications systems, it is unreasonable to expect privacy and security to be inherent in these device networks. Further, information and commands carried over these broadcast channels to IoT devices require security and privacy as they expand to include medical devices (both diagnostic and treatment), vehicles, and industrial control systems, just to name a few.

Despite the misleading description of wireless point-to-point links, we must consider the communications to and from such IoT devices to be broadcast channels; that is, when transmitting, anticipate both legitimate, intended receivers and illegitimate, unintended receivers, called eavesdroppers; reciprocally, when receiving, anticipate a multiple access environment, including both interference and intentional spoofing. Finally, we must enable IoT devices to effectively access broadcast channels while maintaining typically small size, light weight, and minimized power consumption.

For the single-user channel, Shannon famously described the information-theoretic channel capacity bound based on signal and noise entropies [76]. This work was extended to single-user MIMO systems [77] and broadcast channels [78]. Several bounds have been established for MIMO broadcast channels, providing a theoretical maximum achievable sum-rate channel capacity [17], [79], [80]. A technique dubbed “Dirty Paper Coding” was introduced by Costa [72] and later shown to achieve the Sato upper bound for MIMO broadcast channels [17] in the two-user case [73]. Further study has corroborated these claims from an information theoretic standpoint [81]–

[84], and extended the claims to provide bounds for the secrecy capacity of MIMO broadcast channels [85], [86].

The Dirty Paper Coding technique [72] is similar to the Artificial Noise method (Null-Space method), but is designed to accommodate multiple, independent, and legitimate information-bearing signals intended for multiple users. Dirty Paper Coding simultaneously transmits the two information-bearing signals, which reduces the SINR of each signal considerably at both users. To combat this loss of SINR, Dirty Paper Coding transmits a coded signal, $\boldsymbol{w_{DPC}} = \boldsymbol{W_{DPC}}\boldsymbol{u}$, using a precoding matrix, $\boldsymbol{W_{DPC}} \in \mathbb{C}^{N\times S}$, where N is the number of transmit antenna elements and S is the number of receivers considered. The $S\times 1$ codebook vector, $\boldsymbol{u}$, is constrained such that $E[\boldsymbol{u}\boldsymbol{u}^H] = \boldsymbol{I}_R$. The transmitted signal is constrained by the total output power such that $Tr(\boldsymbol{x}\boldsymbol{x}^H) \leq P_t$. The SINR of the information d_m at the primary intended receiver using dirty paper coding ($\gamma_{m,\hat{a}_m}^{DPC}$) is given by

$$\gamma_{m,\hat{a}_m}^{DPC} = \alpha \left|\left|\boldsymbol{v_k^H}(\widehat{\boldsymbol{a}}_m)\boldsymbol{w_{DPC}}\right|\right|^2 P_T = \alpha \left|\left|\boldsymbol{H}_{\widehat{\boldsymbol{a}}_m}\right|\right|^2 P_T, \tag{33}$$

for $\sigma_m = \sigma_n = 1$, given knowledge of the wireless channel transfer function $\boldsymbol{H}_{\widehat{\boldsymbol{a}}_m}$ and noncausal knowledge of the other signals transmitted in the codebook vector, $\boldsymbol{u}$. The parameter $\alpha \in [0,1]$ is a tunable parameter indicating the ratio of the transmitted power allocated to d_m and the total transmitted power P_T for the two-user scenario. The SINR of d_n at the same receiver is designed to be

$$\gamma_{n,\hat{a}_m}^{DPC} = \frac{(1-\alpha)\left|\left|\boldsymbol{H}_{\widehat{\boldsymbol{a}}_m}\right|\right|^2 P_T}{\alpha \left|\left|\boldsymbol{H}_{\widehat{\boldsymbol{a}}_m}\right|\right|^2 P_T + 1}; \tag{34}$$

however, since this receiver has noncausal knowledge of d_n, the interference caused by d_n is subtracted from the received signal. It should be noted that this scheme limits the utility of Dirty Paper Coding from a secrecy capacity standpoint, since one receiver requires non-causal knowledge of all the information-bearing signals.

The second user receives an interference-corrupted version of their signal, observing the first receiver's signal as interference, but without knowledge of d_m. The SINR of d_m at the unintended receiver using dirty paper coding ($\gamma_{m,\hat{a}_n}^{DPC}$) is given by

$$\gamma_{m,\hat{a}_n}^{DPC} = \frac{\alpha \left|\left|\boldsymbol{H}_{\hat{\boldsymbol{a}}_n}\right|\right|^2 P_T}{(1-\alpha) \left|\left|\boldsymbol{H}_{\hat{\boldsymbol{a}}_n}\right|\right|^2 P_T + 1}, \tag{35}$$

and the SINR of d_n at the same receiver is given by

$$\gamma_{n,\hat{a}_n}^{DPC} = \frac{(1-\alpha) \left|\left|\boldsymbol{H}_{\hat{\boldsymbol{a}}_n}\right|\right|^2 P_T}{\alpha \left|\left|\boldsymbol{H}_{\hat{\boldsymbol{a}}_n}\right|\right|^2 P_T + 1}. \tag{36}$$

It has been shown that Dirty Paper Coding achieves the Sato Bound for MIMO broadcast channel capacity [73], [82]; however, the ovarall secrecy capacity is limited by α and $\gamma_{m,\hat{a}_n}^{DPC}$.

We propose a novel coding technique implemented by the proposed beamforming method, first introduced in [67], and show that it can outperform the Dirty Paper Coding technique both in terms of sum rate capacity and secrecy capacity. We achieve this by using time-varying array steering vectors, violating the implicit assumption of available degrees of freedom supporting the proof of optimality of Dirty Paper Coding and its variants [73]. Further, rather than considering multiple users as interference channels [73], the proposed method implements a direction-

dependent overlay modulation, which controls co-channel interference generated by the transmitter in the direction of other users and thus greatly increases the achievable signal-to-interference-plus-noise ratio (SINR) in each channel. We also show that the proposed beamforming method can exceed the Sato Bound [17], which implicitly assumes no time-varying control over the wireless channel transfer function; however, the channel capacity using the proposed method remains well within the Shannon capacity limits. Since the proposed method implements an overlay modulation by time-varying the array steering vector, the Sato Bound [17] does not expressly apply to the proposed method; however the Sato Bound is currently accepted as the current state-of-the-art for sum-rate capacity in a wireless broadcast channel [73].

In further contrast to the Dirty Paper Coding method, the proposed directional modulation method is an overlay modulation scheme that seeks to simultaneously minimize the SINR of both signals at their respective unintended receivers, thereby increasing the achievable sum rate capacity and secrecy capacity. The SINR of d_m at the intended receiver using the proposed method is given by

$$\gamma_{m,\hat{a}_m}^{DM} = \left|\left|\boldsymbol{v}_k^H(\widehat{\boldsymbol{k}}_m)(\boldsymbol{w_0} + \boldsymbol{w_1})\right|\right|^2 \frac{P_T}{2} \tag{37}$$

and the SINR of d_n at the intended receiver is given by

$$\gamma_{n,\hat{a}_n}^{DM} = \left|\left|\boldsymbol{v}_k^H(\widehat{\boldsymbol{k}}_n)(\boldsymbol{w_0} + \boldsymbol{w_1})\right|\right|^2 \frac{P_T}{2}. \tag{38}$$

The interference terms are negligible, that is $\gamma_{n,\hat{a}_m}^{DM} \cong 0$ and $\gamma_{m,\hat{a}_n}^{DM} \cong 0$ if ε is chosen to be sufficiently small.

4.3 Secrecy Capacity in a Broadcast Channel

To the best of our knowledge, determining the capacity region and upper bound for the non-degraded MIMO broadcast channel is still an open problem. Several information theoretic bounds have been established [17], [79], [80] and used to prove the optimality of different coding techniques [73], [81]–[87]. Principally, the Dirty Paper Coding technique [72] was shown to be an optimal coding technique by achieving the Sato upper bound for MIMO broadcast channels in the two-user scenario [73].

We note here that the Sato bound is based on information theory, and does not account for the ability to time-vary the broadcast wireless channel transfer function by electrically steering the antenna array. In doing so, we take advantage of an additional degree of freedom, enabling us to transmit multiple messages simultaneously with sufficient efficiency to outperform the Dirty Paper Coding technique, which has been shown to be tight to the Sato bound in the two-user case. In fact, system models for MIMO and standard broadcast channel bounds may include, but do not take advantage of the direction-dependent and deterministic channel inherent to locally time-invariant, narrowband, line-of-sight, and minimal multipath assumptions, which are typical in array signal processing [1]. For example, in using information theoretic approaches to determining channel capacities, several references treat the MIMO channel purely as a realization of a random variable due to the possibility of significant and unpredictable multipath [17], [77], [73], [82], [83], [85], [87], [88], also called a Rayleigh fading channel. Here, we exploit the known array manifold embedded in the wireless channel transfer function matrix and show that the proposed method can

exceed the performance of Dirty Paper Coding, which achieves the Sato upper bound for MIMO broadcast channels. Numerical comparisons of these coding techniques are shown in Chapter 5.

Chapter 5

Simulation Results

To assess the performance of the proposed method for directional modulation using beamforming, we performed some simulations. First, we consider the cost of using the convex optimization with linear inequality constraints given by (13). Next, we consider the application of (13) to two scenarios: an array receiving a wireless power transfer signal that occupies the same spectrum as a desired information signal where the signals are spatially separated, and an array transmitting a signal that must be secured at the physical layer. By applying the time-varying steering vectors determined from (13), we demonstrate that an array is able to sufficiently separate signals while receiving such that a wireless power transfer signal can be diverted for harvesting using a diplexer with minimal impact to reception of the desired information signal. We also demonstrate that an array is not only able to secure the signal at the PHY-layer while transmitting, but also able to increase the broadcast channel capacity and secrecy capacity as compared to

currently accepted state-of-the-art methods. For each simulation, we implement a signal carrier frequency of 2.35GHz and a free-space path loss model.

5.1 Implementation Cost of the Proposed Beamforming Method

Simulation results of the convex optimization with linear inequality constraints given in (13) are shown in Figure 5.1 for various array manifolds. Specifically, an array consisting of two steerable antenna elements is considered with varied element spacing in wavelengths, δ_p. As a point of comparison, the peak array gain for a uniformly illuminated two-element array is approximately 3dB broadside to the array. Figure 5.1 shows the average array gain between the transmitter and two receivers while the transmit array is subject to time-varying steering vectors, $\boldsymbol{W}$. For this simulation, the primary direction of interest, $\widehat{\boldsymbol{k}}_{\boldsymbol{0}}$, is broadside to the array and the location of the second receiver, $\widehat{\boldsymbol{k}}_{\boldsymbol{1}}$, is varied. The array is subject to two complex steering vectors, $\boldsymbol{w_0}$ and $\boldsymbol{w_1}$, determined by the optimization in (13). The ability to achieve directional modulation, at least in the case of a simple two-element array, is clearly dependent on the array manifold. By varying the array element spacing δ_p, we are able to achieve directional modulation with adequate array gain across a wide field of regard. These results indicate that directional modulation can be leveraged as an overlay modulation technique to create two independent wireless channels by sacrificing less than half of the power in each direction and simultaneously making the entire spectral bandwidth available to both receivers.

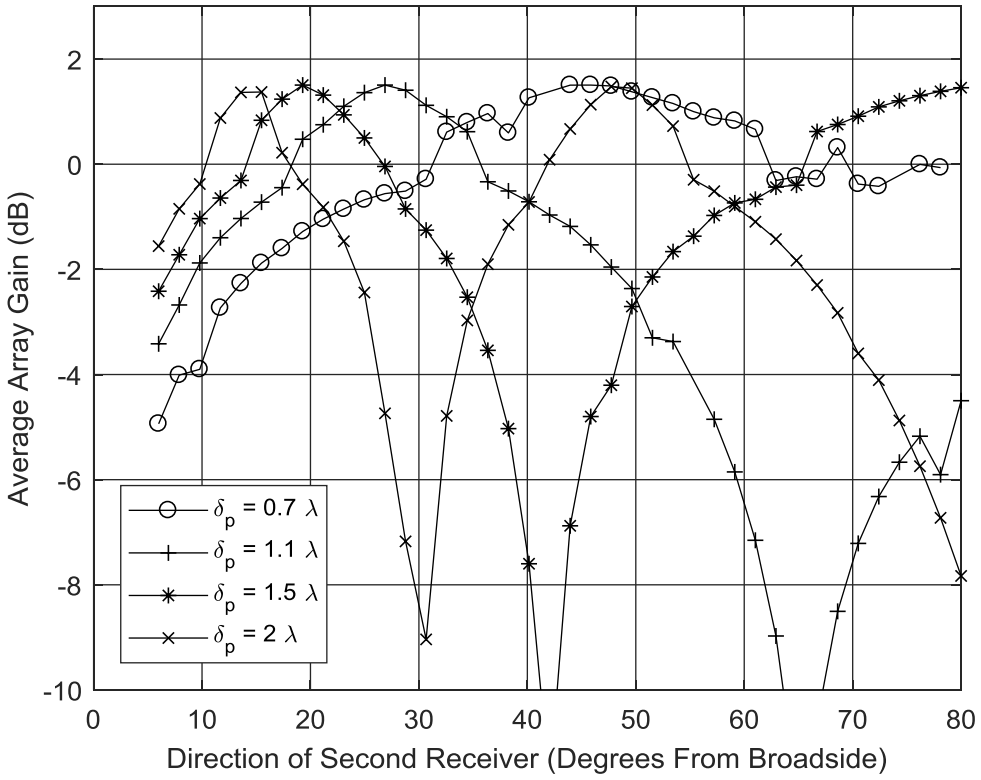

Figure 5.1: Curves of average loss in array gain in dB vs the direction of the second receiver in degrees from broadside for a two-element array with spacing δ_p. In this simulation, the array implements steering vectors resulting from the convex optimization in (13). Here, one receiver is located broadside to the array and the abscissa denotes the direction of the second receiver in degrees from broadside to the array. These results indicate that two independent messages can be sent in different directions more efficiently than by merely equally dividing the available power or bandwidth between the receivers.

We repeat this simulation for the directions of the two receivers, $\widehat{\boldsymbol{k}}_{\boldsymbol{0}}$ and $\widehat{\boldsymbol{k}}_{\boldsymbol{1}}$, equally spaced from broadside to the array. Curves in Figure 5.2 show the average array gain between the transmitter and two receivers while the transmit array is subject to the time-varying steering vectors, $\boldsymbol{W}$, for varied element spacing δ_p in wavelengths. For this simulation, the broadside of the array is aimed directly between the two receivers, and the spacing between the receivers is varied. As a point of comparison, the peak array gain for a uniformly illuminated two-element array is

approximately 3dB. We demonstrate the ability to achieve directional modulation with adequate array gain across a wide field of regard by varying the array element spacing δ_p.

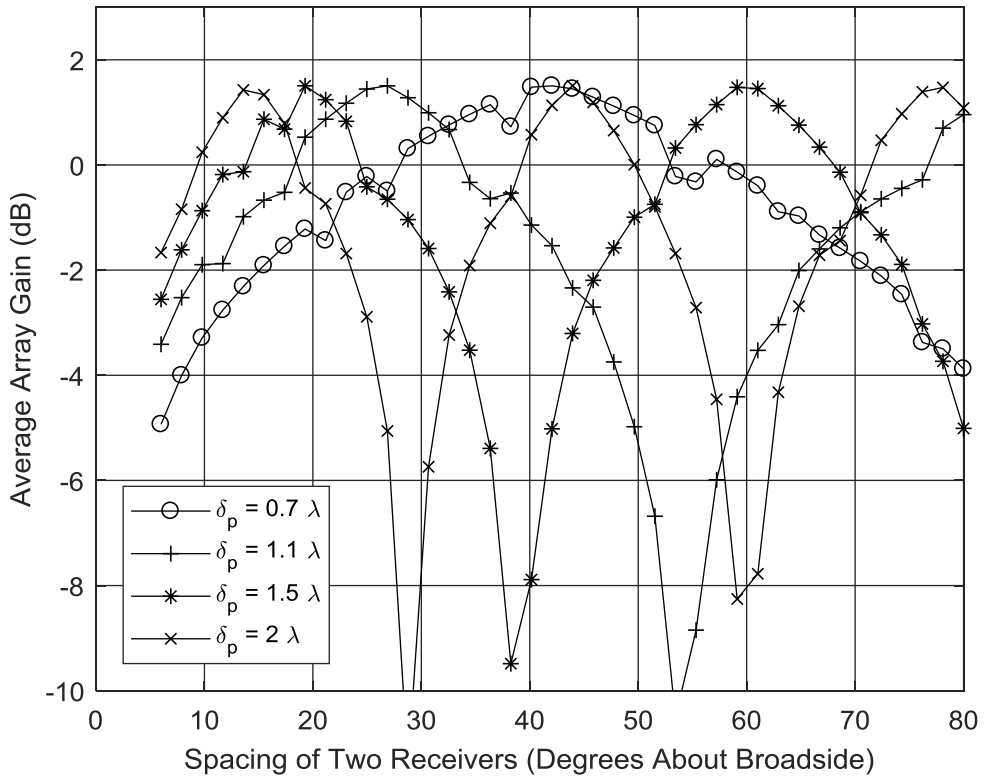

Figure 5.2: Curves of average loss in array gain in dB vs the separation of two receivers in degrees for a two-element array with spacing δ_p. In this simulation, the receivers are equally spaced from broadside to the array and the abscissa denotes spacing between the two receivers. The average loss in array gain is referenced to the ideal array gain of a two-element array at broadside. This plot indicates that two independent messages can be sent in different directions more efficiently than by merely equally dividing the available power or bandwidth between the receivers.

5.2 Simultaneous Wireless Information and Power Transfer

In this Section, we present simulation results indicating that the proposed method for directional modulation using beamforming can be used to effectively separate co-channel signals, even using an array with only two elements. In this simulation, a continuous wireless power transfer signal is centered on the same frequency with the same bandwidth as an information-bearing signal, but the signals are spatially separated. By properly overlaying Binary Offset Carrier (BOC) modulation only onto the wireless power transfer signal using the proposed beamforming method, it is sufficiently separated in frequency from the information-bearing signal. With sufficient frequency separation between the information-bearing signal and the wireless power transfer signal, the latter can be diverted for harvesting using a passive device, such as a diplexer, with minimal impact to reception and bit error rate of the information-bearing signal.

We simulate a simple two-element array with an inter-element spacing of 0.75 wavelengths attempting to separate an information-bearing signal from a wireless power transfer signal. Both signals arbitrarily occupy 20MHz of half-power bandwidth at 2.35GHz center frequency. We apply directional modulation using the proposed method to separate the signals. Despite the time-varying nature of the array steering vector, no discernable modulation or distortion and a minimal increase in bit error rate was observed on the information-bearing signal in the intended direction. Meanwhile, a variety of modulations, including direct sequence spread spectrum and binary offset

carrier, were applied to and observed on the wireless power transfer signal in the unintended direction.

5.2.1 Direct Sequence Spread Spectrum Modulation Overlay

The power spectrum of the unmodulated, undistorted information-bearing signal is shown in Figure 5.3 with a classical BPSK modulation spectrum with $20MHz$ of bandwidth. We compare it to the power spectrum when the information-bearing signal is overlaid with a pseudorandom spreading sequence with a spreading factor of 20. Clearly, we observe the peak power spectral density of the information-bearing signal at the center frequency approximately 20 times greater than the average power spectral density of the direct sequence spread spectrum modulated wireless power transfer signal. While we observe greater than an order of magnitude of suppression within the information bandwidth, we seek to achieve better suppression as explained next.

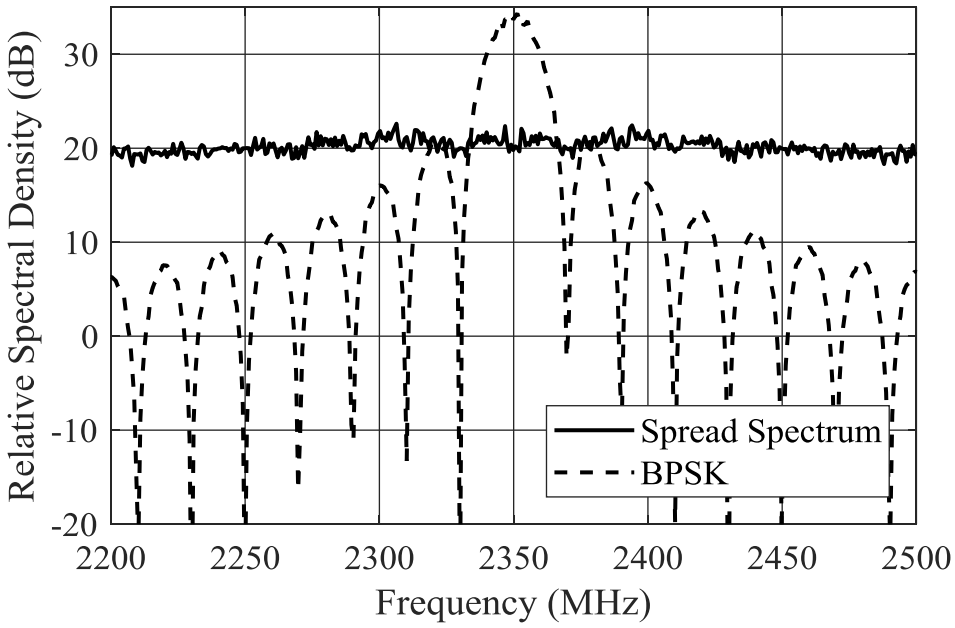

Figure 5.3: Simulation results showing a comparison of the spectrum of a BPSK-modulated signal with the spectrum when direct sequence spread spectrum modulation is overlaid onto the signal using directional modulation, applied by the proposed beamforming method. All of the signals used in these simulations are normalized to the same net power for meaningful comparison of power distribution.We assess the performance of the proposed method over a variety of spreading factors, each during a number of Monte Carlo trials. As expected with direct sequence spread spectrum modulation, larger spreading factors provide better suppression performance. Performance here is measured as the amount of wireless power transfer energy within the information bandwidth that has been shifted out of band. The results for direct sequence spread spectrum modulation are shown in Figure 5.4, indicating that close to 99% of the wireless power transfer signal energy can be spread out of band using a direct sequence spread spectrum overlay with a spreading factor of 100. We note that this would require updating the array steering vector 100 times faster than the information symbol rate, which would impose restrictions on the array hardware. We next show a technique to achieve similar suppression performance with a significantly reduced spreading factor.

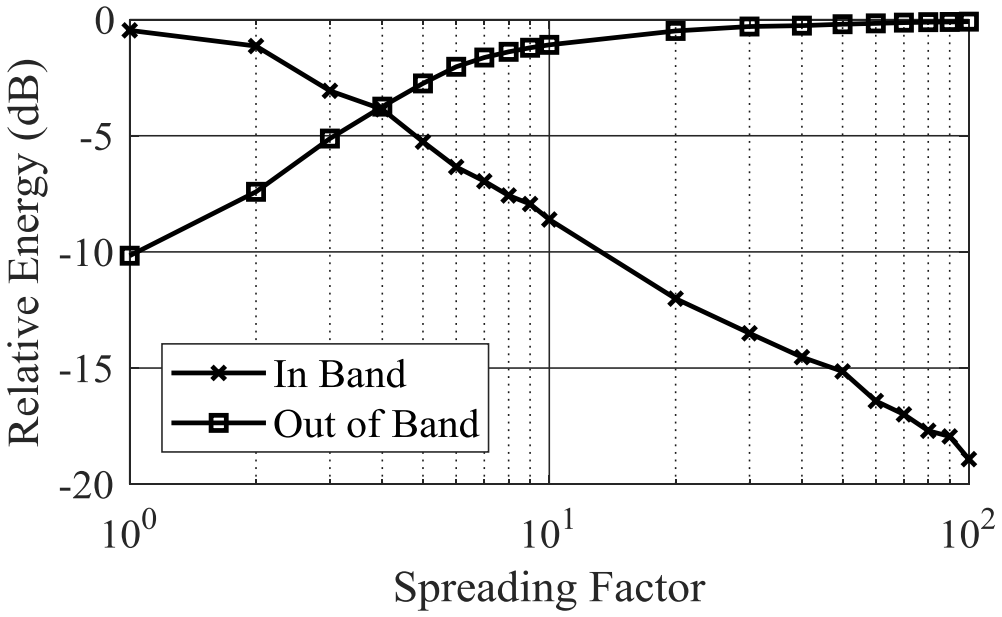

Figure 5.4: Simulation results of direct sequence spread spectrum modulation overlaid onto a BPSK-modulated wireless power transfer signal using directional modulation. These results show the relative amount of energy within the information bandwidth ("in-band") decreasing and spreading outside the information bandwidth ("out-of-band") based on the spreading factor used, which is defined as the ratio of the spread bandwidth to the information bandwidth.

5.2.2 Binary Offset Carrier Modulation Overlay

To achieve better suppression within the information bandwidth and spectrum shifting performance, binary offset carrier modulation was overlaid onto the wireless power transfer signal. The average power spectrum from a number of Monte Carlo trials while using a binary offset carrier with a spreading factor of 5 (BOC(10,2)) is shown in Figure 5.5. The original and undistorted BPSK-modulated signal is at the center frequency showing the information-bearing bandwidth while the BOC(10,2)-modulated wireless power transfer signal is shown with significantly reduced peak power spectral density at the carrier frequency and within the

information bandwidth. A bulk of the signal energy has shifted in spectrum by more than 5 times the information bandwidth.

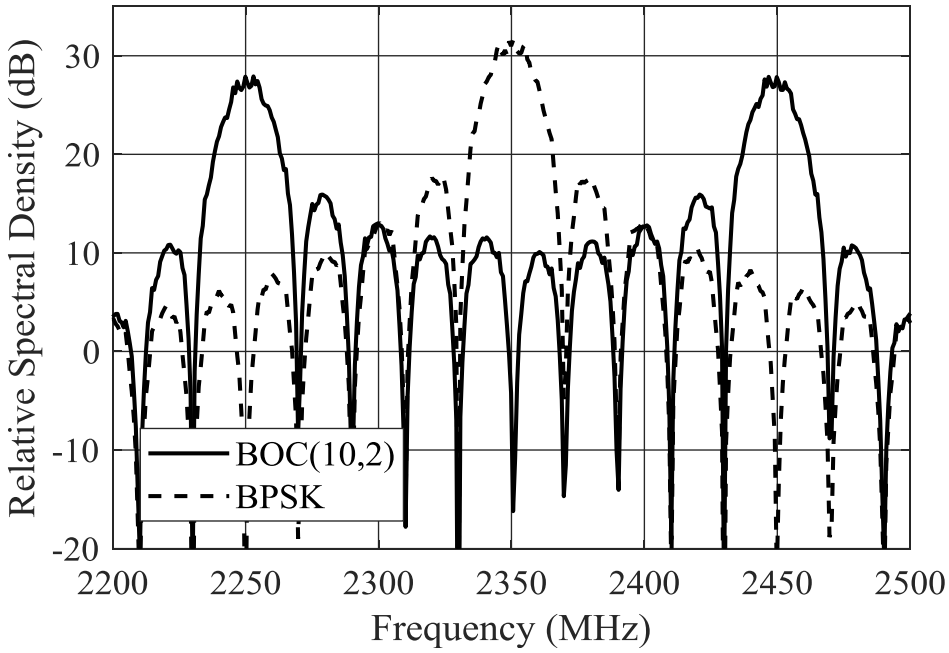

Figure 5.5: Simulation results showing a comparison of the power spectrum of a BPSK-modulated signal with the spectrum when binary offset carrier (BOC) modulation is overlaid onto the signal using directional modulation applied by the proposed beamforming method. In this example, both signals are centered at the same frequency, $2350MHz$.

As observed in Figure 5.6, binary offset carrier modulation shows considerably more favorable results, removing the same 99% of wireless power transfer signal energy out of band as direct sequence spread spectrum modulation, with only a spreading factor of 10. Overlaying BOC(10,2) modulation using the proposed technique would require significantly less complex array hardware since the array steering vectors would need to be updated an order of magnitude less frequently for the same performance. Simulation results show that binary offset carrier modulation with a spreading factor of 100 can achieve greater than 40dB reduction of wireless

power transfer energy within the information bandwidth by shifting the energy out of band, to where it can be harvested using conventional circuitry.

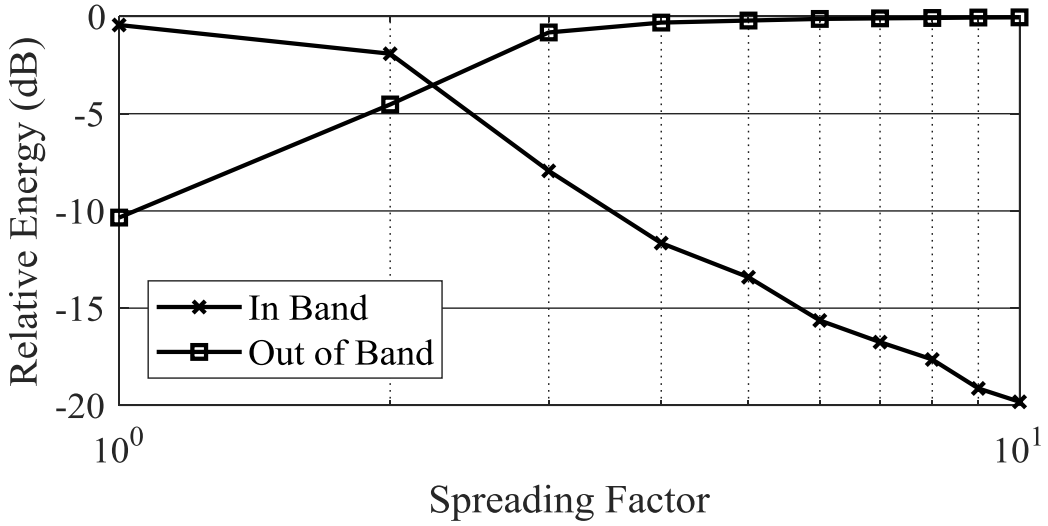

Figure 5.6: Simulation results of direct binary offset carrier modulation overlaid onto a BPSK-modulated wireless power transfer signal using directional modulation. These results show the relative amount of energy within the information bandwidth ("in-band") decreasing and spreading outside the information bandwidth ("out-of-band") based on the spreading factor used, which is defined as the ratio of the spread bandwidth to the information bandwidth.

5.3 Disguising Transmissions for Physical Layer Secrecy

In this Section, we provide simulation results indicating that directional modulation using only the proposed passive beamforming method can provide additional physical layer security by modulating the information-bearing signal into a valid, spoofed signal only in the direction of the eavesdropper. Not only does this method of selectively overlaying modulation reduce the SNR of the information-bearing signal in the direction of the eavesdropper, but it even moreso reduces the

SINR of information-bearing signal by replacing it with an arbitrarily different signal. Throughout this section, the transmitter considered is an array of 2 elements spaced 0.75 wavelengths apart. The intended receiver is located broadside to the transmitter array in the direction $\widehat{\boldsymbol{k}}_{\boldsymbol{m}}$, and the eavesdropper is located 30° from broadside to the transmitter array in the direction $\widehat{\boldsymbol{k}}_{\boldsymbol{n}}$.

A randomly generated binary information sequence denoted by $d_m(t)$ is modulated and routed to each array element, reproduced in Figure 5.7. Then, the array steering vector $\boldsymbol{w}(t)$ is determined from (13) and modulated according to the exclusive disjunction of the genuine binary information sequence and the spoofed binary information sequence, $d_n(t)$, given by $d_m(t) \oplus d_n(t)$. The bit error rates are recorded at the receiver in the direction $\widehat{\boldsymbol{k}}_{\boldsymbol{m}}$ and at the eavesdropper in the direction $\widehat{\boldsymbol{k}}_{\boldsymbol{n}}$ for a variety of bit energy to noise ratios, using $d_m(t)$ as the signal template for the receiver, and $d_n(t)$ as the signal template for the eavesdropper. Otherwise static channel coefficients were assumed for this simulation, and a line of sight channel model free of multipath and dispersion is used.

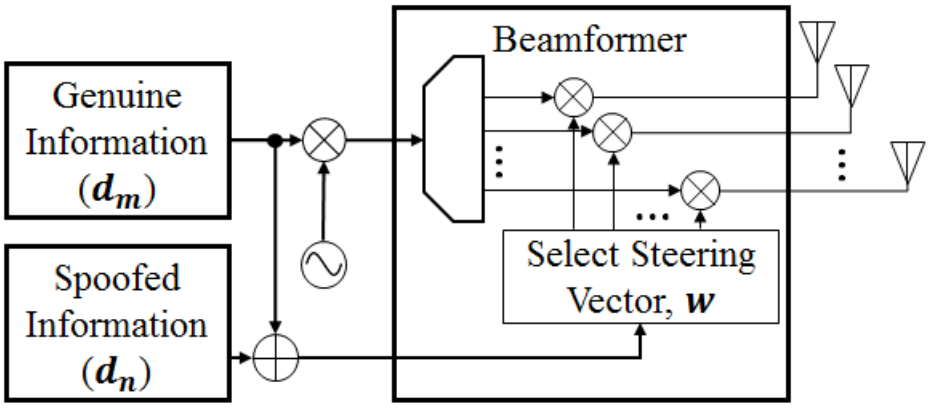

Figure 5.7: Schematic diagram showing a genuine binary information sequence, d_m being sent to the beamformer which is modulated according the exclusive disjunction of d_m and d_n. This results in the genuine information sequence, d_m, being transmitted in the direction $\hat{k}_m$, and the spoofed information sequence, d_n, being transmitted in the direction $\hat{k}_n$. This directional modulation technique provides physical layer security since the genuine information sequence, d_m, becomes unrecoverable in the direction $\hat{k}_n$.

The simulated bit error rates are recorded at the receiver in the direction $\hat{\boldsymbol{k}}_{\boldsymbol{m}}$ and at the eavesdropper in the direction $\hat{\boldsymbol{k}}_{\boldsymbol{n}}$ for a variety of bit energy to noise ratios are shown in Figure 5.8. The performance of the array using the proposed beamforming method for directional modulation is compared to the theoretical performance of an otherwise identical single element transmitter, and an otherwise identical, ideal two-element array transmitter without time-varying beamforming. The performance results indicate that bit error rate achievable using the propsed method is higher than for an ideal array steered towards one of the receivers; however, the bit error rate achievable by directional modulation outperforms the single element transmitter. It should be noted that the ideal two element array must be steered towards only one of the receivers, and must time division multiplex to address both receivers independently, which provides no additional physical layer security. Using the proposed method, we achieve low bit error rates for the respective, independent information signals in both the direcrtion of the recevier and the

eavesdropper. We should also note that the bit error rate performance achieved is highly dependent of the array manifold for this geometry, as shown in Figure 5.1 and Figure 5.2. These results indicate that an array transmitter can establish secrecy for a transmitted signal at the physical layer using only beamforming by spoofing eavesdroppers and sacrificing less than half of the ideal array gain in the both directions.

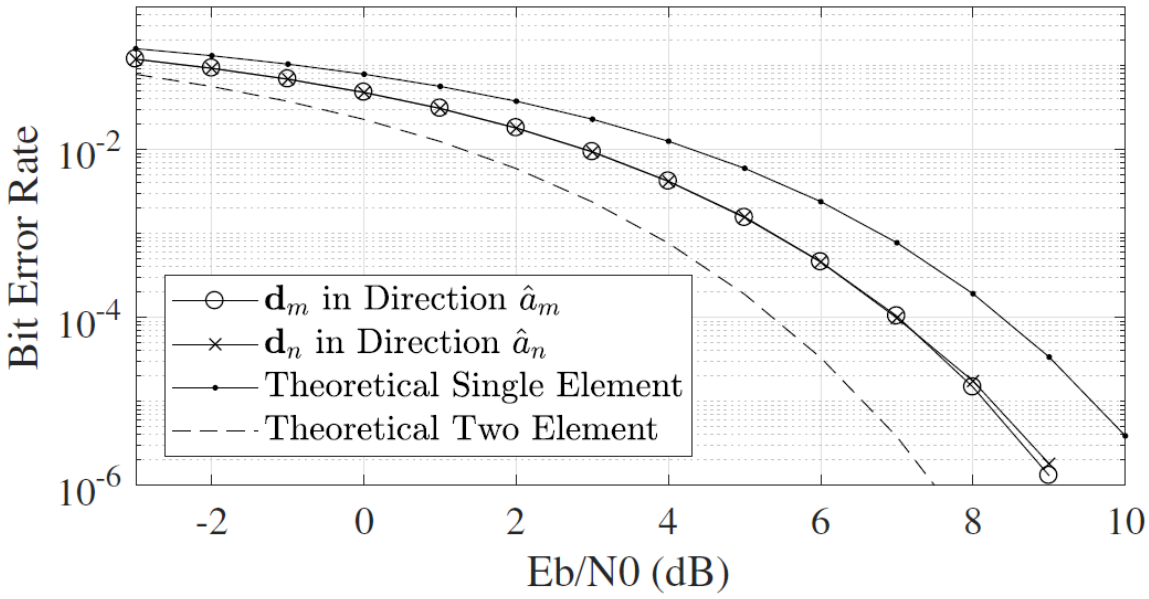

Figure 5.8: Simulation of bit error rates for BPSK modulation applied using directional modulation in the directions $\hat{\boldsymbol{a}}_{\boldsymbol{m}}$ and $\hat{\boldsymbol{a}}_{\boldsymbol{n}}$ compared to bit error rates for single-channel BPSK without beamforming.The data sent in the direction $\hat{\boldsymbol{a}}_{\boldsymbol{n}}$ is independent of the data sent in the direction $\hat{\boldsymbol{a}}_{\boldsymbol{m}}$, and only modulated by beamforming.

For these simulations, randomly generated binary information sequences intended for both the receiver and eavesdropper were used for these simulations to show that the signal received by the eavesdropper can be independently and arbitrarily manipulated from the original signal. We recognize that depending on the signal parameters and concept of operations, the spoofed signal may closely resemble the genuine signal.

5.4 Increasing the Capacity of Confidential Messages over Wireless Broadcast Channels

We executed several simulations to assess the sum-rate capacity and secrecy capacity performance of the proposed beamforming method for directional modulation. First, we compute the achievable capacity region for a two-user directional modulation scenario using the system model reproduced in Figure 5.9 and the proposed beamforming method. We compare this performance to theoretical bounds and the current state-of-the-art coding approaches for MIMO broadcast channels assuming narrowband, static, direct line-of-sight channels. Next, we compare the achievable multi-user secrecy capacity of directional modulation to these same published techniques. For all simulations, the time-varying steering vectors for directional modulation are determined from the optimization in (13) and implemented as shown in Figure 5.10.

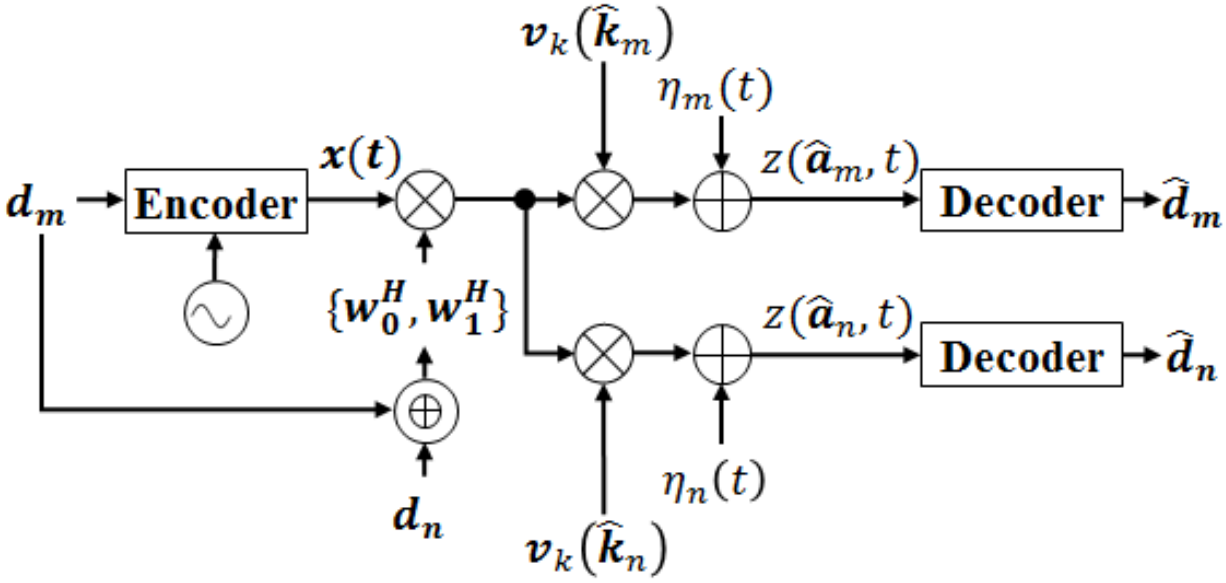

Figure 5.9: Graphical representation of the signal model for implementation of directional modulation in the two-user scenario. The information, d_m, is phase-modulated and encoded onto a carrier signal and transmitted by the array. The array steering vector is time-varied per the exclusive disjunction between the information d_m and the information d_n. Given the known array manifold in the directions $\hat{\boldsymbol{k}}_{\boldsymbol{m}}$ and $\hat{\boldsymbol{k}}_{\boldsymbol{n}}$, and the appropriately designed steering vectors $\boldsymbol{w}_0^{\boldsymbol{H}}$ and $\boldsymbol{w}_1^{\boldsymbol{H}}$, the information signal decoded in the direction $\hat{\boldsymbol{k}}_{\boldsymbol{m}}$ yields d_m, and the information signal decoded in the direction $\hat{\boldsymbol{k}}_{\boldsymbol{n}}$ yields d_n.

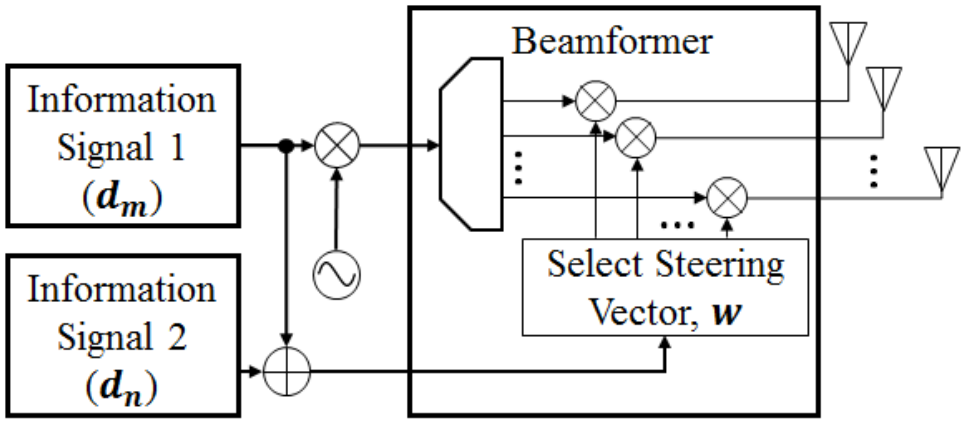

Figure 5.10: Schematic diagram showing two genuine binary information sequences, d_m and d_n being transmitted in the directions $\hat{k}_m$ and $\hat{k}_n$, respectively. The beamformer time-varies the array steering vector per the exclusive disjunction of d_m and d_n. This directional modulation technique enables the simultaneous transmission of d_m and d_n with high sum-rate capacity.

For the purposes of this simulation, we assume that each receiver separately calibrates the symbol decision threshold for the received constellation based on the first few received symbols, as typically done in practice with known pilot sequences. The signal-to-noise ratio (SNR) is measured from the simulated received symbols, and the mean SNR of all symbols to each receiver is reported. The achievable performance of the transmit array using the proposed beamforming method is highly dependent on the array manifold, which includes the array element spacing δ_p, the spatial separation of the receivers in question $\Delta\theta$, and the implementation loss parameter ε. We exercised and explored these parameters through each of the simulations presented.

Considering the terminology outlined in Figure 5.11, we identify two receivers, User 0 and User 1, each the legitimate, intended recipient of a confidential message. Both receivers are susceptible to interference from the other confidential message, and capable of eavesdropping on the other confidential message. In order to assess the effectiveness of the proposed beamforming method for broadcasting confidential messages, we consider the secrecy capacity introduced by Barros [74], and slightly modified here as

$$C_m = \begin{cases} C_{m,\hat{\boldsymbol{a}}_m} - C_{m,\hat{\boldsymbol{a}}_n}, & \gamma_{m,\hat{\boldsymbol{a}}_m} > \gamma_{m,\hat{\boldsymbol{a}}_n} \\ 0, & \gamma_{m,\hat{\boldsymbol{a}}_m} \leq \gamma_{m,\hat{\boldsymbol{a}}_n} \end{cases}, \tag{39}$$

where C_m is the secrecy capacity of the message $d_m(t)$, $C_{\boldsymbol{m},\hat{\boldsymbol{a}}_m}$ is the acheivable channel capacity per unit bandwidth of the intended recipient of $d_m(t)$ in the direction $\hat{\boldsymbol{a}}_m$ given by $C_{m,\hat{\boldsymbol{a}}_m} = \log_2(1 + \gamma_{m,\hat{\boldsymbol{a}}_m})$, $\gamma_{\boldsymbol{m},\hat{\boldsymbol{a}}_m}$ is the SINR of $d_m(t)$ at the intended recipient of $d_m(t)$, $C_{m,\hat{\boldsymbol{a}}_n}$ is the acheivable channel capacity per unit bandwidth of the unintended recipient of $d_m(t)$ in the direction $\hat{\boldsymbol{a}}_n$ specific to the signal $d_m(t)$, and $\gamma_{n,\hat{\boldsymbol{a}}_m}$ is the SINR of $d_m(t)$ at the unintended

recipient. We can similarly compute the secrecy capacity for the second message, $d_n(t)$ as C_n. The sum-rate secrecy capacity of the system is simply given as $C_S = C_m + C_n$.

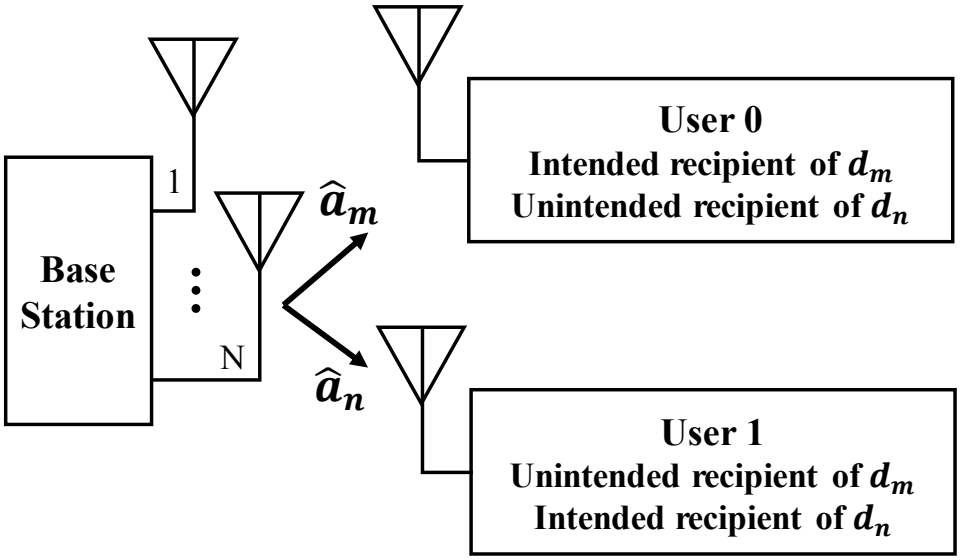

Figure 5.11: Diagram of Base Station transmitter array servicing User 0 and User 1, which are spatially separated with respect to the transmitter array. The Base Station possesses two messages: d_m intended for User 0 and d_n intended for User 1. Due to the broadcast nature of the Base Station and expected wireless channels, we expect that both messages are perceptible by their respective unintended receivers.

To maximize the sum-rate secrecy capacity of the system, we must simultaneously maximize the SINR of each signal at the respective intended receiver while minimizing the SINR of each signal at the respective unintended receiver. We have shown that directional modulation inherintly provides this simultaneous maximizing and minimizing of SINRs in contrast to other MIMO broadcast coding techniques. A typical array transmitter may use beamforming to focus a signal onto an intended user and steer a null towards the direction of the unintended user, maximizing the acheivable secrecy capacity for that particular signal; however, half of the secrecy capacity is sacrificed to similarly transmit the second message. This simple trade-off, also refered to as Time-

division multiplexing (TDM), establishes the lower achievable threshold for performance comparison.

First, we compare the simulated broadcast performance of the proposed beamforming method for directional modulation to the Dirty Paper Coding achievable rate region, due to the complexity in computing the Sato upper bound for MIMO broadcast channels [17], since Dirty Paper Coding achieves the Sato Bound for MIMO broadcast channel capacity [73], [82]. Using Dirty Paper Coding, an achievable rate vector for the ith of K users is given by [89]

$$R_{\pi(i)}^{DPC} = log\left(\frac{\left|\boldsymbol{I_N} + \boldsymbol{H_{\pi(i)}}\left(\sum_{\boldsymbol{j\geq i}} \boldsymbol{\Sigma_{\pi(j)}}\right)\boldsymbol{H_{\pi(i)}^H}\right|}{\left|\boldsymbol{I_N} + \boldsymbol{H_{\pi(i)}}\left(\sum_{\boldsymbol{j>i}} \boldsymbol{\Sigma_{\pi(j)}}\right)\boldsymbol{H_{\pi(i)}^H}\right|}\right), for\ i = 1, \dots, K, \tag{40}$$

for any positive semidefinite covariance matrices satisfying $Tr(\Sigma_1, \dots, \Sigma_K) < P_T$ and MIMO channel matrix $\boldsymbol{H}$, where $\boldsymbol{I}_N$ is the identity matrix of size N. The achievable capacity region using Dirty Paper Coding is the convex hull of the union of all achievable rate vectors given in (40).

Steering vector solutions for a two-element transmit array and two spatially separated users are computed using the convex optimization in (13) for varying angular separation of users, $\Delta\theta$. Using the proposed beamforming method for directional modulation, an achievable rate vector for the user in the direction $\widehat{\boldsymbol{k}}_{\boldsymbol{r}}$ is given by

$$R_r^{DM} = \frac{\mathbf{1}}{\mathbf{2}} log\left(\left(1 + \frac{\boldsymbol{\beta_{r,0}P_T}}{\boldsymbol{\eta_r}}\right)\left(1 + \frac{\boldsymbol{\beta_{r,1}P_T}}{\boldsymbol{\eta_r}}\right)\right), \tag{41}$$

where $\beta_{r,s}$ is a measure of the loss from the maximum possible array gain, given by

$$\beta_{r,s} = 1 - \left|\boldsymbol{v_k^H}\left(\widehat{\boldsymbol{k}}_{\boldsymbol{r}}\right)\boldsymbol{w}_s\right|. \tag{42}$$

The achievable rate vectors and, consequently, the broadcast channel capacity are dependent on the array manifold, indicating that the proposed directional modulation technique may not outperform other techniques for every given array and receiver geometry. Figure 5.2 shows the average achievable loss of array gain β, for various array manifolds given that boresight of the array is aimed in between two receivers. The proposed beamforming method for directional modulation is generalized for arrays with an arbitrary number of elements and arbitrary receiver locations. Of note is that an average array loss of $3dB$ would have equivalent channel capacity performance to the simple time-division multiplexing (TDM) scheme for two receivers.

The resulting, achievable broadcast channel rates for each user by using the proposed method are shown in Figure 5.12 for various array element spacing, δ_p, and spatial separation of the receivers, $\Delta\theta$. The Dirty Paper Coding achievable rate region is computed as in (40) and shown in Figure 5.12 for comparison against achievable rates for the proposed beamforming method. Of note is that there are many array and receiver geometries where the achievable capacity using the proposed method is beyond the achievable capacity of the Dirty Paper Coding scheme, which has been considered an optimal coding scheme for non-time-varying channels [73]. We submit that prior discussions have conflated time-varying wireless channel transfer functions, such as fading channels treated as random variables, with time-varying spatial coding schemes, which we have used here.

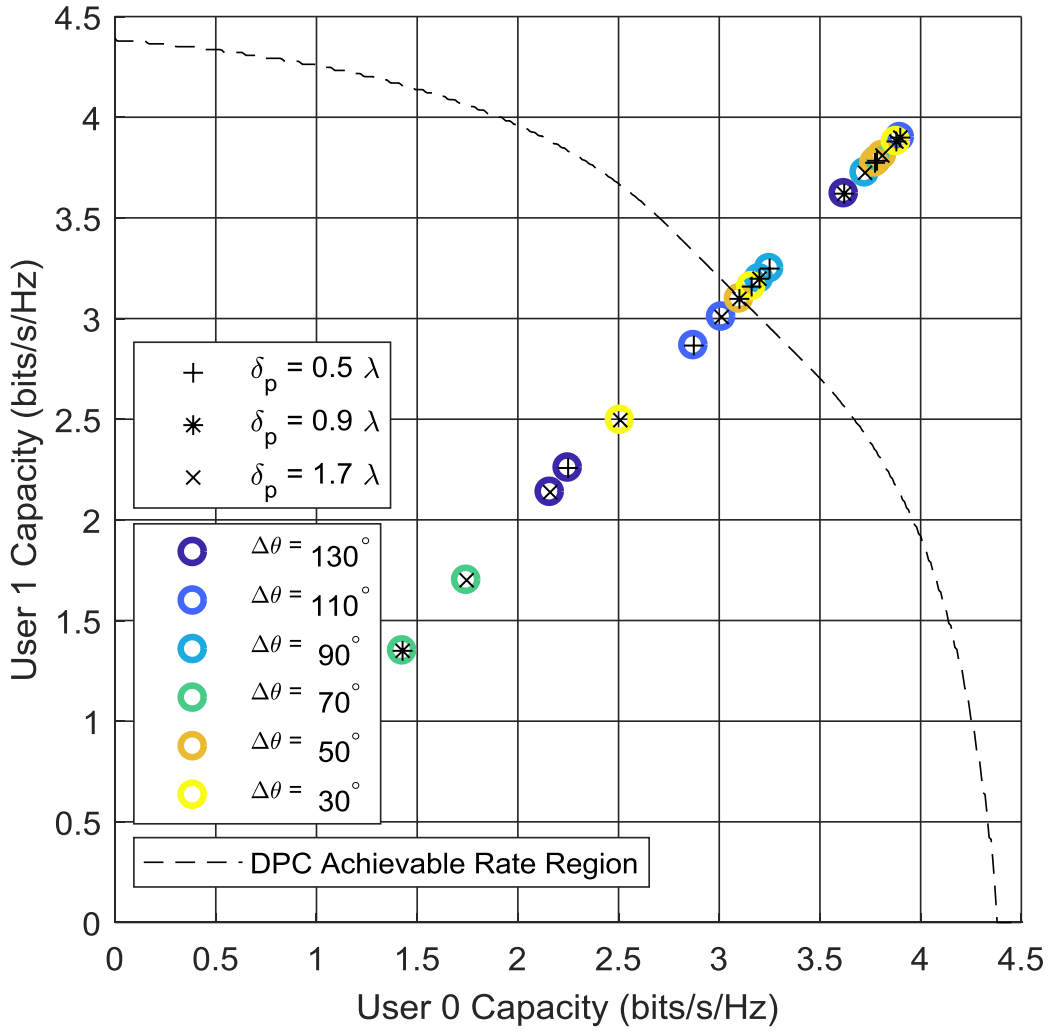

Figure 5.12: Maximum achievable broadcast channel capacities in bits/s/Hz for a two-element array transmitting to two users. The element spacing in the array, δ_p in wavelengths, and the spatial separation of the receivers is varied, showing the dependence of the sum-rate broadcast channel capacity performance on the array manifold. The points shown are solutions to the optimization in (13) and can exceed the Dirty Paper Coding (DPC) achievable rate region in a broadcast channel given the proper system geometry. Here, the DPC achievable rate region is tight to the Sato upper bound for MIMO broadcast channels.

The benefits of increased achievable sum-rate capacity due to the proposed beamforming method for directional modulation are clear, and stem from the fact that the implementation of the overlay modulation using time-varying array steering vectors produces minimal interference to either User from message intended for the other User. For these simulation results, the efficiency

metric, ε, used in the optimization in (13) is selected as $\varepsilon = 0.05$, which corresponds to a negligible modulation error ratio of $-26dB$. Consequently, these achievable capacities have the added benefit of being inherently confidential at the physical layer, leading to even greater performance in secrecy capacity.

5.5 Robustness of the Proposed Method to Angle and Frequency

We have demonstrated the dependence of the performance of the proposed beamforming method on the array manifold. A practical consideration is the performance of the steering vectors designed using (13) for a single frequency, a fixed element spacing, and for two receivers at fixed locations when the operating frequency changes or the receivers' locations are known only to finite accuracy. While the steering vectors can be recomputed for changing center frequency, if the directions towards both receivers is not precisely known or is slowly time-varying, constantly re-computing the steering vectors becomes both impractical and ineffective. Further, in the case of secrecy and physical layer security, it is useful to know the spatial extents to which the confidential signals are recoverable by unknown eavesdroppers.

To this end, we simulate the system describe in Figure 5.11 using the signal model shown in Figure 5.9. The optimization in (13) is used to compute the steering vectors for an array with two elements spaced at 1.1λ, operating at a center frequency of $2.4GHz$. Here, User 0 is located broadside to the two-element array, and User 1 is located $20°$ from broadside. Figure 5.13 shows a greyscale image of the phase modulation achieved in degrees when the steering vectors are time-

varied, with the average array gain contour overlay. Of note is that the transition between regions where modulation is applied and is not applied falls into either a peak or a null of the array gain pattern. Further, we note that the precise location of both Users is not required since this particular steering vector design allows for at least $15°$ of uncertainty in the direction of both Users at the design frequency. Further, if the operating frequency is changed, the modulation regions hold sufficiently stable over more than $2GHz$. Finally, we note that the modulation region for the User located $20°$ from broadside is also observable $20°$ from broadside opposite the User. This can be mitigated by designing a set of steering vectors that assumes 3 Users, one at $+20°$ from broadside, one at broadside, and one at $-20°$ from broadside. The design and implementation method for designing steering vectors with 3 Users is given in Figure 2.2 and (15).

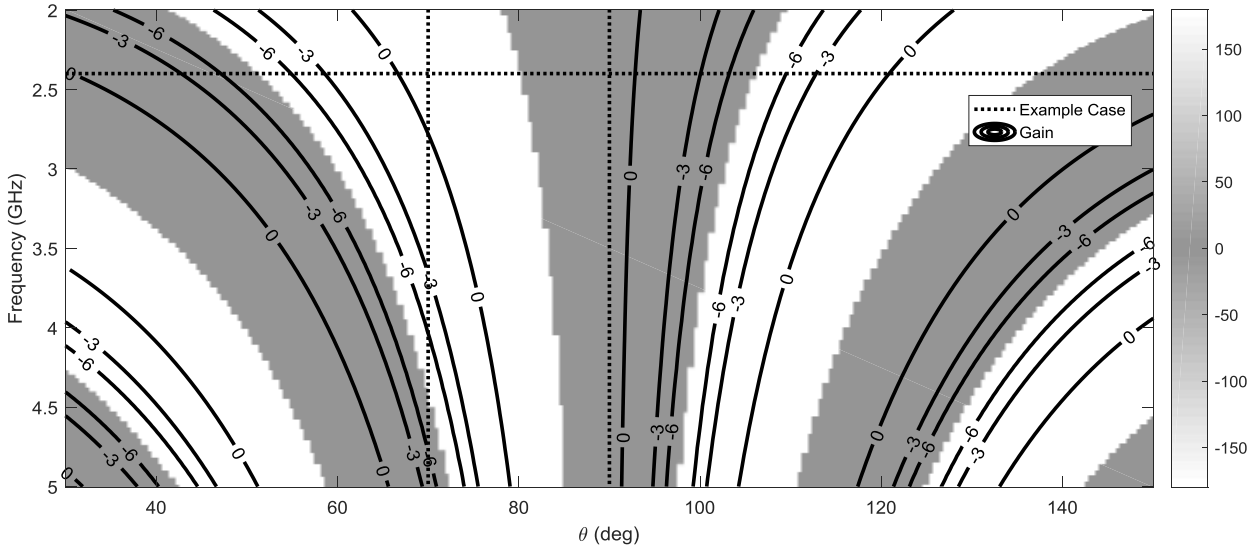

Figure 5.13: Greyscale image indicating the direction-dependent phase modulation in degrees due to time-varying the steering vector state for the array. Directional modulation is implemented using a two-element array spaced by 1.1λ at $2.4GHz$. Dotted lines show an example operating point at $2.4GHz$ with one User at broadside and the other at $20°$ from broadside. The contour indicates the achieved array gain using the proposed method.

We repeat the simulation and use the optimization in (13) to compute the steering vectors for an array with two elements spaced at 1.1λ, operating at a center frequency of $2.4GHz$. Here, we have modified the location of User 0 and User 1, such that they are separated by 5° and are both off-broadside. Figure 5.14 shows a greyscale image of the phase modulation achieved in degrees when the steering vectors are time-varied, with the average array gain contour overlay. Of note here is that the transition between regions where modulation is and is not applied falls exclusively into a null of the array gain pattern. Further, we show here that the region where directional modulation is applied is extremely narrow compared to where directional modulation is applied, less than 5°. This can be advantageous for a confidential communication signal that must be spoofed in all other directions, or in a scenario where most of the incident energy outside of a designed direction is to be used for power harvesting. We also show that the designed steering vectors here are sensitive to the operating frequency given that the two Users are close in proximity. Finally, we note again here that a unique modulation region can be designed by pursuing a set of steering vectors that assumes 3 Users, particularly by using the design and implementation method given in Figure 2.2 and (15).

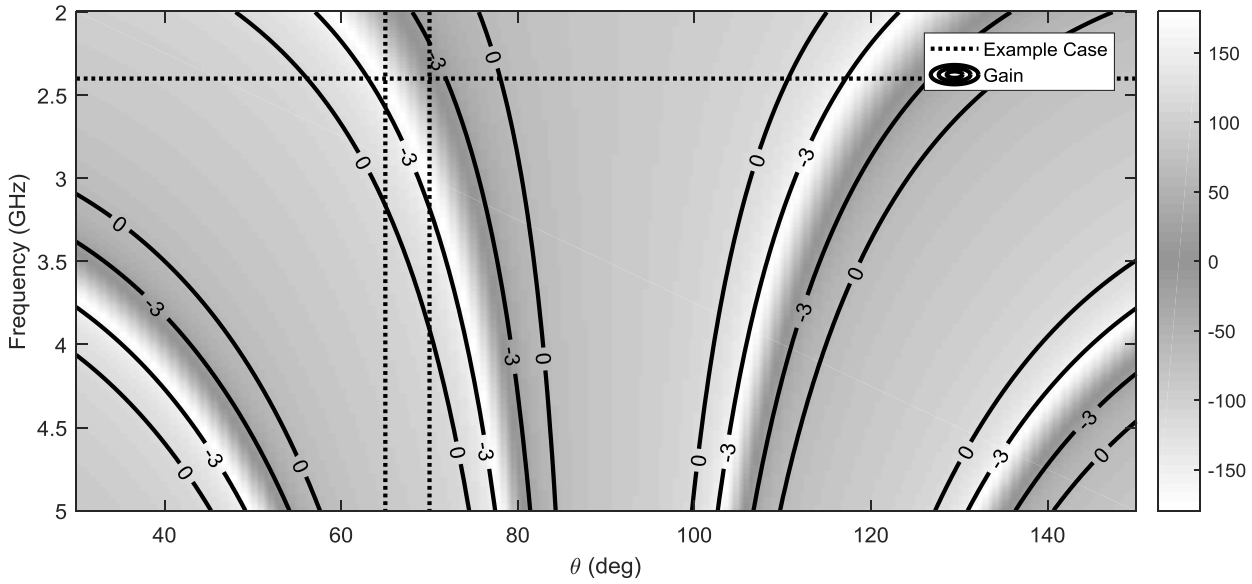

Figure 5.14 Greyscale image indicating the direction-dependent phase modulation in degrees due to time-varying the steering vector state for the array. Directional modulation is implemented using a two-element array spaced by 1.1λ at $2.4GHz$. Dotted lines show an example operating point at $2.4GHz$ with Users separated by 5°. The contour indicates the achieved array gain using the proposed method. The narrow modulation regions can be particularly advantageous for a confidential communication signal that must be spoofed in all other directions, or where most of the incident energy on the array is to be used for power harvesting.

We again repeat the simulation and use the optimization in (13) to compute the steering vectors for an array with two elements spaced at 3λ, operating at a center frequency of $2.4GHz$. Here, we have again modified the location of User 0 and User 1, such that they are separated by 10° and one is located broadside to the array. Figure 5.15 shows a greyscale image of the phase modulation achieved in degrees when the steering vectors are time-varied, with the average array gain contour overlay. Of note here is that the transition between regions where modulation is and is not applied is particularly sharp. Again, we show here that the regions where directional modulation is applied repeats, and can be mitigated by pursuing a set of steering vectors that assumes 3 Users, particularly by using the design and implementation method given in Figure 2.2 and (15). The repetitive pattern below can be particularly useful where the array is in receive mode

and designed for simultaneous wireless information and power transfer. The regularly spaced and repetitive regions can be advantageous to a receiver with wireless power transfer transmitters and information transmitters periodically spaced, such as in the layout shown in Figure 3.2.

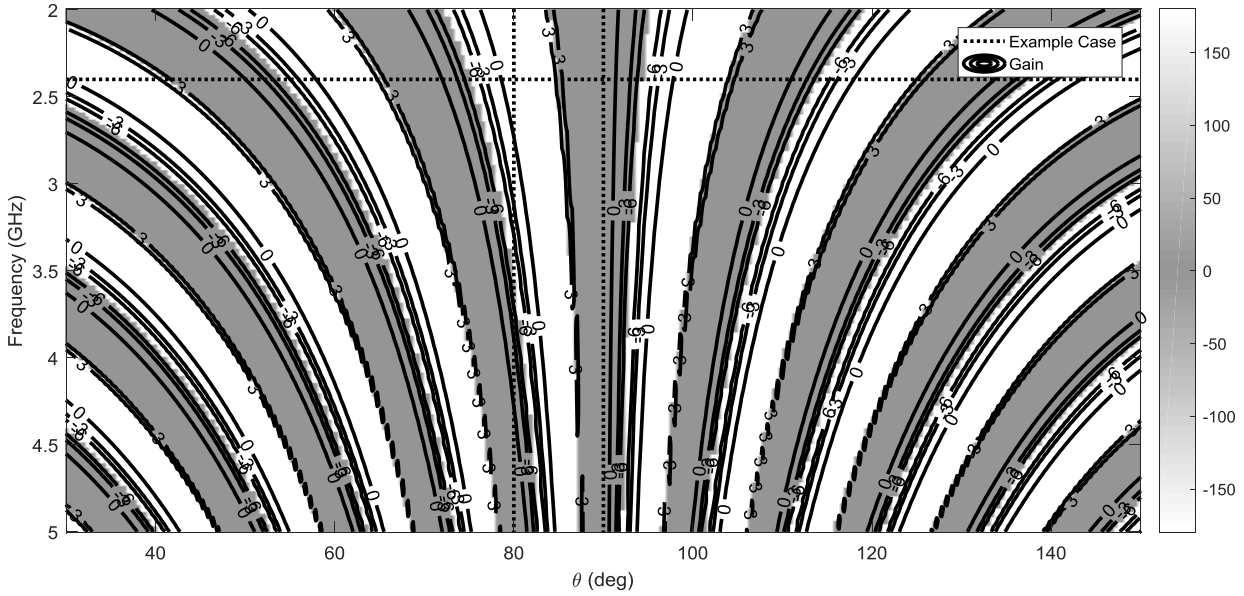

Figure 5.15: Greyscale image indicating the direction-dependent phase modulation in degrees due to time-varying the steering vector state for the array. Directional modulation is implemented using a two-element array spaced by 3λ at $2.4GHz$. Dotted lines show an example operating point at $2.4GHz$ with one User at broadside and the other at 10° ofrom broadside. The contour indicates the achieved array gain using the proposed method. The regular spacing of the modulation regions can be advantageous to communications systems with geometrically planned layouts, such as in the layout shown in Figure 3.2.

Chapter 6

Experimentation

The proposed method for directional modulation was experimentally verified in a laboratory setting using a phased array transmitter and two receivers with single horn antennas. The experimental setup, including the hardware used and the wireless channels, was calibrated to the extent possible and practical. It should be noted that the instantaneous channel state information (CSI) is necessary for implementation of directional modulation as proposed; however, sufficiently line-of-sight channels free of multipath are sufficient to prove the utility of the proposed method. The following experiment shows that simple calibration of the wireless channel is sufficient to achieve directional modulation.

This experiment was performed in coordination between the author and Ryan Christopher of New Mexico State University. Mr. Christopher provided access to the experimental setup, including all hardware. Of particular note in this experimental setup are the programmable and time-variable array steering controls as well as the channel environment with minimal multipath.

The author was responsible for the experiment design, calibration of the wireless channels, and processing of the experimental results.

6.1 Objective

The objective of this experiment is to verify the differing and direction-dependent effects of the proposed array control method on the physical layer of wireless information signals. By verifying the effect on the physical layer, we can extrapolate the ability of the proposed method to achieve simultaneous wireless information and power transfer and to increase the capacity of confidential messages over broadcast channels. The time-varying steering vectors induce direction-dependent phase modulation at the cost of array gain. In this experiment, we demonstrate selectively inducing binary phase-shift keying (BPSK) modulation to different receivers over a broadcast channel at will, thereby enabling independent modulation of signals to different receivers. We also measure the cost of implementing the proposed method by comparing the achieved array gain to the array gain measured using conventional beam steering.

6.2 Experimental Setup

The experimental setup consists of a transmit antenna array and two receivers. The transmit array is an array of 6 patch antennas designed for optimum response at a center frequency of 2.35GHz. Each transmit Antenna Element is mated to an Analog Transmit Module that includes programmable amplifiers, phase-delay circuits, and attenuators. The Analog Transmit Modules are coherently coupled to the same source using a corporate feed. Throughout each of the experiments,

4 of the 6 array elements were effectively disabled by terminating the amplifiers and implementing the maximum in-path attenuation. During the experiment, the transmit array with two active elements was oriented in the azimuth plane towards two receivers, each with a single antenna. A block diagram of the experimental setup is shown in Figure 6.1.

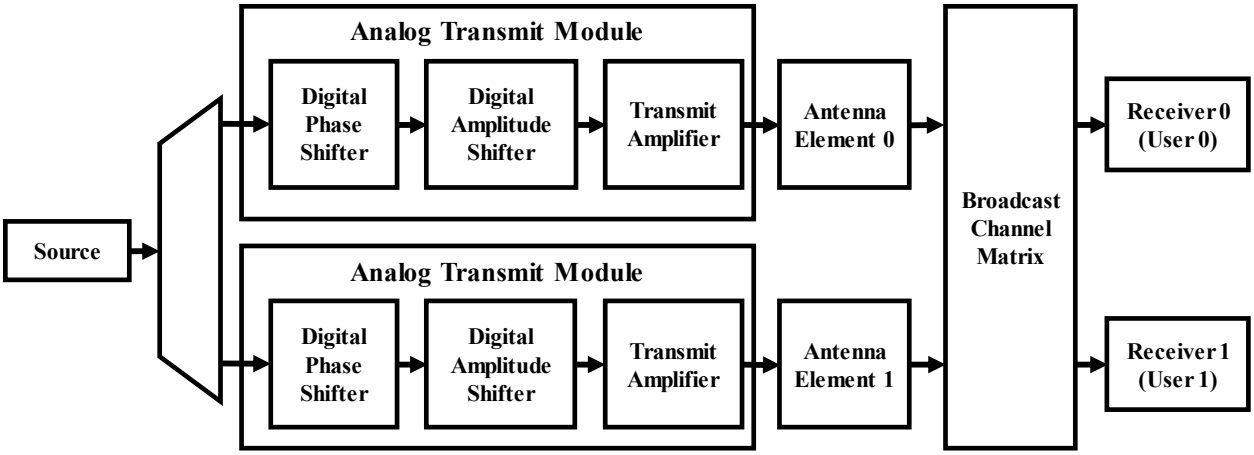

Figure 6.1: Block diagram of the experimental setup, consisting of a transmit antenna array oriented in the azimuth plane towards two receivers. Each transmit Antenna Element is mated to an Analog Transmit Module that includes programmable amplifiers, phase-delay circuits, and attenuators, and is coherently coupled to a signal source using a corporate feed.

The receivers are spaced by 36° about boresight of the array and in the azimuth plane with no obstacles in line-of-sight between the transmitter and receivers. A photograph of the experimental setup is shown in Figure 6.2. Microwave absorptive material is placed surrounding the entire experimental setup to minimize the multipath in the wireless channels. All experiments are conducted within the unlicensed industrial, scientific and medical (ISM) radio band, at a center frequency of 2.35GHz.

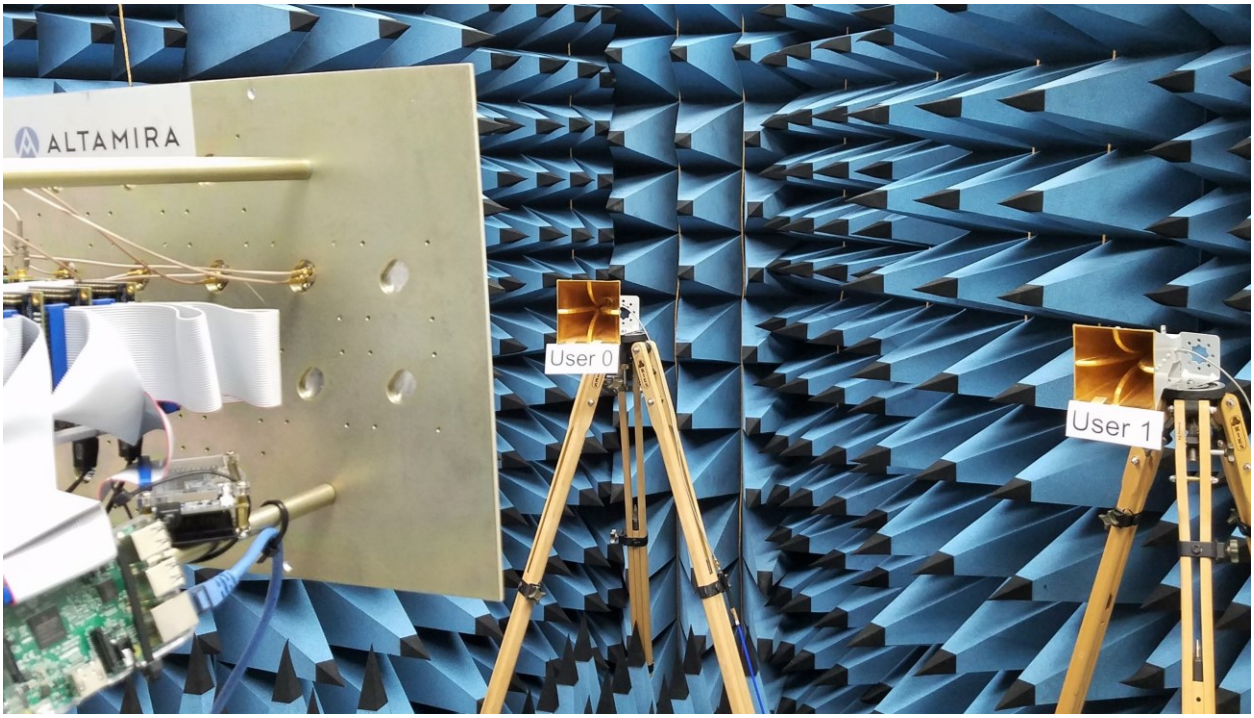

Figure 6.2: Experimental setup consisting of a transmit antenna array (left) and two receivers (center and right). The transmit array is an array of 6 patch antennas designed for optimum response at a center frequency of 2.35GHz, each mated to a programmable Analog Transmit Module that are coherently coupled to the signal source using a corporate feed. Throughout each of the experiments, 4 of the 6 array elements were disabled by terminating Analog Transmit Module. Each of the receivers uses a single horn antenna connected directly to a network analyzer. Image courtesy of Ryan Christopher.

6.3 Calibration

Prior to and throughout the experiments, we calibrate the wireless channel (broadcast channel matrix), all active and passive components in each Analog Transmit Module, and the Antenna Elements. One differing aspect between the proposed technique and information-theoretic approaches to broadcast channel capacity bounds lies in the estimation of the wireless channel. In these experiments, a line-of-sight channel is setup and precautions are taken to minimize multipath contribution by covering nearby surfaces with microwave absorptive material. As expected,

calibration measurements indicate that the wireless channel can be reasonably predicted by the array manifold; however, it should be noted that obtaining channel state information is practical in current wireless communications systems and pure prediction is not required.

We calibrated the entire experimental setup using automated scripts prior to each experimental collection, including the programmable Analog Transmit Module and the wireless channels. Due to the static nature of the experimental setup, calibration values remained stable over the course of the experiments.

6.3.1 Analog Transmit Front End Hardware Calibration

Each of the Analog Transmit Modules used in this experiment resides on a multi-function Analog Transmit/Receive Board. The programmable phase and amplitude control circuitry within the Analog Transmit Module was calibrated by measuring the complex transfer function of each control bit available on each Analog Transmit/Receive Board using a 2-port network analyzer, as shown in Figure 6.3. Each Analog Transmit/Receive Board can route the input connector to a passive path, a receive path with low-noise amplifier (LNA), or a transmit path with a power amplifier (PA) based on the supplied command. Throughout the experiments and calibration, each Analog Transmit/Receive Board was commanded to activate the transmit path and terminate the input and outputs of the passive path and the receive path.

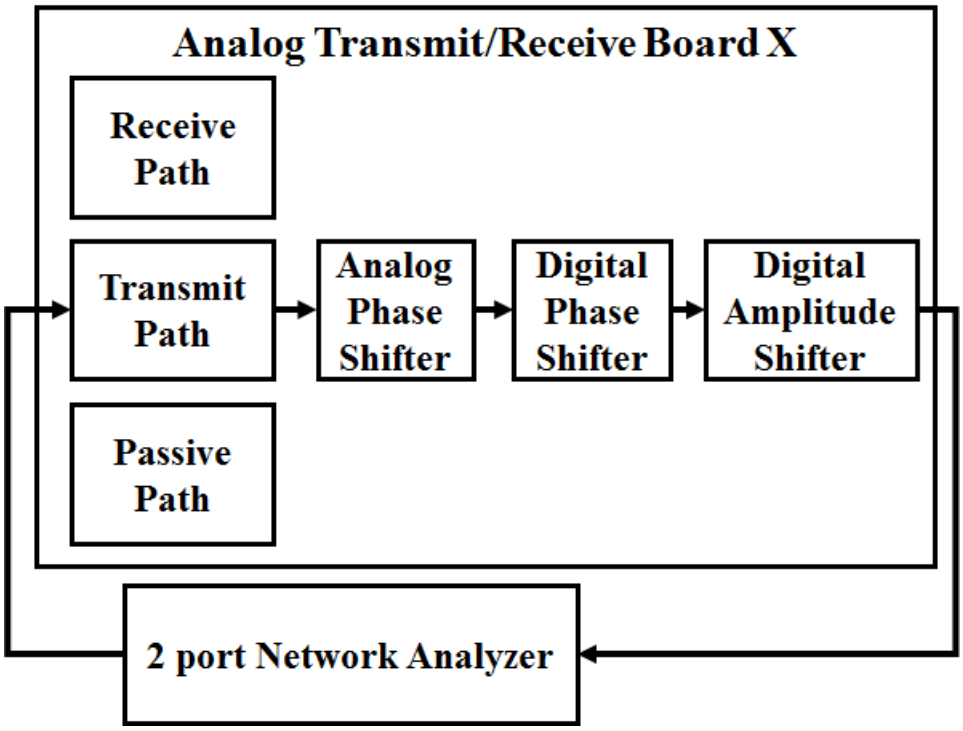

Figure 6.3: Diagram of the measurement setup for calibrating each multi-function Analog Transmit/Receive Board. The programmable phase and amplitude control circuitry was calibrated by measuring the complex transfer function using a 2-port network analyzer, exercising each available control bit when configured to operate in the transmit mode. Throughout the experiments and calibration, each Analog Transmit/Receive Board was commanded to terminate the input and outputs of the passive path and the receive path.

Each Analog Transmit/Receive Board is designed to implement steering vectors with least significant bit precision of $5.625°$ in phase and $0.25dB$ in attenuation. The Analog Transmit/Receive Boards operate the power amplifier near saturation when switched to the transmit path. The theoretically achievable complex transfer function for steering vectors based on specified component performance at $2.35GHz$ while operating near amplifier saturation is shown in Figure 6.4. We note that since the steering vectors are implemented using phase shift and amplitude attenuation, there is no observed gain in the steering vectors (i.e., the maximum norm of the theoretically achievable steering vector is 1). Further, we note that low amplitude steering

vectors are not achievable using this hardware; however, we do not expect this to be a problem given that low amplitude steering vectors will cause significant loss of array gain, which is undesirable. A detailed study of the effect of steering vector resolution on directional modulation performance is suggested for future research.

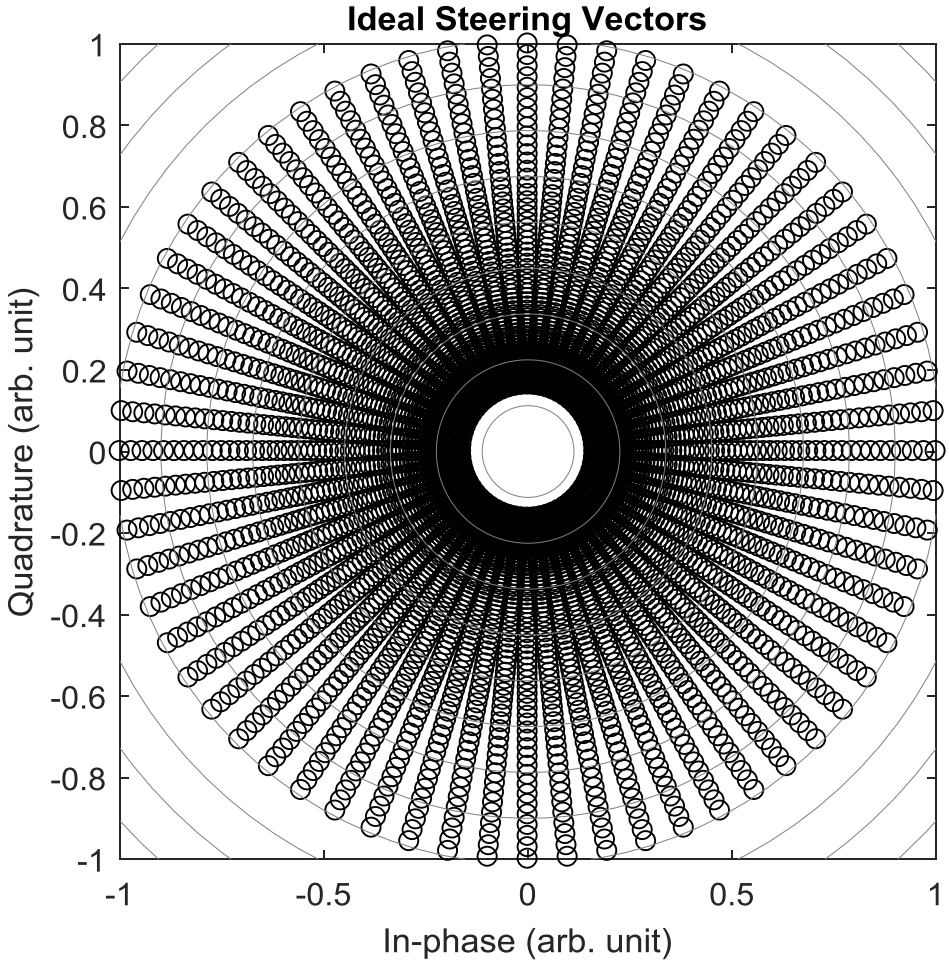

Figure 6.4: Theoretically achievable steering vectors for the Analog Transmit/Receive Board at 2.35GHz based on specified component control precision of 5.625° in phase and 0.25dB in attenuation. Since the power amplifier operates near saturation when switched to the transmit path, and the steering vectors are implemented using phase shift and amplitude attenuation, there is no observed gain in any of the steering vectors.

Though advertised with a minimum achievable phase shift per bit of $5.625°$, we measure each Analog Transmit/Receive Board at closer to $10°$ minimum achievable phase shift per bit. Though the MACOM MAPS-010164 6-bit digital phase shifter is rated for operation at $2.35GHz$, the advertised mean root mean square (RMS) phase error at that frequency is approximately $3°$. As such, the achievable steering vectors that can be realized using Analog Transmit/Receive Board #4 and #9 are shown in Figure 6.5 and Figure 6.6, respectively. The coarse resolution of achievable steering vectors is common to both Analog Transmit/Receive Board #4 and #9, and limit the performance of directional modulation.

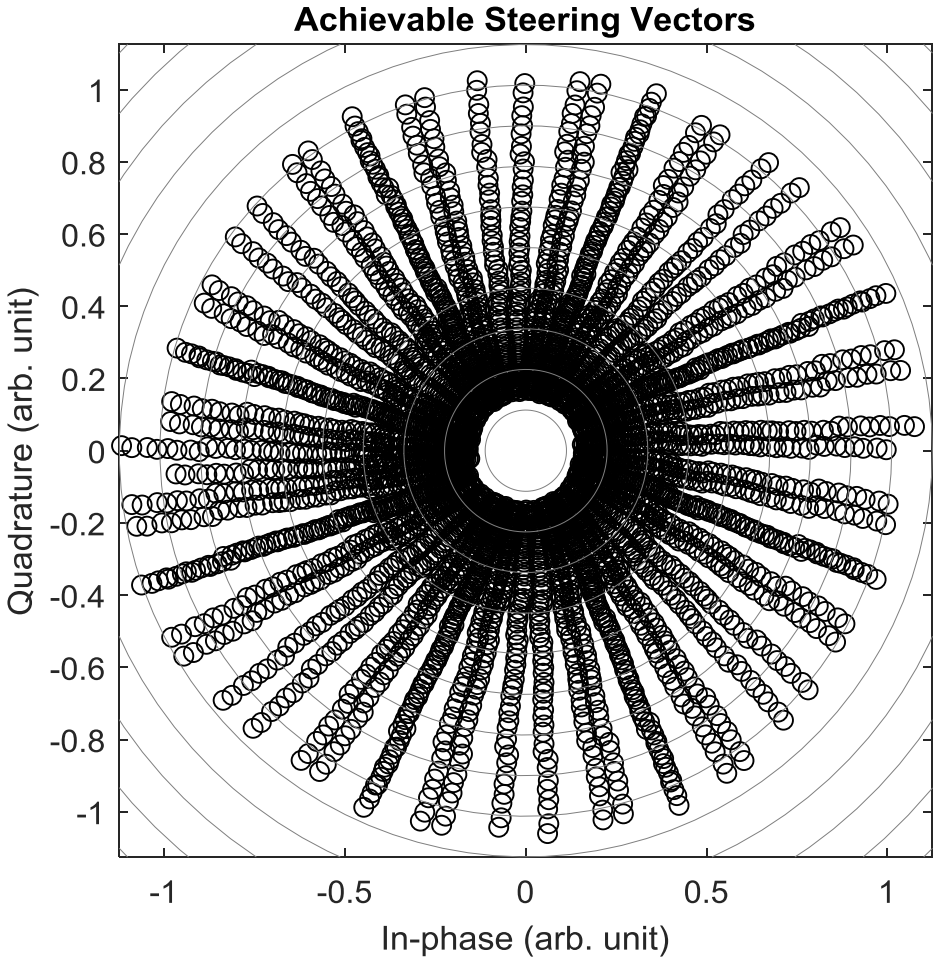

Figure 6.5: Graphical depiction of all possible complex steering vectors that can be realized using Analog Transmit/Receive Board #4, given measured component performance at 2.35GHz. Though advertised with a phase shift resolution of 5.625°, calibration of Analog Transmit/Receive Board #4 shows approximately 10° minimum phase resolution per control bit, likely due to the RMS phase error performance of the MACOM MAPS-010164 6-bit digital phase shifter. The coarse resolution of achievable steering vectors limit the performance of directional modulation.

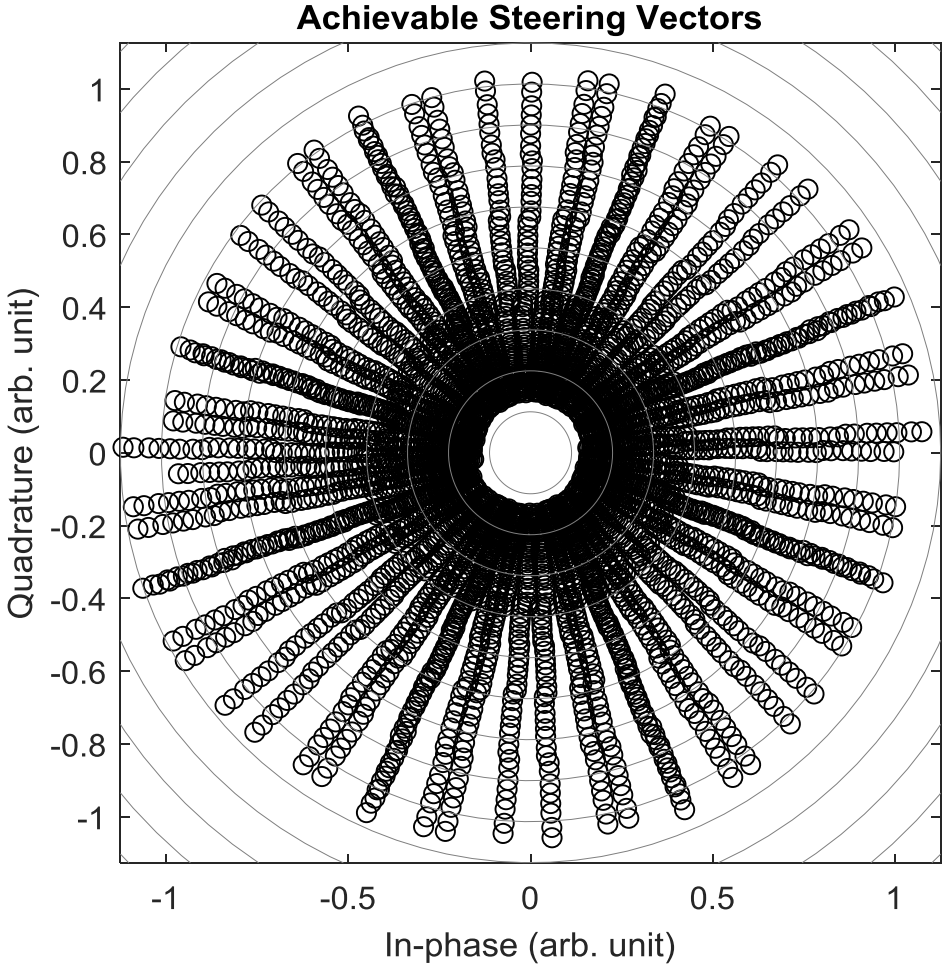

Figure 6.6: Graphical depiction of all possible complex steering vectors that can be realized using Analog Transmit/Receive Board #9, given measured component performance at 2.35GHz. Though advertised with a phase shift resolution of 5.625°, calibration of Analog Transmit/Receive Board #9 shows approximately 10° minimum phase resolution per control bit, likely due to the RMS phase error performance of the MACOM MAPS-010164 6-bit digital phase shifter. The coarse resolution of achievable steering vectors limit the performance of directional modulation.

6.3.2 Channel Calibration

Once the Analog Transmit/Receive Boards are mated to their respective Antenna Elements and the corporate feed, we calibrate the wireless channel, the corporate feed, passive components, and the power amplifiers housed within the Transmit Path. We employ a 3-port network analyzer

providing the source to the corporate feed and coherently measuring the output of both receivers, as shown in Figure 6.7. Each Analog Transmit/Receive Board is software-addressable and programmable, so we are able to measure each Analog Transmit/Receive Board and Antenna Element pair independently. Though the array is fitted with 6 Antenna Elements, only 5 Analog Transmit/Receive Boards were operational, so the unmated Antenna Element and corporate feed output were terminated to a 50Ω load.

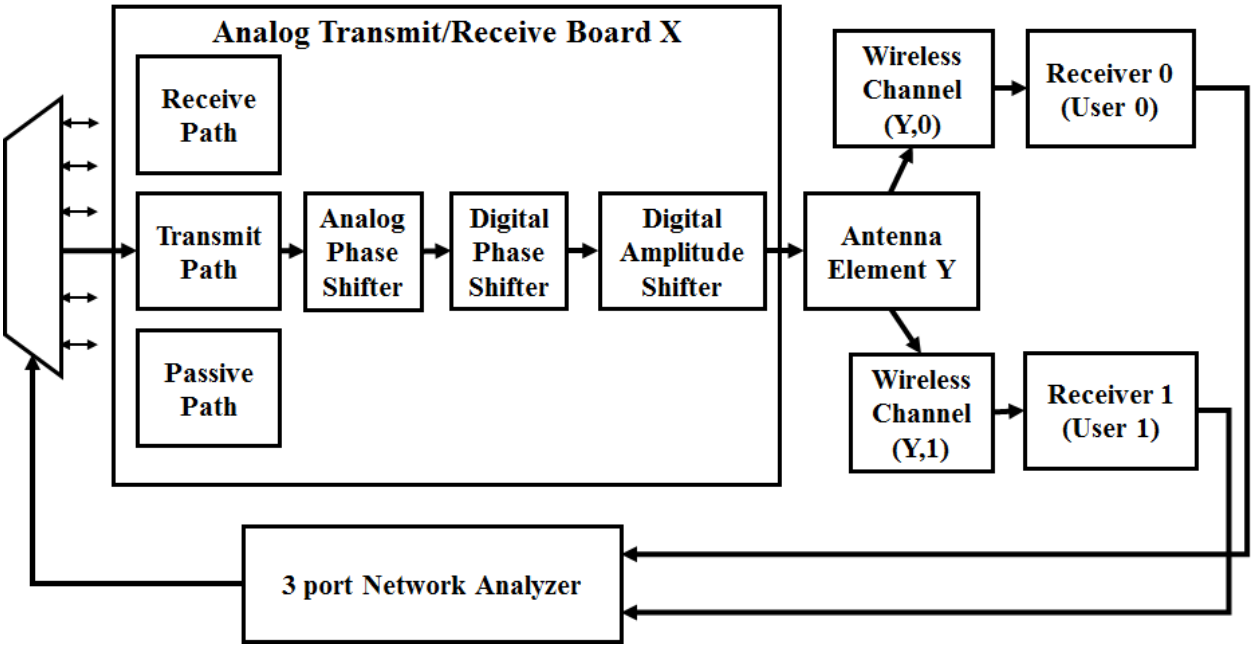

Figure 6.7: Diagram of the experimental setup for calibrating the wireless channels between each Antenna Element and both receivers. The measurements include the complex transfer functions of the corporate feed, passive components, and the power amplifiers housed within the Transmit Path of each Analog Transmit/Receive Board. We use a 3-port network analyzer to coherently record the output of both receivers while transmitting from each Analog Transmit/Receive Board and Antenna Element pair independently, with unused elements terminated to a 50Ω load.

One differing aspect between the proposed technique and information-theoretic approaches to broadcast channel capacity bounds [82] is in the estimation and knowledge of the complex transfer function induced by the wireless channel. For example, in [82] the wireless channel transfer

functions are explicitly assumed to be uniform random variables, then used to compute the broadcast channel capacity bounds. For the proposed technique, we assume full channel state information is available to the transmitter; however, it should be noted that given a sufficiently line-of-sight channel with minimal multi-path contribution, the full channel state information is not necessary for directional modulation.

Throughout the experiments described in this chapter, line-of-sight channels are setup and precautions are taken to minimize multipath, as described in Section 6.2. We measure the wireless channels using the configuration shown in Figure 6.7, and show that the wireless channels can be reasonably predicted for the 5 Antenna Elements and 2 receivers after a bulk phase rotation, as shown in Figure 6.8. The wireless channels were predicted using the array manifold shown in (1) and fit to the measured channels using a minimum mean square error (MMSE) criterion for a bulk rotation of the channel constellation. Though the calibration results indicate that perhaps a Rician fading model is more accurate for this experimental setup, a line-of-sight channel model is assumed. It is important to note that since the proposed method is a beamforming method, the relative offset between the various wireless channels is critical; however, the bulk rotation common to all the wireless channels for the Antenna Elements towards a receiver will not affect the performance of the induced directional modulation. Notwithstanding, we note that obtaining channel state information is practical and a reasonable requirement in modern wireless communications systems such that prediction is not required. The tolerance of this method to multipath is left as a subject of future research.

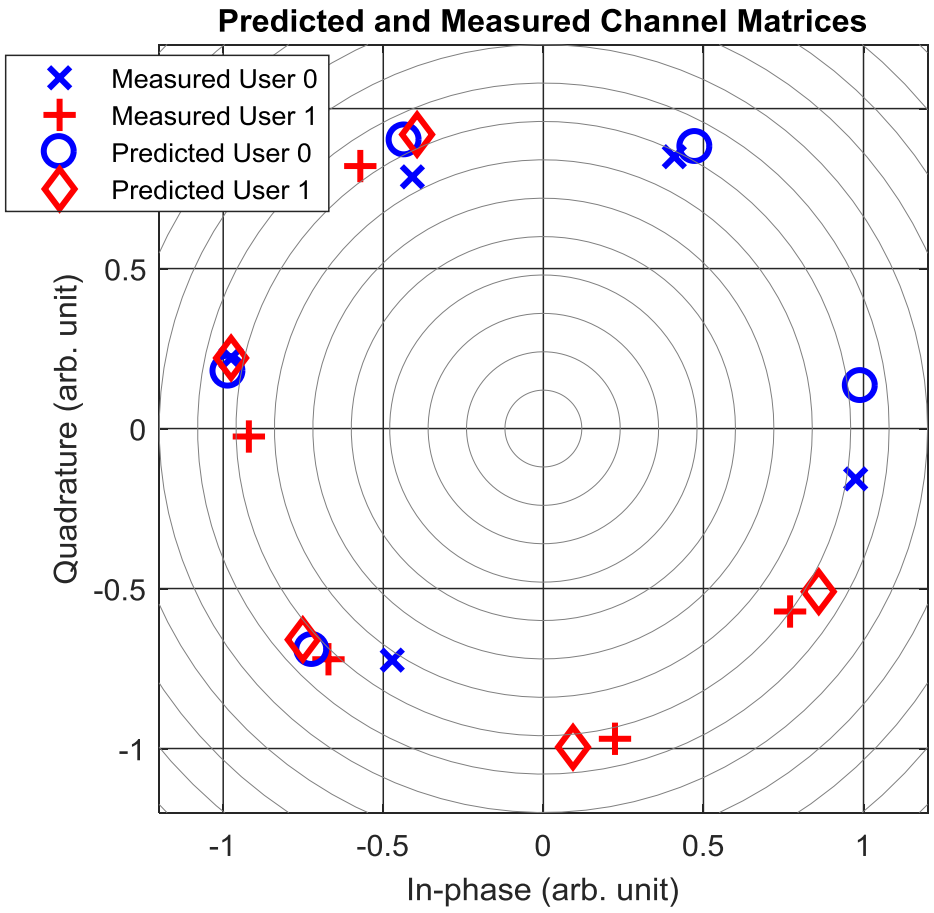

Figure 6.8: Measured wireless channels between 5 Antenna Elements and 2 receivers (Users) compared to theoretical predictions based on the array manifold. In this manuscript, we assume the full channel state information for line-of-sight channels with minimal multipath is available to the transmitter for computation of the steering vectors. These measurements show that the wireless channels used in this experiment fit sufficiently to a line-of-sight channel model. These measurements were taken on May 20, 2017.

6.4 Experimental Procedure

Once the Analog Transmit Front End Hardware and Channel calibration measurements have been obtained, we execute a software function to generate machine-readable command files for the array, which is detailed in Figure 6.9. We estimate the wireless channel transfer functions from

the channel calibration measurements and compare them to theoretical expected channel measurements to confirm that the channels are subject to a minimal amount of multipath. We use the estimated channel state information to seed the proposed optimization function in (13) and compute the ideal steering vector solutions for directional modulation, denoted $\boldsymbol{W} = [\boldsymbol{w}_0 \ \cdots \ \boldsymbol{w}_{S-1}]$. Using the measured Analog Transmit Front End Hardware calibration measurements, we identify the hardware control settings closest to the optimal steering vectors computed in minimum mean square error. We denote $\boldsymbol{W}$ as implemented by the discretized Analog Transmit Front End Hardware as $\ddot{\boldsymbol{W}}$. We then write the proper control settings for each Analog Transmit/Receive Board to a machine-readable command file. We also develop steering vectors in the same way for beamformers steered towards each of the receivers, where the ideal steering vector towards the receiver in the direction $\widehat{\boldsymbol{k}}_{\boldsymbol{r}}$ in wavenumber space is computed as $\dot{\boldsymbol{w}}_{\boldsymbol{r}} = \boldsymbol{v}_{\boldsymbol{k}}(\widehat{\boldsymbol{k}}_{\boldsymbol{r}})$ [1]. We denote $\dot{\boldsymbol{w}}_{\boldsymbol{r}}$ as implemented by the discretized Analog Transmit Front End Hardware as $\ddot{\boldsymbol{w}}_{\boldsymbol{r}}$. The different machine-readable command files are uploaded to the array controller to implement time-varying steering vectors. In this case, two steering vectors are generated for each transmit array Antenna Element and are varied in a controlled pattern.

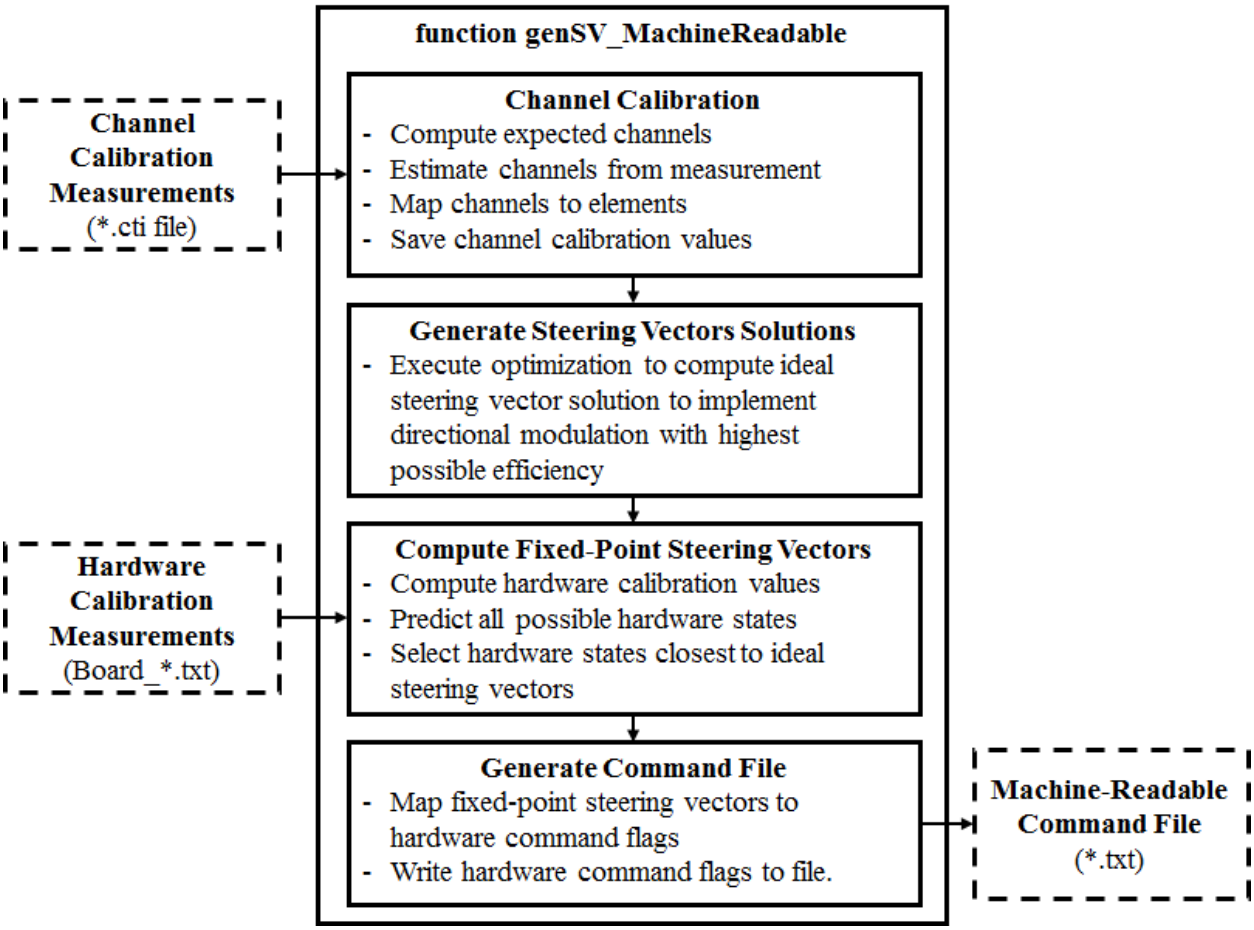

Figure 6.9: After the calibration measurements are obtained, the depicted software function computes steering vector solutions for directional modulation using the proposed method and produces machine-readable array commands to implement time-varying steering vectors. This function uses calibration measurements and channel state information to compute the hardware control settings closest to the optimal steering vectors for directional modulation, and to steer towards each receiver.

The experimental setup in Figure 6.7 is used again to measure the wireless channels between the transmitter and receivers using the generated steering vectors. A 3-port network analyzer is used to simultaneously estimate the channel transfer functions observed by each receiver as the array controller asynchronously updates the steering vector. The intent is to observe a stable channel transfer function at one receiver, and a bi-modal channel transfer function at the other

receiver while the array is steered by $\ddot{\boldsymbol{W}}$. The desire is to observe sufficient amplitude and signal-to-noise ratio at each receiver as compared to the array under $\ddot{\boldsymbol{w}}_{\boldsymbol{0}}$ and $\ddot{\boldsymbol{w}}_{\boldsymbol{1}}$.

6.5 Results

To establish a reference peak performance of the array, we implement steering vectors designed to steer towards Receiver 0, $\ddot{\boldsymbol{w}}_{\boldsymbol{0}}$, then implement steering vectors to steer towards Receiver 1, $\ddot{\boldsymbol{w}}_{\boldsymbol{1}}$. The centroids of each group of measurements are shown in Figure 6.10. As expected, each Receiver experiences a relatively favorable SNR when the array is steered towards them, and a poor SNR when the array is steered away. The relative signal strength can be visually estimated as the absolute distance of the centroids to the origin. In this round of experiments, the Receivers observed losses of approximately $9dB$ and $7dB$ when the array was steered away from them. The SNR loss in computed relative to the average wireless channel transfer functions measured during the channel calibration, as describe in Section 6.3.2. The average SNR loss measured at each Receiver subject to different steering vectors is summarized in Table 6.1. In this case, the orientations of the channels are meaningless since a receiver would synchronize to the centroid. The transmitter would encode information by inverting the phase of the channel transfer function. For clarity, Figure 6.10 and Table 6.1 only describe the channel transfer functions associated with the '0' bit and not the '1' bit.

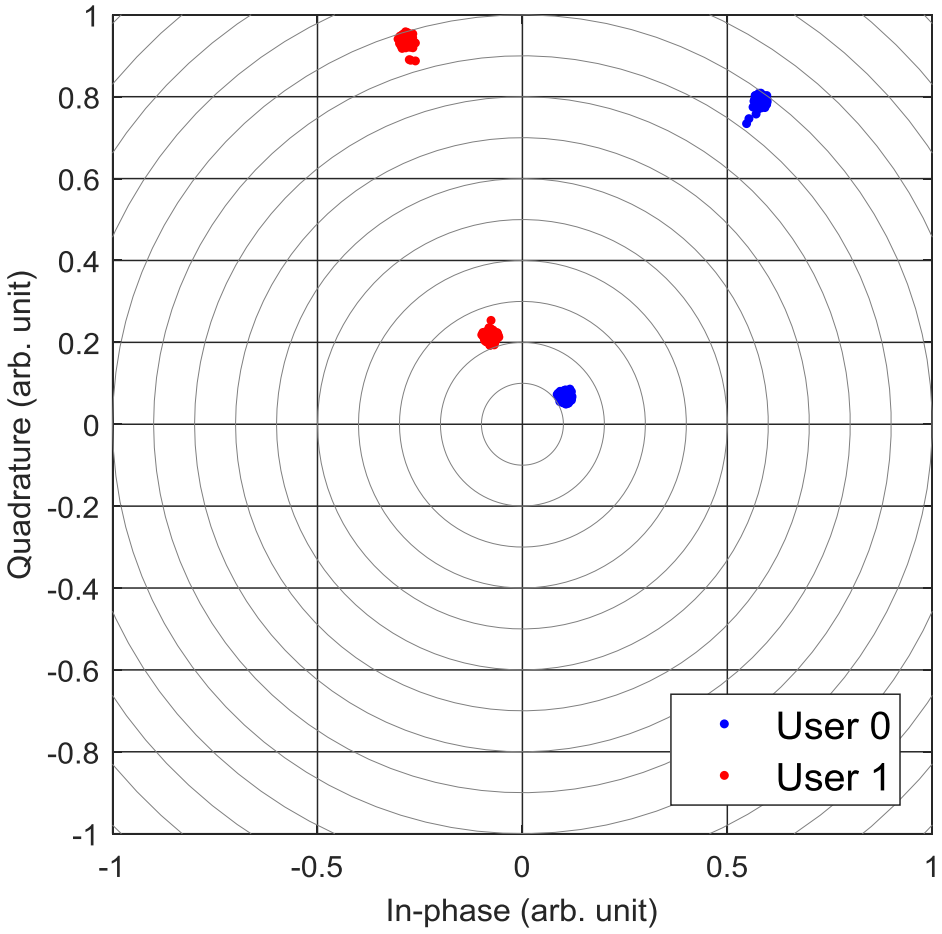

Figure 6.10: Graphical depiction of the wireless channel transfer functions observed by User 0 and User 1 when the array is subject to a beamformer designed to steer towards User 0 ($\ddot{\boldsymbol{w}}_{\boldsymbol{0}}$) and a beamformer designed to steer towards User 1 ($\ddot{\boldsymbol{w}}_{\boldsymbol{1}}$). The measurements indicate good array efficiency observed by each User when the array is steered towards and poor efficiency when the array is steered away.

Table 6.1: Average SNR loss measured by each user for the array subject to each steering vector relative to peak SNR for conventional beam steering towards each user as measured during the wireless channel calibration.

	Steering Vector 0 ($\ddot{\boldsymbol{w}}_{\boldsymbol{0}}$)	**Steering Vector 1 ($\ddot{\boldsymbol{w}}_{\boldsymbol{1}}$)**
User 0	$-0.7dB$	$-6.6dB$
User 1	$-9.7dB$	$-0.3dB$

The steering vectors computed from the optimization in (10) to implement directional modulation are designed to selectively modulate the wireless channel for User 1 and have minimal effect on the wireless channel for User 0. The centroids of the measured channel transfer functions for each of the two steering vectors ($\ddot{\boldsymbol{W}}$) are shown in Figure 6.11. As expected, the channel transfer function observed by User 0 is minimally affected as the steering vector is time-varied. In contrast, User 1 would likely interpret a symbol transition due to the change in steering vector, which results in an observed phase shift in excess of 170° only for User 1. We assume that each receiver would synchronize to their received centroids prior to demodulation and decoding. The SNR measured for each User subject to each steering vector is measured and compared to the maximum measured beamforming gain throughout the experiments. In all cases, the average SNR loss when implementing directional modulation was within $3dB$ of the average SNR loss when steering directly towards each User. The average SNR measurements are shown in Table 6.2 and were nearly identical over thousands of measurements during 3 separate collections.

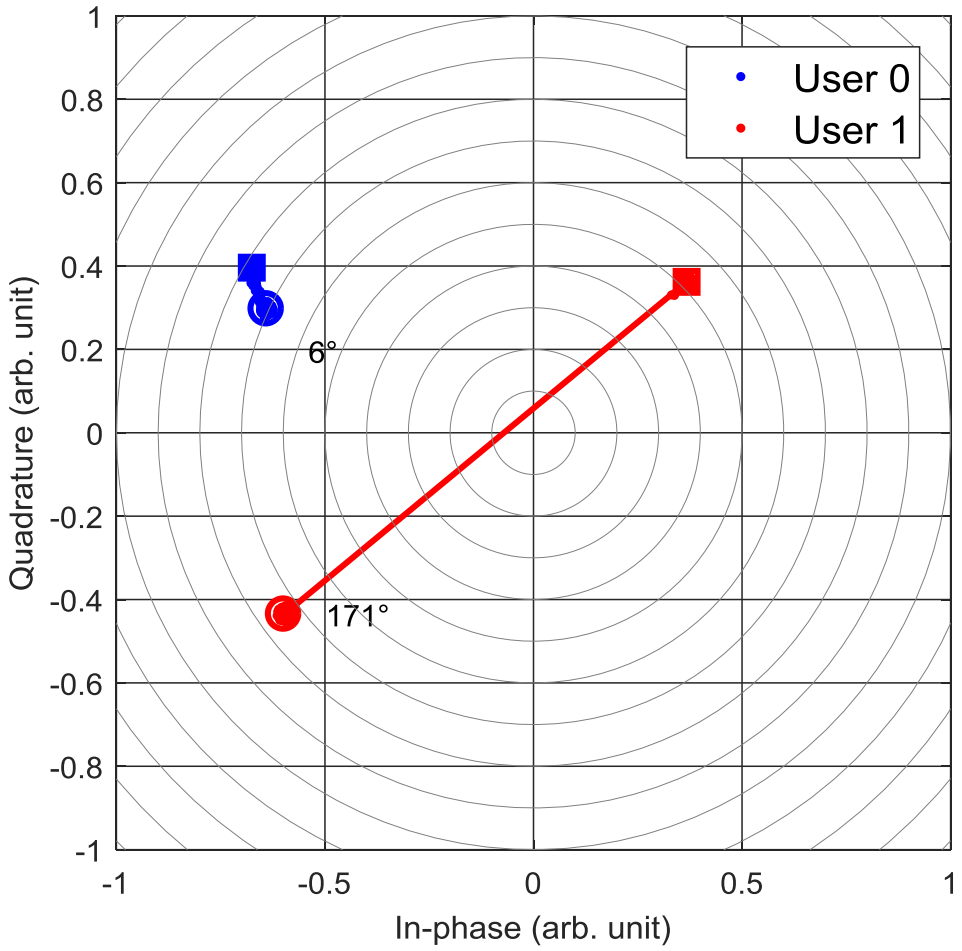

Figure 6.11: Graphical depiction of the wireless channel transfer functions observed by User 0 and User 1 using a time-varying beamformer designed for directional modulation ($\ddot{\boldsymbol{W}}$). Notably, these results show that User 0 and User 1 can selectively receive independent information purely based on the applied steering vectors.

Table 6.2: Average SNR loss measured by each user for the array subject to each directional modulation steering vector relative to peak SNR for conventional beam steering towards each user as measured during the wireless channel calibration.

	Steering Vector 0 (First Column of $\ddot{\boldsymbol{W}}$)	Steering Vector 1 (Second Column of $\ddot{\boldsymbol{W}}$)
User 0	$-1.0dB$	$-1.2dB$
User 1	$-1.4dB$	$-2.7dB$

During a third experiment, we attempt to steer the array using both the directional modulation steering vectors ($\ddot{\boldsymbol{W}}$) and the individual steering vectors ($\ddot{\boldsymbol{w}}_{\boldsymbol{0}}$ and $\ddot{\boldsymbol{w}}_{\boldsymbol{1}}$) consecutively and in a repeating pattern. This experiment will enable direct comparison of these steering vectors to verify the validity and the efficiency of directional modulation. The centroids of each group of measurements are shown in Figure 6.12, where the directional modulation channel transfer function centroids are connected by a line, and the individually steered channel transfer function centroids are not. Again, as expected, User 0 does not experience a symbol transition as the steering vector is time-varied, while simultaneously, User 1 would likely interpret a symbol transition given the change in steering vector, given that a phase shift in excess of $170°$. Here, again, we assume that the receivers would synchronize to their observed centroids. The channel transfer functions when the array is subject to the steering vectors $\ddot{\boldsymbol{w}}_{\boldsymbol{0}}$ and $\ddot{\boldsymbol{w}}_{\boldsymbol{1}}$ outperform directional modulation at the intended recipient, User 0 and User 1, respectively; however, the unintended recipient observes reduced SNR. The SNR measured for each User subject to each steering vector is measured and compared relative to the peak SNR measured when the array is steered directly to that receiver. In three cases, the SNR loss was less than $1.6dB$, and approximately $2.7dB$ in the fourth case, as shown in Table 6.3. The tabulated results were nearly identical over 3 separate collections and thousands of measurements using the same steering vectors. We recognize that the observed performance is somewhat decreased due to imperfections in the hardware and fixed-point nature of the steering vectors that were implemented, and some presence of multipath in the channel calibration.

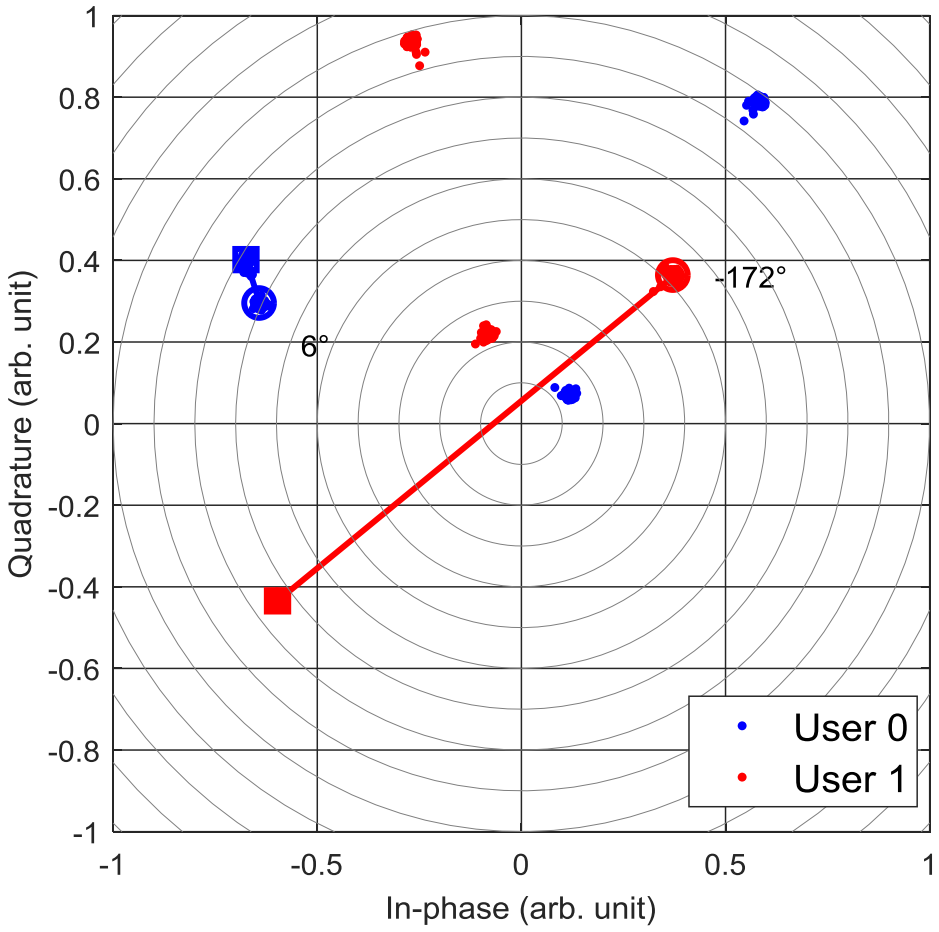

Figure 6.12: Graphical depiction of the wireless channel transfer functions observed by User 0 and User 1 using a time-varying beamformer that consecutively induces directional modulation then steers directly towards User 0 then towards User 1.

Table 6.3: Average SNR loss measured by each user for the array subject to each steering vector relative to peak SNR for conventional beam steering towards each user as measured during the wireless channel calibration.

	Steering Vector $\ddot{w}_0$ User 0 is the intended recipient	**Steering Vector $\ddot{w}_1$** User 1 is the intended recipient	**Steering Vector $\ddot{W}$ (Column 1)** Directional Modulation	**Steering Vector $\ddot{W}$ (Column 2)** Directional Modulation
User 0	$0dB$	$-6.2dB$	$-1.0dB$	$-1.2dB$
User 1	$-8.6dB$	$0dB$	$-1.4dB$	$-2.7dB$

Chapter 7

Conclusions and Scope of Future Work

7.1 Conclusions

In this dissertation, we develop a passive array beamforming technique to implement directional modulation. Application of directional modulation to communications systems enables a receiver to extract information and harvest wireless energy simultaneously from signals occupying the same time and frequency subspaces. The same technique can also provide a transmitter with additional PHY-layer secrecy by purposefully overlaying a spoofed signal onto the transmitted signal in the direction of an eavesdropper. In both applications, this technique surpasses the state of the art by time-varying the spatial degrees of freedom inherent in an array. The proposed directional modulation technique enables energy efficient and secure wireless communications.

We also described and produced simulation and experimental results for a coding technique that exploits the directional modulation overlay not only as a spoofed signal, but as a second, legitimate, and confidential signal intended for a second User. The proposed coding technique can outperform the Dirty Paper Coding technique both in terms of sum rate capacity and secrecy capacity. Unlike Dirty Paper Coding, the proposed technique time-varies array steering vectors to achieve a direction-dependent overlay modulation, which eliminates co-channel interference generated by the transmitter and thus greatly increases the achievable SINR in each channel. We also showed that the proposed technique exceeds the Sato Bound [17] since the Sato Bound implicitly assumes no time-varying control or knowledge of the channel via steering vector manipulation. The proposed technique can benefit IoT systems by increasing the overall secrecy capacity of a wireless broadcast system without increasing the size, weight, or power consumption of the devices.

7.2 Topics for Future Research

The following topics are recommended for future research in the interest of further developing the proposed beamforming method, further characterizing the performance of the proposed method, and developing extended applications of the proposed method.

7.2.1 Effects of Channel State Information and the Channel Model

Future study of the effects of channel state information and the assumed channel model on the performance of directional modulation is encouraged. First, the relationship between the accuracy of the channel state information to the performance of directional modulation should be established, both in terms of the modulation quality (e.g., modulation error ratio) and in the overall loss of array gain. Further, the effectiveness of the proposed method should be investigated as the line-of-sight channel observes increasing amounts of multipath and more closely resembles a Rician channel then a Rayleigh channel. The proposed method relies on the knowledge of the relative phase difference between the dominant multipath components of the two users. It may be possible to overcome loss of the line-of-sight channels if the channels are Rician but sufficiently sounded, even if the maximum amplitude component is not the line-of-sight component. It is unclear if the proposed method will maintain effectiveness in a Rayleigh channel environment. As such, the robustness of the proposed method to varying multipath is suggested as an area of future research.

7.2.2 Effects of Hardware Implementation

Further study of the effect of steering vector implementation in hardware on the performance of directional modulation is suggested. First, the discrete nature of the control of amplitude and phase modulating components can be quantified, and the effect of the discrete implementation on such performance parameters as modulation error ratio and loss of array gain can be bounded.

Second, it is possible that a possibly brute-force, alternative formulation of (13), while possibly not convex, may provide better performance when the possible solution space is discretized. For example, amplitude and phase modulation with 6-bit control each has only 4096 possible control combinations per Analog Transmit/Receive Board. It is feasible to evaluate all of the directional modulation constraints and the objective function for each of the possible control combinations. This will not scale favorably to larger dimensions (e.g., additional Antenna Elements, higher resolution of control); however, these studies may provide simpler, non-optimal implementations for practical purposes.

7.2.3 Convex Optimization of Steering Vectors for Directional Modulation

Continued investigation into the capacity of these techniques is recommended. Critical to the sum-rate capacity and the secrecy capacity of the system relies upon the efficiency of the proposed technique. The existence of a transformation of (13) that preserves convexity and linearizes the gradient remains an open problem. The existence of a reformulation of (13) that develops directional modulation steering vectors with greater secrecy capacity and remains convex should be investigated.

7.2.4 Effects of Imperfect Synchronization

While unnecessary in the implementation of directional modulation for transmit, future study of the effects of imperfect synchronization on directional modulation for receive is recommended. Specifically, the direct effect of imperfect synchronization on power transfer performance and

degree of corruption of simultaneous wireless information and power transfer should be studied. Further, the existence of optimal layout planning for co-channel information and power transfer should be studied, including the existence of optimal layouts for performance with sub-optimal synchronization.

7.2.5 Effects of Inequality Constraint Parameters

The selection of the parameter ε in the linear inequality constraints for directional modulation as in (12), (15), and (17), is not only critical to the performance in terms of achieved modulation error ratio, but also affects the achievable array gain. It is not necessary for the inequality constraint parameter to be applied uniformly across each inequality constraint. We suggest a future study of the achievable gain by varying the parameter ε in different directions of interest while maintaining the convexity of Ψ.

7.2.6 Performance Benefits Using Non-Uniform Array Layouts

Continued investigation and qualification of the performance of the proposed directional modulation method for an irregular array, possibly sparse or volumetric is recommended. For example, a swarm of Array Elements that are cooperating for a given mission would be both sparse and volumetric, and able to change element positions should the need arise. The proposed method may be applied to increase the performance of the cooperating swarm, or perhaps provide additional multiple access performance within the swarm. For example, directional modulation can provide enhanced performance to radar direction finding by directionally-coding the

transmitted signal as considered in [51]. Further, non-uniform array layouts that maximize the utility of these applications should be investigated.

7.2.7 Applications to Multi-Rate, Multiple Access Communications

The linear inequality constraints and predicted performance for achieving variable symbol rates to multiple users should be developed. Applications where one user receives a low symbol-rate communication (e.g., BPSK) and a second user receives high symbol-rate communication (e.g., QPSK or 16-QAM) should be explored, and may be of particular relevance to military communications applications.

7.2.8 Additional Laboratory Experimentation

Additional laboratory experimentation to verify and explore the practical implementation of directional modulation is recommended. Further, more extensive experimentation to validate and quantify the observed capacity gains of the proposed method over Dirty Paper Coding is suggested. Lastly, detailed investigation of the stability of solutions of the proposed method over broad swaths of angular coverage is suggested.

Bibliography

[1] H. L. Van Trees, *Optimum array processing*. New York: Wiley-Interscience, 2002.

[2] Y.-W. P. Hong, P.-C. Lan, and C.-C. J. Kuo, *Signal processing approaches to secure physical layer communications in multi-antenna wireless systems*. Springer, 2013.

[3] Q. Li, Q. Zhang, and J. Qin, "Secure Relay Beamforming for SWIPT in Amplify-and-Forward Two-Way Relay Networks," *IEEE Transactions on Vehicular Technology*, vol. 65, no. 11, pp. 9006–9019, Nov. 2016.

[4] Y. Yang, Q. Li, W.-K. Ma, J. Ge, and P. C. Ching, "Cooperative Secure Beamforming for AF Relay Networks With Multiple Eavesdroppers," *IEEE Signal Processing Letters*, vol. 20, no. 1, pp. 35–38, Jan. 2013.

[5] N. Yang, S. Yan, J. Yuan, R. Malaney, R. Subramanian, and I. Land, "Artificial Noise: Transmission Optimization in Multi-Input Single-Output Wiretap Channels," *IEEE Transactions on Communications*, vol. 63, no. 5, pp. 1771–1783, May 2015.

[6] O. N. Alrabadi and G. F. Pedersen, "Directional space-time modulation: A novel approach for secured wireless communication," in *Communications (ICC), 2012 IEEE International Conference on*, 2012, pp. 3554–3558.

[7] X. Zhou, R. Zhang, and C. K. Ho, "Wireless Information and Power Transfer: Architecture Design and Rate-Energy Tradeoff," *IEEE Transactions on Communications*, vol. 61, no. 11, pp. 4754–4767, Nov. 2013.

[8] A. Salem, K. A. Hamdi, and K. M. Rabie, "Physical Layer Security With RF Energy Harvesting in AF Multi-Antenna Relaying Networks," *IEEE Transactions on Communications*, vol. 64, no. 7, pp. 3025–3038, Jul. 2016.

[9] Z. Xiang and M. Tao, "Robust Beamforming for Wireless Information and Power Transmission," *IEEE Wireless Communications Letters*, vol. 1, no. 4, pp. 372–375, Aug. 2012.

[10] Q. Li, Q. Zhang, and J. Qin, "Beamforming for Information and Energy Cooperation in Cognitive Non-Regenerative Two-Way Relay Networks," *IEEE Transactions on Wireless Communications*, vol. 15, no. 8, pp. 5302–5313, Aug. 2016.

[11] I. Krikidis, S. Sasaki, S. Timotheou, and Z. Ding, "A Low Complexity Antenna Switching for Joint Wireless Information and Energy Transfer in MIMO Relay Channels," *IEEE Transactions on Communications*, vol. 62, no. 5, pp. 1577–1587, May 2014.

[12] R. Zhang and C. K. Ho, "MIMO Broadcasting for Simultaneous Wireless Information and Power Transfer," *IEEE Transactions on Wireless Communications*, vol. 12, no. 5, pp. 1989–2001, May 2013.

[13] S. Timotheou and I. Krikidis, "Joint information and energy transfer in the spatial domain with channel estimation error," in *Online Conference on Green Communications (GreenCom), 2013 IEEE*, 2013, pp. 115–120.

[14] M. P. Daly and J. T. Bernhard, "Directional Modulation Technique for Phased Arrays," *IEEE Transactions on Antennas and Propagation*, vol. 57, no. 9, pp. 2633–2640, Sep. 2009.

[15] Y. Ding and V. Fusco, "Directional modulation transmitter synthesis using particle swarm optimization," in *Antennas and Propagation Conference (LAPC), 2013 Loughborough*, 2013, pp. 500–503.

[16] M. P. Daly and J. T. Bernhard, "Directional modulation and coding in arrays," in *Antennas and Propagation (APSURSI), 2011 IEEE International Symposium on*, 2011, pp. 1984–1987.

[17] H. Sato, “An outer bound to the capacity region of broadcast channels (Corresp.),” *IEEE Transactions on Information Theory*, vol. 24, no. 3, pp. 374–377, 1978.

[18] H. E. Shanks and R. W. Bickmore, “Four-dimensional electromagnetic radiators,” *Canadian Journal of Physics*, vol. 37, no. 3, pp. 263–275, 1959.

[19] W. H. Kummer, A. T. Villeneuve, T. Fong, and F. Terrio, “Ultra-low sidelobes from time-modulated arrays,” *Antennas and Propagation, IEEE Transactions on*, vol. 11, no. 6, pp. 633–639, 1963.

[20] R. E. Crotty and C. G. Goss, “Side Lobe Response Reducing System,” 3412405, 19-Nov-1968.

[21] B. L. Lewis and J. B. Evins, “A New Technique for Reducing Radar Response to Signals Entering Antenna Sidelobes,” *Antennas and Propagation, IEEE Transactions on*, vol. 31, no. 6, pp. 993–996, 1983.

[22] E. J. Baghdady, “Novel techniques for counteracting multipath interference effects in receiving systems,” *Selected Areas in Communications, IEEE Journal on*, vol. 5, no. 2, pp. 274–285, 1987.

[23] Shiwen Yang, Yeow Beng Gan, and T. Peng Khiang, “A new technique for power-pattern synthesis in time-modulated linear arrays,” *IEEE Antennas and Wireless Propagation Letters*, vol. 2, no. 1, pp. 285–287, 2003.

[24] X. Zhu, S. Yang, and Z. Nie, “Full-Wave Simulation of Time Modulated Linear Antenna Arrays in Frequency Domain,” *IEEE Transactions on Antennas and Propagation*, vol. 56, no. 5, pp. 1479–1482, May 2008.

[25] Fondevila, Bregains, Ares, and Moreno, “Optimizing uniformly excited linear arrays through time modulation,” *IEEE Antennas and Wireless Propagation Letters*, vol. 3, no. 1, pp. 298–301, Dec. 2004.

[26] A. Babakhani, D. B. Rutledge, and A. Hajimiri, "Transmitter Architectures Based on Near-Field Direct Antenna Modulation," *IEEE Journal of Solid-State Circuits*, vol. 43, no. 12, pp. 2674–2692, Dec. 2008.

[27] M. P. Daly and J. T. Bernhard, "Beamsteering in Pattern Reconfigurable Arrays Using Directional Modulation," *IEEE Transactions on Antennas and Propagation*, vol. 58, no. 7, pp. 2259–2265, Jul. 2010.

[28] Tao Hong, Mao-Zhong Song, and Yu Liu, "Dual-Beam Directional Modulation Technique for Physical-Layer Secure Communication," *IEEE Antennas and Wireless Propagation Letters*, vol. 10, pp. 1417–1420, 2011.

[29] M. P. Daly, E. L. Daly, and J. T. Bernhard, "Demonstration of Directional Modulation Using a Phased Array," *IEEE Transactions on Antennas and Propagation*, vol. 58, no. 5, pp. 1545–1550, May 2010.

[30] Y. Ding and V. Fusco, "BER-driven synthesis for directional modulation secured wireless communication," *International Journal of Microwave and Wireless Technologies*, vol. 6, no. 02, pp. 139–149, Apr. 2014.

[31] V. Pellegrini, F. Principe, G. de Mauro, R. Guidi, V. Martorelli, and R. Cioni, "Cryptographically secure radios based on directional modulation," in *Acoustics, Speech and Signal Processing (ICASSP), 2014 IEEE International Conference on*, 2014, pp. 8163–8167.

[32] Shiwen Yang, Y.-B. Gan, and Peng Khiang Tan, "Linear antenna arrays with bidirectional phase center motion," *IEEE Transactions on Antennas and Propagation*, vol. 53, no. 5, pp. 1829–1835, May 2005.

[33] Shiwen Yang, Yeow Beng Gan, and Anyong Qing, "Sideband suppression in time-modulated linear arrays by the differential evolution algorithm," *IEEE Antennas and Wireless Propagation Letters*, vol. 1, no. 1, pp. 173–175, 2002.

[34] S. Yang, "Study of Low Sidelobe Time Modulated Linear Antenna Arrays at Millimeter-Waves," *International Journal of Infrared and Millimeter Waves*, vol. 26, no. 3, pp. 443–456, Mar. 2005.

[35] E. Aksoy and E. Afacan, "Thinned Nonuniform Amplitude Time-Modulated Linear Arrays," *IEEE Antennas and Wireless Propagation Letters*, vol. 9, pp. 514–517, 2010.

[36] P. Rocca, Q. Zhu, E. T. Bekele, S. Yang, and A. Massa, "4-D Arrays as Enabling Technology for Cognitive Radio Systems," *IEEE Transactions on Antennas and Propagation*, vol. 62, no. 3, pp. 1102–1116, Mar. 2014.

[37] Q. Zhu, S. Yang, R. Yao, and Z. Nie, "Directional Modulation Based on 4-D Antenna Arrays," *IEEE Transactions on Antennas and Propagation*, vol. 62, no. 2, pp. 621–628, Feb. 2014.

[38] S. Yang, Q. Zhu, P. Rocca, and Z. Nie, "Signal-to-noise ratio and time-modulated signal spectrum in four-dimensional antenna arrays," *IET Microwaves, Antennas & Propagation*, vol. 9, no. 3, pp. 264–270, Feb. 2015.

[39] N. Valliappan, A. Lozano, and R. W. Heath, "Antenna Subset Modulation for Secure Millimeter-Wave Wireless Communication," *IEEE Transactions on Communications*, vol. 61, no. 8, pp. 3231–3245, Aug. 2013.

[40] A. Babakhani, D. B. Rutledge, and A. Hajimiri, "A near-field modulation technique using antenna reflector switching," in *Solid-State Circuits Conference, 2008. ISSCC 2008. Digest of Technical Papers. IEEE International*, 2008, pp. 188–605.

[41] A. Babakhani, D. Rutledge, and A. Hajimiri, "Near-field direct antenna modulation," *IEEE Microwave Magazine*, vol. 10, no. 1, pp. 36–46, Feb. 2009.

[42] A. H. Chang, A. Babakhani, and A. Hajimiri, "Near-field direct antenna modulation (NFDAM) transmitter at 2.4 GHz," in *Antennas and Propagation Society International Symposium, 2009. APSURSI'09. IEEE*, 2009, pp. 1–4.

[43] J. Lavaei, A. Babakhani, A. Hajimiri, and J. C. Doyle, "A study of near-field direct antenna modulation systems using convex optimization," in *American Control Conference (ACC), 2010*, 2010, pp. 1065–1072.

[44] Y. Zhang, Y. Ding, and V. Fusco, "Sidelobe Modulation Scrambling Transmitter Using Fourier Rotman Lens," *IEEE Transactions on Antennas and Propagation*, vol. 61, no. 7, pp. 3900–3904, Jul. 2013.

[45] V. Fusco and Y. Ding, "Directional modulation transmitter radiation pattern considerations," *IET Microwaves, Antennas & Propagation*, vol. 7, no. 15, pp. 1201–1206, Dec. 2013.

[46] Y. Ding and V. F. Fusco, "Establishing Metrics for Assessing the Performance of Directional Modulation Systems," *IEEE Transactions on Antennas and Propagation*, vol. 62, no. 5, pp. 2745–2755, May 2014.

[47] Y. Ding and V. F. Fusco, "Constraining directional modulation transmitter radiation patterns," *IET Microwaves, Antennas & Propagation*, vol. 8, no. 15, pp. 1408–1415, Dec. 2014.

[48] V. F. Fusco and Y. Ding, "Directional modulation far-field pattern separation synthesis approach," *IET Microwaves, Antennas & Propagation*, vol. 9, no. 1, pp. 41–48, Jan. 2015.

[49] V. Fusco and Y. Ding, "Directional modulation-enhanced retrodirective array," *Electronics Letters*, vol. 51, no. 1, pp. 118–120, Jan. 2015.

[50] T. Hong, M.-Z. Song, and Y. Liu, "RF DIRECTIONAL MODULATION TECHNIQUE USING A SWITCHED ANTENNA ARRAY FOR COMMUNICATION AND DIRECTION-FINDING APPLICATIONS," *Progress In Electromagnetics Research*, vol. 120, pp. 195–213, 2011.

[51] T. Snow and W. J. Chappell, "Applications for Directional Modulation on a Digital Phased Array," in *Phased Array Systems & Technology, 2013 IEEE International Symposium on*, 2013, pp. 529–533.

[52] T. Hong, M. Song, and Y. Liu, “Directional spread-spectrum modulation signal for physical layer security communication applications: Physical layer security communication,” *Security and Communication Networks*, vol. 6, no. 2, pp. 182–193, Feb. 2013.

[53] R. M. Christopher, “OPTIMIZATION OF SYMBOL DISTANCE METRIC IN DIRECTIONAL MODULATION SYSTEMS,” in *International Telemetering Conference Proceedings*, 2016.

[54] Y. Ding and V. F. Fusco, “A Vector Approach for the Analysis and Synthesis of Directional Modulation Transmitters,” *IEEE Transactions on Antennas and Propagation*, vol. 62, no. 1, pp. 361–370, Jan. 2014.

[55] S. S. Haykin and M. Moher, *Modern wireless communications*. Upper Saddle River, N.J: Pearson/Prentice Hall, 2005.

[56] Stephen P Boyd and Lieven Vandenberghe, *Convex optimization*. Cambridge, UK, New York: Cambridge University Press, 2004.

[57] S. Jontz, “DISA Seeks Software Solution To Manage Spectrum,” *Signal*, vol. 69, no. 11, pp. 34–36, Jul-2015.

[58] W. C. Brown and R. George, “Rectification of microwave power,” *Spectrum, IEEE*, vol. 1, no. 10, pp. 92–97, 1964.

[59] W. C. Brown, “Experiments involving a microwave beam to power and position a helicopter,” *Aerospace and Electronic Systems, IEEE Transactions on*, no. 5, pp. 692–702, 1969.

[60] A. H. Sakr and E. Hossain, “Cognitive and Energy Harvesting-Based D2D Communication in Cellular Networks: Stochastic Geometry Modeling and Analysis,” *IEEE Transactions on Communications*, vol. 63, no. 5, pp. 1867–1880, May 2015.

[61] S. Lee, R. Zhang, and K. Huang, "Opportunistic Wireless Energy Harvesting in Cognitive Radio Networks," *IEEE Transactions on Wireless Communications*, vol. 12, no. 9, pp. 4788–4799, Sep. 2013.

[62] I. Krikidis, S. Timotheou, S. Nikolaou, G. Zheng, D. W. K. Ng, and R. Schober, "Simultaneous wireless information and power transfer in modern communication systems," *IEEE Communications Magazine*, vol. 52, no. 11, pp. 104–110, 2014.

[63] D. W. K. Ng, E. S. Lo, and R. Schober, "Robust Beamforming for Secure Communication in Systems With Wireless Information and Power Transfer," *IEEE Transactions on Wireless Communications*, vol. 13, no. 8, pp. 4599–4615, Aug. 2014.

[64] A. F. Molisch, *Wireless communications*. Chichester, West Sussex, U.K.: Wiley : IEEE, 2011.

[65] J. W. Betz, "The Offset Carrier Modulation for GPS Modernization," in *Proceedings of the 1999 National Technical Meeting of The Institute of Navigation*, San Diego, CA, 1999, pp. 639 – 648.

[66] X. Zhu and F. Wang, "The signal design of present satellite navigation system and its inspiration," 2005, pp. 598557–598557–5.

[67] R. M. Yamada, A. O. Steinhardt, and L. Mili, "Beamforming for Simultaneous Energy and Information Transfer and Physical-Layer Secrecy," *IEEE Transactions on Wireless Communications*, vol. Submitted, Mar. 2017.

[68] Q. Zhu, S. Yang, R. Yao, and Z. Nie, "A directional modulation technique for secure communication based on 4D antenna arrays," in *Antennas and Propagation (EuCAP), 2013 7th European Conference on*, 2013, pp. 125–127.

[69] R. Poisel, *Introduction to communication electronic warfare systems*. Boston: Artech House, 2002.

[70] R. Poisel, *Modern communications jamming: principles and techniques*, 2nd ed. Boston: Artech House, 2011.

[71] C. Cox, *An introduction to LTE LTE, LTE-advanced, SAE, VoLTE and 4G mobile communications*. Chichester, West Sussex, United Kingdon ; Hoboken, New Jersey: John Wiley & Sons, Inc, 2014.

[72] M. Costa, "Writing on dirty paper (corresp.)," *IEEE transactions on information theory*, vol. 29, no. 3, pp. 439–441, 1983.

[73] G. Caire and S. Shamai, "On the achievable throughput of a multiantenna Gaussian broadcast channel," *IEEE Transactions on Information Theory*, vol. 49, no. 7, pp. 1691–1706, Jul. 2003.

[74] J. Barros and M. R. Rodrigues, "Secrecy capacity of wireless channels," in *Information Theory, 2006 IEEE International Symposium on*, 2006, pp. 356–360.

[75] A. Nordrum, "The Internet of Fewer Things," *IEEE Spectrum*, vol. 53, no. 10, pp. 12–13, 2016.

[76] C. E. Shannon, "A Mathematical Theory of Communication," *Bell System Technical Journal*, vol. 27, no. 4, pp. 623–656, Oct. 1948.

[77] G. J. Foschini and M. J. Gans, "On limits of wireless communications in a fading environment when using multiple antennas," *Wireless personal communications*, vol. 6, no. 3, pp. 311–335, 1998.

[78] T. Cover, "Broadcast channels," *IEEE Transactions on Information Theory*, vol. 18, no. 1, pp. 2–14, 1972.

[79] K. Marton, "A coding theorem for the discrete memoryless broadcast channel," *IEEE Transactions on Information Theory*, vol. 25, no. 3, pp. 306–311, 1979.

[80] I. Csiszar and J. Korner, “Broadcast channels with confidential messages,” *IEEE Transactions on Information Theory*, vol. 24, no. 3, pp. 339–348, May 1978.

[81] N. Jindal, S. Vishwanath, and A. Goldsmith, “On the duality of Gaussian multiple-access and broadcast channels,” *IEEE Transactions on information Theory*, vol. 50, no. 5, pp. 768–783, 2004.

[82] S. Vishwanath, N. Jindal, and A. Goldsmith, “Duality, achievable rates, and sum-rate capacity of gaussian mimo broadcast channels,” *IEEE Transactions on Information Theory*, vol. 49, no. 10, pp. 2658–2668, Oct. 2003.

[83] A. Bennatan and D. Burshtein, “On the fading-paper achievable region of the fading MIMO broadcast channel,” *IEEE Transactions on Information Theory*, vol. 54, no. 1, pp. 100–115, 2008.

[84] P. Viswanath and D. N. C. Tse, “Sum capacity of the vector Gaussian broadcast channel and uplink-downlink duality,” *IEEE Transactions on Information Theory*, vol. 49, no. 8, pp. 1912–1921, 2003.

[85] F. Oggier and B. Hassibi, “The Secrecy Capacity of the MIMO Wiretap Channel,” *IEEE Transactions on Information Theory*, vol. 57, no. 8, pp. 4961–4972, Aug. 2011.

[86] R. Liu and H. V. Poor, “Secrecy Capacity Region of a Multiple-Antenna Gaussian Broadcast Channel With Confidential Messages,” *IEEE Transactions on Information Theory*, vol. 55, no. 3, pp. 1235–1249, Mar. 2009.

[87] J. Brehmer, A. Molin, P. Tejera, and W. Utschick, “A low complexity approximation of the MIMO broadcast channel capacity region,” in *Communications, 2006. ICC’06. IEEE International Conference on*, 2006, vol. 7, pp. 3111–3116.

[88] A. Goldsmith, S. A. Jafar, N. Jindal, and S. Vishwanath, “Capacity limits of MIMO channels,” *IEEE Journal on Selected Areas in Communications*, vol. 21, no. 5, pp. 684–702, Jun. 2003.

[89] E. Biglieri, Ed., *MIMO wireless communications*. Cambridge: Cambridge University Press, 2007.